Studies on Grasping and Manipulation by Robotic Multifingered Hands and Arm-Hand Systems(Dissertation_全文)

AUTHOR(S):

Nagai, Kiyoshi

STUDIES ON GRASPING AND MANIPULATION BY ROBOTIC MULTIFINGERED HANDS AND ARM-HAND SYSTEMS

Kiyoshi NAGAI

1994

ABSTRACT

The major purpose of this thesis is to discuss the various problems of the grasping and manipulation by robotic multifingered hands and arm-hand systems.

This thesis consists of two parts. In the first part of Chapters 2 through 4, discussions are made on grasping and manipulation by multifingered hands. In the second part of Chapters 5 and 6, cooperative manipulations with grasping by macro-micro manipulators and arm-hand systems are dealt with.

In the grasping and manipulation by multifingered hands, the fingertip force must be applied to an object suitably for the secure grasping and desired manipulation. In Chapter 2, the grasping and manipulating forces are defined as the components of fingertip force for the above aim. Based on the concept of these forces, a control scheme of multifingered hands for grasping and manipulation is proposed in Chapter 3, and adaptation of the grasping force for the secure grasping is proposed in Chapter 4 as an adaptive grasping.

It is a matter of fact that the rolls of the arms and hands are important to the cooperative manipulations with grasping by arm-hand systems. In the comparison of their abilities, the arms are considered as macro manipulator, and the multifingered hands are considered as micro manipulator. That is, the arms generally have big motion ranges, but are not suitable for compliant motions because of their big masses. On the other hand, the multifingered hands are suitable for compliant motions because of their small masses, but they have relatively small motion ranges. Consequently, by connecting an arm and multifingered hand, a redundant macro-micro manipulator is constructed. In Chapter 5, a motion control scheme of such redundant macro-micro manipulators is proposed, based on the impedance control. In Chapter 6, a control scheme of arm-hand systems for the secure grasping and cooperative manipulation is proposed.

The results of this study surely contribute to advanced manipulation technologies, and help to realize dexterous manipulation, appears in the cooperative motions by the human arm and hand.

ACKNOWLEDGEMENT

I would like to express my gratitude to Professor Tsuneo Yoshikawa for his patient guidance. His intense criticism and deep insight in the discussions have been the base of this thesis.

I would also like to express my gratitude to Professor Hideo Hanafusa for giving me a opportunity to study in the robotics field. He has encouraged me since I was a student of Kyoto University and enables me to complete this thesis.

I wish to thank to the late Professor Keiichiro Miyata. He gave me a chance to continue my research at Ritsumeikan University.

I also wish to thank to the professors in Ritsumeikan University. Especially, Professor Hirokazu Mayeda, Professor Tohru Watanabe, Professor Hidekatsu Tokumaru, Professor Eiji Okubo and Professor Sadao Kawamura have encouraged me to finish this thesis. Professor Tsuneshichi Tanaka shows me preparedness as a researcher.

I also wish to thank to Dr. Toshiharu Sugie and Dr. Yoshihiko Nakamura for their valuable suggestions at the Automation Research Laboratory of Kyoto University.

I also wish to thank to the members in our laboratory. Especially, Mr. Kazuhiro Waki helped me in the simulation of the hand, Mr. Hiromi Totani, Mr. Hiromichi Hanai and Mr. Hidetoshi Mizuno helped me in the experiment, and Mr. Koichi Watanabe intently helped me to finish this thesis.

Finally, I am deeply grateful to my family for their support.

Contents

Chapter 1

Introduction

1.1 Grasping and Manipulation

Grasping and *manipulation* are two of the most important topics in the robotics field, which are very closely related to each other. Grasping by robot hands comes first to manipulate an object by robotic mechanisms. The robot hands can be classified into two groups by considering whether they have the ability of manipulation or not. That is, the robot hands with this ability are called *multifingered hand*, discussed in this thesis, and the others are called as gripper. In case of the multifingered hands, a desired manipulation of the object becomes important. Especially, if the multifingered hand is attached to a robot arm, manipulations can be executed by both the hand and arm. This means such mechanisms have redundancy, and they are called *arm-hand system* in this thesis.

Multifingered hands generally have several articulated fingers. The number of fingers of each hand is not always five different from a human hand. Human hands are good examples of multifingered hands, but their ability of manipulation are too advanced to be realized by robotic multifingered hands. Human hands can manipulate an object arbitrarily by dexterous cooperative motions of the fingers, and this is the interesting point of the research on robot hands.

The redundancy of the arm-hand systems in the manipulation as mentioned above is important. In the case of mankind, highly advanced cooperative motions of arms and hands with this sort of redundancy are often observed in daily life and in sports. When we write a letter with a pen, a rough motion of our arm and a fine motion of the hand are combined dexterously. Indeed the motion of the pen is a combination of the motions of the arm and hand, in which the fine motion of the hand modifies the rough motion of the pen produced by the arm. This sort of the cooperative motion of the arm and hand is a good model of the advanced manipulation by the robotic arm-hand systems.

1.2 Background of Multifingered Hands

1.2.1 History of Multifingered Hands

The study on multifingered hands began in 1960s for the automation of material handling. Yamashita[61] developed a three-fingered hand driven by pneumatic actuators in 1964, in which each finger of the hand has three DOF (Degrees Of Freedom), and it could manipulate an object by the sequential control.

Since the later half of the 1970s, many papers have been published on the multifingered hands. In 1977, Hanafusa and Asada[12] discussed the stable grasping by using the potential energy of the grasping system. Regarding the research on the mechanisms, in 1979, Okada[40] developed a three-fingered hand and realized a manipulation of a stick and a bowl, paying attention to its kinematics. In 1985, Kobayashi[27], [28] developed a three-fingered hand whose fingers have four DOF. Jacobsen[17] developed a four-fingered hand considering the structure of human hands.

Regarding the research on kinematics, Salisbury[43] discussed the contact condition between fingers and an object, and discussed the concept of mobility in 1982. Kobayashi[27], [28] discussed a kinematical necessary and sufficient condition for manipulation by introducing the virtual joints at the contact points. Yoshikawa[56] discussed the optimal posture by using the concept of the manipulability in 1985.

Analytical researches have been published since the latter half of the 1980s. Cutkosky and Wright[7] discussed the contact where the fingertips have elasticity. Kerr and Roth[22] discussed the grasping configurations where the grasped object is underconstrained or overconstrained. Abel et al.[1] and Trinkle et al.[50] discussed the grasping and manipulation by two-fingered hands in planar motion. Cai[5] discussed a path planning as the problem of linear programing.

Recently, Montana[33], Cole, Hauser, and Sastry[6], Li and Canny[31] discussed the rolling contact between fingers and an object. Cutkosky[8] analyzed the motion by human hand, and discussed an expert system for the manipulation by the robotic hand. Starr[47] discussed an implementation of stiffness control of grasped object by a three-fingered hand. Bicchi[3] presented a control algorithm for the power grasping that minimizes the risk of slippage.

Of course, many papers have been published on grasping and manipulation, described in the following subsection.

1.2.2 Stability in Grasping and Manipulation

So far the grasping and manipulation have been discussed with a keyword *stability*. However, there are two meanings of stability: *stability of motion* and *stability of contact*.

Stability of motion means the ability to return a grasped object to its statically equilibrium position when its position is changed, and this is a topic of manipulation. On the other hand, stability of contact means the ability to maintain the contact against any disturbance of external forces on the object, and this is a topic of grasping.

Among the researches of manipulation, the research by Hanafusa and Asada[12], as mentioned above, was the initial study of this topic. Fearing[11], Cutkosky and Kao[9] discussed a resultant compliance on the object produced by a compliance of each finger. Li and Sastry[29] discussed the static stability by considering the manipulation task. Nguyen[38], [39] discussed this topic as the force closure. It is, however, noted that these researches are mainly on the static stability of the grasped object. Recently, several control algorithms have been proposed[49], [30], [59], considering the dynamics of the fingers and the object. Li et al.[30] consider the dynamics of the system, and propose the control algorithm which includes both the position control of the object and internal force control. This controller is based on the dynamic coordinative manipulation[35].

On the other hands, the grasping problem has been discussed as the problem of determining internal forces. It has been well known that the internal force is an important factor in the analysis and synthesis of fingertip forces for grasping and manipulation. Hanafusa et al.[14] discussed the magnitude of grasping force. Mason and Salisbury[32] gave the conditions for complete restraint of the grasped object in terms of internal forces. Kerr and Roth[21] proposed the method of determining the optimal internal force with the minimum norm under an approximated frictional constraint. Kumar and Waldron[25], [26] have a computationally efficient suboptimal solution to this problem. Ji and Roth[18] proposed a method of determining the fingertip forces of three-fingered hands by finding the internal forces that minimize the maximum angles between the contact normals and the internal force components.

1.2.3 Grasping and Manipulating Forces

Most of the efforts in the above mentioned research involve the decomposition of each fingertip force into two components by using the pseudoinverse of a coefficient matrix that relates the resultant forces exerted on the object to the fingertip forces. One of the components is given by premultiplying the pseudoinverse of the coefficient matrix to the resultant force. This component is characterized as that having the minimum norm among those producing the specified resultant force. The other component, which is given by a vector belonging to the null space of the coefficient matrix, is an internal force.

In spite of their mathematical simplicity and clear meaning in terms of vector norm, this may not be adequate from a physical point of view as will be shown in the next chapter. In this paper, a grasping force is considered as a component of a fingertip force

that contributes to the secure grasping, which is independent of a manipulating force that produces the required force for the manipulation.

1.3 Background of Arm-Hand Systems

1.3.1 Problems of Arm-Hand Systems

Since the both of the arm and multifingered hand in this thesis have the manipulation ability, a system that consists of the arm and the multifingered hand has a sort of redundancy. Hanafusa, Yoshikawa and Nakamura[13] utilize this redundancy for changing the arm posture to avoid obstacles. Tsuji, Takahashi and Ito[51],[52],[53], Yokoi, Maekawa and Tanie[55], Newman and Dohring[37] utilize the redundancy of the arm for the compliance control.

However, there are two different points between ordinary redundant arms and arm-hand systems. The first point is that grasping by multifingered hands must be considered simultaneously during manipulation. Therefore, a required control scheme should utilize the redundancy to maintain non-slip grasping. The second point is that multifingered hands are suitable to compliant motion because of their small inertia compared to that of arms, but, the motion range of the multifingered hands are small compared to that of the arms. These points means that arm-hand systems have a same feature as redundant macro-micro manipulators, described in the following subsection.

1.3.2 Redundant Macro-Micro Manipulators

The merits of using a micro manipulator were discussed mentioned in several papers. Khatib[23] pointed out that by attaching a micro manipulator to a macro manipulator the inertia of the endpoint is generally reduced. Sharon, Hogan and Hardt[46] reported that the performance of the position and force controllers is improved by using a micro manipulator. Yoshikawa, Hosoda and Doi[60] utilize a micro manipulator to improve the tracking ability of flexible manipulators. For compensation of small motion range of the micro manipulator, Kawase et al.[20] proposed to utilize a big motion range of the arm. However, above researches do not mention the behavior when an external force is applied at the endpoint of the manipulator.

1.4 The Goal of this Study and the Composition of this Thesis

The goal of this study is to develop a control algorithm of multifingered hands and arm-hand systems for the secure grasping and arbitrary manipulation.

This thesis consists of two parts. In the first part of Chapters 2 through 4, discussions are made on analysis and control of multifingered hands. In the second part of Chapters 5 and 6, control schemes of macro-micro manipulators and arm-hand mechanisms are dealt with.

In Chapter 2, the grasping and manipulating forces for multifingered robot hands are newly defined. A short discussion of the grasping and manipulating forces for two-fingered hands with linear motion is first given to explain the motivation more clearly and to provide the basic idea of the new definition. Then, based on an analysis of the internal force, the grasping force for three-fingered hands is defined as an internal force that satisfies the static friction constraint. The concept of grasp mode is also introduced. Subsequently, the manipulating force is defined as a fingertip force that satisfies the following three conditions: 1) It produces the specified resultant force. 2) It is not in the inverse direction of the grasping force. 3) It is orthogonal to the grasping force component. An algorithm is presented for decomposing a given fingertip force into the manipulating and grasping forces. Discussions are made on the extensions of the obtained results to the case of two-fingered hands with planar motion and to that of four-fingered hands. Finally, a simple example of synthesizing fingertip forces for a given manipulation task is given to illustrate the usefulness of the proposed definition.

In Chapter 3, a dynamic manipulation/grasping controller of multifingered robot hands is proposed, based on the dynamic control and hybrid position/force control. Using a concept of the manipulating and grasping forces proposed in Chapter 2, this controller consists of a compensator which linearizes the whole grasping system and a servo controller for the linearized system. The distinctive features of the proposed controller are: 1) It uses the grasp parameters, which have the same number of elements as that of the essential dimension of the internal force, as the controlled variables for the grasping control. 2) It decomposes the total force required grasping of the object into the manipulating force which is a part of the fingertip force. First, the basic equations are formulated for the kinematical constraint among the fingers and the equations of motion of the fingers and the object. Second, the dynamic manipulation/grasping controller is proposed, whose validity is shown by simulation results.

In Chapter 4, discussions are made on a new method of the adaptive grasping for multifingered hands with the constraints of static friction and the joint torques, under the repeated manipulation tasks. First, the dynamic manipulation/grasping controller, proposed in Chapter 3, are described for two-fingered hands. This controller makes it possible to give the desired grasp parameters which determining the grasping force, in spite of the desired trajectory of the object. Second, the scalar functions are defined to evaluate the manipulation and the grasping, and the effects on these functions by the given grasp parameter are shown. Then, a new algorithm of the adaptive grasping is proposed, based on

these functions. This algorithm realizes the desired manipulation without the fingertip slips by adjusting the grasp parameter to the given manipulation task. Finally, the effectiveness of the proposed method is shown by several experiments.

In Chapter 5, an impedance control scheme of redundant macro-micro manipulators is proposed, which specifies not only the desired mechanical impedance of the end effector, but also that of the macro manipulator by considering the internal force applied to the tip of the macro manipulator. This control scheme can utilize both merits of the macro and micro manipulators. That is, by specifying a suitable set of the desired mechanical impedance, a compliant motion can be realized without any excessive joint torque of the macro manipulator, and a big motion range of the macro manipulator can be used effectively to compensate a small motion range of the micro manipulator. The validity of the proposed control scheme is shown by several simulation results.

In Chapter 6, a control scheme for grasping and manipulation by arm-hand systems is proposed. The arm-hand systems, consisting of arm and multifingered hand, have the same feature as that of redundant macro-micro manipulators concerning manipulation. That is: 1) manipulations are possible by both the arms and hands, 2) the hands are suitable for the compliant motions compared to the arms because of their small inertia, and the motion ranges of the arms are bigger than those of the hands. The control scheme can utilize both merits of the arms and hands. Simultaneously, it can realize the secure grasping during manipulations. Several simulation and experimental results illustrate the validity of the proposed control scheme.

In Chapter 7, concluding remarks and further research topics are described.

Chapter 2

Manipulating and Grasping Forces in Manipulation by Multifingered Robot Hands

2.1 Introduction

This chapter discusses the question of whether we can define grasping and manipulating forces for multifingered hands in a reasonable way.

It has been well recognized that internal force is an important factor in the analysis and synthesis of fingertip forces for grasping and manipulation. Mason and Salisbury [32] gave conditions for complete restraint of an object by a grasp in terms of internal force. Kerr and Roth [21] proposed to determine the optimal internal force as that with the minimum norm under an approximated frictional constraint. Kumar and Waldron [25] have a computationally efficient suboptimal solution to this problem. Ji and Roth [18] proposed a method of determining fingertip force of three-fingered hands by first finding the internal force that minimizes the maximum of the angles between the contact normals and the internal force components. Demmel and Lafferriere [10] proposed a different scheme for the same problem. Schwartz and Sharir [45] defined the optimality as minimizing the coefficient of friction needed to attain a grasp in the presence of a given external force and torque, and gave a complexity analysis of the solution algorithm.

Most of these research efforts involve the decomposition of the fingertip force into two components by using the pseudoinverse of a coefficient matrix that relates the resultant force exerted on the object to the fingertip force. One component is given by premultiplying the resultant force by the pseudoinverse of the coefficient matrix. This component is characterized as the one with the minimum norm among those producing the specified resultant force. The other component, which is given by a vector belonging to the null space of the coefficient matrix, is an internal force. Because of their mathematical simplicity and

clear meaning in terms of vector norm, we are tempted to define these two components as manipulating and grasping forces (see, e.g., [27]). However,this is not adequate from a physical point of view as will be shown in the next section.

In this chapter, a new physically reasonable definition of manipulating force and grasping force is given for two-, three-, and four-fingered hands. First, for a simple case of two-fingered hands with linear motion, the irrelevance of the pseudoinverse decomposition of fingertip force as the basis of defining grasping and manipulating forces is shown, and a new physically reasonable definition is proposed. Then for three-fingered hands a representation of the internal force is given. Based on this representation, the grasping force and the manipulating force are defined. An algorithm for decomposing a given fingertip force into manipulating and grasping forces is presented. It is shown that this definition can be extended to two-fingered hands with planar motion and four-fingered hands. Finally, the usefulness of the obtained analytical result is shown by an example of synthesizing the fingertip force for a given manipulation task.

Note that only fingertip grasps with point contact are treated, and the Coulomb model is used for friction in this paper.

2.2 Two-Fingered Hand with Linear Motion

To explain the motivation and the main idea of our study, we first consider the problem of decomposing a given fingertip force into grasping and manipulating force components for a simple two-fingered hand as shown in Fig. 2.1.

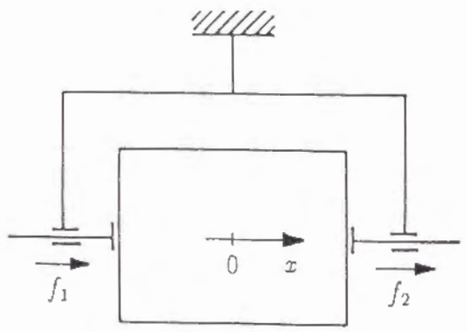

Fig. 2.1. Two-fingered hand with linear motion.

Assume that the two fingers have one degree of freedom and can move in the x direction. Let $f_i \in \mathrm{R}^1$ (R^n is the set of all n-dimensional real vectors) denote the force applied by the i-th finger ($i = 1, 2$) on the object along the x axis. We assume that both fingers can only

push, that is, $f_1 \geq 0$ and $f_2 \leq 0$. The relation between the fingertip force $\boldsymbol{F} = [f_1 \quad f_2]^{\mathrm{T}}$ and the resultant force $t \in \mathrm{R}^1$ exerted on the object is given by

$$t = f_1 + f_2 = \boldsymbol{A}\boldsymbol{F} \tag{2.1}$$

where $\boldsymbol{A} = [1 \quad 1]$.

When a resultant force t is given, fingertip force $\boldsymbol{F}$ that produces this t is given by the general solution of Eq. (2.1):

$$\boldsymbol{F} = \boldsymbol{A}^{\dagger}t + (\boldsymbol{E}_2 - \boldsymbol{A}^{\dagger}\boldsymbol{A})\boldsymbol{y} \tag{2.2}$$

where $\boldsymbol{A}^{\dagger}$ is the pseudoinverse [4] of $\boldsymbol{A}$, $\boldsymbol{y} \in \mathrm{R}^2$ is an arbitrary constant vector, and $\boldsymbol{E}_n \in \mathrm{R}^{n\times n}$ ($\mathrm{R}^{n\times n}$ is the set of all $n \times n$ real matrices) denotes the unity matrix. The right hand first term of Eq. (2.2) represents the fingertip force with the minimum norm among those that produce the resultant force t. The second term represents an internal force. Now assume that we are given a fingertip force $\boldsymbol{F}$ first instead of t. Substituting Eq. (2.1) into Eq. (2.2) yields

$$\boldsymbol{F} = \boldsymbol{A}^{\dagger}\boldsymbol{A}\boldsymbol{F} + (\boldsymbol{E}_2 - \boldsymbol{A}^{\dagger}\boldsymbol{A})\boldsymbol{F} \tag{2.3}$$

This equation represents a decomposition of the fingertip force into two components. We are tempted to define the manipulating force by the first term $\boldsymbol{A}^{\dagger}\boldsymbol{A}\boldsymbol{F} \triangleq [\tilde{f}_{m1} \quad \tilde{f}_{m2}]^{\mathrm{T}}$ and the grasping force by the second term $(\boldsymbol{E}_2 - \boldsymbol{A}^{\dagger}\boldsymbol{A})\boldsymbol{F} \triangleq [\tilde{f}_{g1} \quad \tilde{f}_{g2}]^{\mathrm{T}}$, on the right-hand side of Eq. (2.3). However, this is not adequate from a physical point of view as is shown in the following.

Since $\boldsymbol{A}^{\dagger} = \boldsymbol{A}^{\mathrm{T}}(\boldsymbol{A}\boldsymbol{A}^{\mathrm{T}})^{-1} = [1/2 \quad 1/2]^{\mathrm{T}}$, we have

$$\begin{bmatrix} \tilde{f}_{m1} \\ \tilde{f}_{m2} \end{bmatrix} = \begin{bmatrix} \frac{f_1+f_2}{2} \\ \frac{f_1+f_2}{2} \end{bmatrix} \tag{2.4}$$

$$\begin{bmatrix} \tilde{f}_{g1} \\ \tilde{f}_{g2} \end{bmatrix} = \begin{bmatrix} \frac{f_1-f_2}{2} \\ -\frac{(f_1-f_2)}{2} \end{bmatrix} \tag{2.5}$$

If we consider the case of $f_1 \geq 0$ and $f_2 = 0$ which is schematically shown in Fig. 2.2(a), we have $[\tilde{f}_{g1} \quad \tilde{f}_{g2}]^{\mathrm{T}} = [f_1/2 \quad -f_1/2]^{\mathrm{T}}$, implying that the force component for grasping is not zero [see Fig. 2.2(b)]. However, since $f_2 = 0$, the object will slip out of the two fingers by an application of any external force perpendicular to the x axis however small it may be. Therefore, according to our institution, the grasping force for this case should be zero. Note also that $\tilde{f}_{m2}$ given by Eq. (2.4) is negative, implying that the manipulating force for the second finger is a pulling force. Hence, $[\tilde{f}_{m1} \quad \tilde{f}_{m2}]^{\mathrm{T}}$ and $[\tilde{f}_{g1} \quad \tilde{f}_{g2}]^{\mathrm{T}}$ are not suitable for the definition of manipulating and grasping forces.

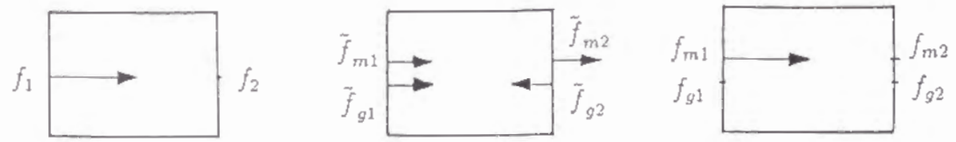

(a) Fingertip force (b) Decomposition by Eqs. (2.4) and (2.5) (c) Decomposition by Eqs. (2.6) and (2.7)

Fig. 2.2. Decomposition of fingertip force.

Based on this consideration, we now propose to define the manipulating force $[\tilde{f}_{m1} \quad \tilde{f}_{m2}]$ and the grasping force $[\tilde{f}_{g1} \quad \tilde{f}_{g2}]^{\mathrm{T}}$ by the following equations:

$$\begin{bmatrix} f_{m1} \\ f_{m2} \end{bmatrix} = \begin{bmatrix} k \\ -(1-k) \end{bmatrix} |f_1 + f_2| \tag{2.6}$$

$$\begin{bmatrix} f_{g1} \\ f_{g2} \end{bmatrix} = \begin{bmatrix} 1 \\ -1 \end{bmatrix} \min(|f_1|, |f_2|) \tag{2.7}$$

where k is an auxiliary parameter that takes a value of 1 when $f_1 + f_2 \geq 0$ and a value of 0 when $f_1 + f_2 \leq 0$. According to this definition, we always have $f_{m1} \geq 0$, $f_{g1} \geq 0$, $f_{m2} \leq 0$, and $f_{g2} \leq 0$. Also, when $f_1 > 0$ and $f_2 = 0$, we have $[\tilde{f}_{m1} \quad \tilde{f}_{m2}]^{\mathrm{T}} = [f_1 \quad 0]^{\mathrm{T}}$ and $[f_{g1} \quad f_{g2}]^{\mathrm{T}} = [0 \quad 0]^{\mathrm{T}}$ [see Fig. 2.2(c)]. This result agrees with our intuitive picture of the grasping force.

We will extend the definition of grasping and manipulating forces given by Eqs. (2.6) and (2.7) for two-fingered hands to the case of three-fingered hands in Sections 2.3 through 2.5.

2.3 A Representing of Internal Force for Three-Fingered Hands

The basic relations of forces in manipulation of a rigid object by a three-fingered hand and a representation of the internal force will be given in this section under the following assumptions.

A1) Each fingertip makes a frictional point contact with the object.

A2) The three contact points are not located on a straight line.

A3) The mechanism of each finger is such that each fingertip can exert a force to the object in any direction.

Assumption A1 means that the interaction between each finger and the object can be modeled as a pure force through some point, which we call a contact point. Assumptions A2 and A3 are necessary for arbitrary manipulation of the object.

Figure 2.3 shows a robot hand and an object under consideration. In the figure, $\Sigma_O(O - xyz)$ is the object coordinate frame fixed to the object, C_i is the contact point of the i-th finger ($i = 1, 2, 3$), $\boldsymbol{r}_i = [r_{ix} \quad r_{iy} \quad r_{iz}]^{\mathrm{T}} \in \mathrm{R}^3$ is the position vector of C_i from the origin of Σ_0, and $\boldsymbol{f}_i \in \mathrm{R}^3$ is the fingertip force applied to the object by the i-th finger.

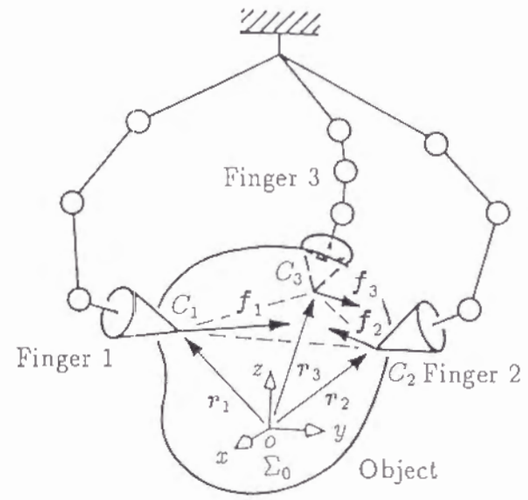

Fig. 2.3. Three-fingered hand and object.

The resultant force $\boldsymbol{f} \in \mathrm{R}^3$ and resultant moment $\boldsymbol{n} \in \mathrm{R}^3$ due to ($\boldsymbol{f}_i, i = 1, 2, 3$) are given by

$$\boldsymbol{f} = \sum_{i=1}^{3} \boldsymbol{f}_i \tag{2.8}$$

$$\boldsymbol{n} = \sum_{i=1}^{3} (\boldsymbol{r}_i \times \boldsymbol{f}_i). \tag{2.9}$$

From Eqs. (2.8) and (2.9) we obtain the basic relation between the total fingertip force $\boldsymbol{F} \triangleq [\boldsymbol{f}_1^{\mathrm{T}} \quad \boldsymbol{f}_2^{\mathrm{T}} \quad \boldsymbol{f}_3^{\mathrm{T}}]^{\mathrm{T}}$ and the total resultant force $\boldsymbol{T} \triangleq [\boldsymbol{f}^{\mathrm{T}} \quad \boldsymbol{n}^{\mathrm{T}}]^{\mathrm{T}}$:

$$\boldsymbol{T} = \boldsymbol{A}\boldsymbol{F} \tag{2.10}$$

where

$$\boldsymbol{A} \triangleq \begin{bmatrix} \boldsymbol{E}_3 & \boldsymbol{E}_3 & \boldsymbol{E}_3 \\ \boldsymbol{R}_1 & \boldsymbol{R}_2 & \boldsymbol{R}_3 \end{bmatrix} \in \mathrm{R}^{6\times 9} \tag{2.11}$$

$$\boldsymbol{R}_i \triangleq \begin{bmatrix} 0 & -r_{iz} & r_{iy} \\ r_{iz} & 0 & -r_{ix} \\ -r_{iy} & r_{ix} & 0 \end{bmatrix} \in \mathrm{R}^{3\times 3} \tag{2.12}$$

The general solution $\boldsymbol{F}$ of Eq. (2.10) for a given $\boldsymbol{T}$ is written as

$$\boldsymbol{F} = \boldsymbol{A}^{\dagger}\boldsymbol{T} + (\boldsymbol{E}_9 - \boldsymbol{A}^{\dagger}\boldsymbol{A})\boldsymbol{y} \tag{2.13}$$

where $\boldsymbol{y} \in \mathrm{R}^9$ is an arbitrary constant vector. Although the second term, $(\boldsymbol{E}_9 - \boldsymbol{A}^{\dagger}\boldsymbol{A})\boldsymbol{y}$, in Eq. (2.13) represents the internal force among the fingers, this expression is not convenient due to the following fact. From assumption A2 the rank of $\boldsymbol{A}$ is 6 and $\mathrm{rank}(\boldsymbol{E}_9 - \boldsymbol{A}^{\dagger}\boldsymbol{A}) = 3$. Hence, the number of independent unknown parameters of the internal force is three. Determining the internal force by vector $\boldsymbol{y}$ means determining a three-dimensional quantity by specifying a nine-dimensional quantity. In order to avoid this inconvenience, another expression of the internal force will now be given. Let

$$\boldsymbol{e}_{ij} \triangleq \frac{\boldsymbol{r}_j - \boldsymbol{r}_i}{||\boldsymbol{r}_j - \boldsymbol{r}_i||}, \quad i,j = 1,2,3,\ i \neq j \tag{2.14}$$

where $||\boldsymbol{r}||$ denotes the Euclidian norm of vector $\boldsymbol{r}$. The vector $\boldsymbol{e}_{ij}$ is the unit vector directing from C_i to C_j on the grasp plane Q including the three contact points, and $\boldsymbol{e}_{ij} = -\boldsymbol{e}_{ji}$ (see Fig. 2.4). We have:

Proposition 1: A total fingertip force $\boldsymbol{F}$ is an internal force if and only if there exists a vector $\boldsymbol{z} = [z_{23} \quad z_{31} \quad z_{12}]^{\mathrm{T}} \in \mathrm{R}^3$ such that

$$\boldsymbol{F} = \boldsymbol{G}\boldsymbol{z} \tag{2.15}$$

where

$$\boldsymbol{G} \triangleq \begin{bmatrix} 0 & \boldsymbol{e}_{13} & \boldsymbol{e}_{12} \\ \boldsymbol{e}_{23} & 0 & \boldsymbol{e}_{21} \\ \boldsymbol{e}_{32} & \boldsymbol{e}_{31} & 0 \end{bmatrix} \in \mathrm{R}^{9\times 3} \tag{2.16}$$

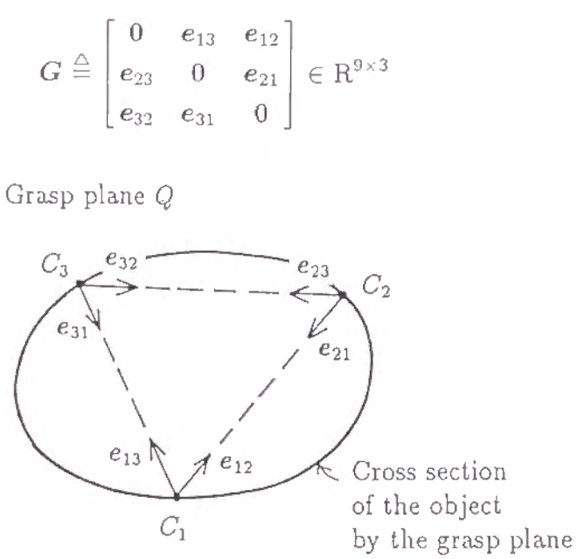

Fig. 2.4. Vectors e_{ij}.

Proof: From Eqs. (2.11), (2.12), (2.14), and (2.16), we obtain $\boldsymbol{A}\boldsymbol{G} = \boldsymbol{0}$. Hence, $\mathrm{Range}(\boldsymbol{G}) \subset \mathrm{Range}(\boldsymbol{E}_9 - \boldsymbol{A}^{\dagger}\boldsymbol{A})$ where $\mathrm{Range}(\cdot)$ is the range space of a matrix. On the other hand, from assumption A2 and the fact that $\mathrm{rank}(\boldsymbol{A}\boldsymbol{G} = \boldsymbol{0}) = 3$, we have $\mathrm{rank}(\boldsymbol{G}) = \mathrm{rank}\ (\boldsymbol{E}_9 - \boldsymbol{A}^{\dagger}\boldsymbol{A})$. Hence, we obtain $\mathrm{Range}\ (\boldsymbol{G}) = \mathrm{Range}(\boldsymbol{E}_9 - \boldsymbol{A}^{\dagger}\boldsymbol{A})$, completing the proof. ∎

The property of the internal force expressed by Eqs. (2.15) and (2.16) has been recognized by many researchers (e.g., [43], [21], [25],[18], and [44]). For example, Salisbury and Craig [43] introduced the concept of grasp matrix, which includes $\boldsymbol{G}^{\mathrm{T}}$ as a submatrix. Expression (2.15) is presented here and proved rigorously because it plays a key role in the following development.

It can be easily shown that any internal force $\hat{\boldsymbol{F}} = [\hat{\boldsymbol{f}}_1^{\mathrm{T}} \quad \hat{\boldsymbol{f}}_2^{\mathrm{T}} \quad \hat{\boldsymbol{f}}_3^{\mathrm{T}}]^{\mathrm{T}}$ given by Eq. (2.15) has the following well known geometric characteristics (see, e.g., [44], [18]). As shown in Fig. 2.5, the load lines of the three fingertip forces $\hat{\boldsymbol{f}}_i$ generally intersect at a point P on plane Q, and the three forces form a closed triangle (force triangle) due to the balance of force and moment. The three degrees of freedom of the internal force can be interpreted as the sum of the two degrees of freedom in the position of the point P on the plane Q, and one degree of freedom in the scale of the force triangle. Therefore, there is one-to-one relation between choosing an internal force and determining both the position of P and the scale of the force triangle. The point P is called the focus of the internal force. Note that when the three load lines are parallel to each other, the point P does not exist. However, the argument developed in this paper is valid by regarding this situation as a limiting case where point P goes to infinity.

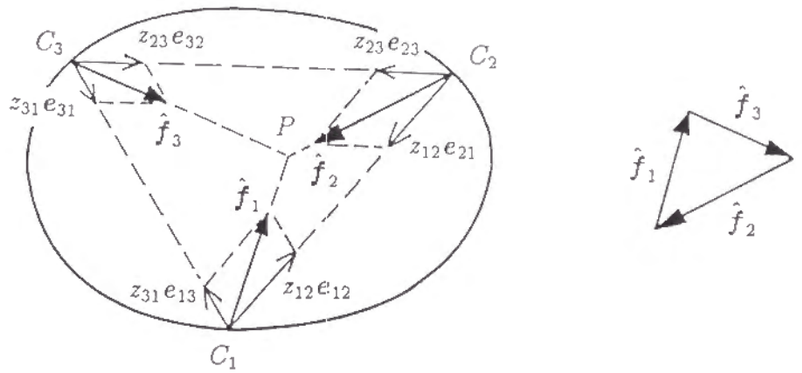

(a) Internal force (b) Force triangle

Fig. 2.5. Internal force and force triangle.

2.4 Grasping Force for Three-Fingered Hands

Based on the result in the previous section, the grasping force is defined and the concept of grasp mode is introduced for three-fingered hands in this section.

Definition 1: A fingertip force $\boldsymbol{F}$ is called a grasping force if the following two conditions are satisfied.

Condition 1:

$$\boldsymbol{A}\boldsymbol{F} = 0 \tag{2.17}$$

Condition 2:

$$\frac{\boldsymbol{f}_i^{\mathrm{T}}\boldsymbol{a}_i}{||\boldsymbol{f}_i||} > \frac{1}{\sqrt{1+\mu_i^2}}, \quad i = 1,2,3 \tag{2.18}$$

where $\boldsymbol{a}_i$ is the inward unit normal vector of the object surface and μ_i is the static friction coefficient at the contact point C_i.

Condition 1 implies that $\boldsymbol{F}$ is an internal force. Condition 2 means that each fingertip force should satisfy the friction constraint. Due to this constraint, the location of point P on plane Q in Fig. 2.5 for grasping force $\boldsymbol{F}$ is also restricted. This restriction will now be analyzed and a condition for the existence of a grasping force will be derived for a given set of three contact points on an object.

Let the position vector of focus P be $\boldsymbol{r}_p$, and

$$\boldsymbol{e}_{pi} \stackrel{\triangle}{=} \frac{\boldsymbol{r}_p - \boldsymbol{r}_i}{||\boldsymbol{r}_p - \boldsymbol{r}_i||}, \quad i = 1,2,3. \tag{2.19}$$

The vector $\boldsymbol{e}_{pi}$ is the unit vector directing from contact point C_i to focus P. In the case of Fig. 2.5, the fingertip force $\hat{\boldsymbol{f}}_i$ and the $\boldsymbol{e}_{pi}$ are in the same direction. However, this does not necessarily hold for all cases. For example, in the case of Fig. 2.6, $\hat{\boldsymbol{f}}_2$ and $\boldsymbol{e}_{p2}$, and $\hat{\boldsymbol{f}}_3$ and $\boldsymbol{e}_{p3}$ are in the opposite direction. Taking this point into consideration, the constraint of Eq. (2.18) can be shown to be equivalent to the following two relations:

$$\boldsymbol{f}_i = \mathrm{sgn}(\boldsymbol{e}_{pi}^{\mathrm{T}}\boldsymbol{a}_i)||\boldsymbol{f}_i||\boldsymbol{e}_{pi} \tag{2.20}$$

$$|\boldsymbol{e}_{pi}^{\mathrm{T}}\boldsymbol{a}_i| > \frac{1}{\sqrt{1+\mu_i^2}}, \quad i = 1,2,3 \tag{2.21}$$

In order to express the state of the internal force described by Eq. (2.15), let

$$\begin{aligned} \boldsymbol{\alpha} &\stackrel{\triangle}{=} [\alpha_1, \alpha_2, \alpha_3] \\ \alpha_i &\stackrel{\triangle}{=} \mathrm{sgn}(\, z_{(i+1)(i+2)}\,), \quad i = 1,2,3 \end{aligned} \tag{2.22}$$

where the subscript $j(=i+1, i+2)$ is interpreted as $(j-3)$ when $j \geq 4$ for notational convenience, and $\mathrm{sgn}(a)$ denotes the sign of a, i.e.,

$$\mathrm{sgn}(a) = \begin{cases} +1, & \text{if } a > 0 \\ \pm 1, & \text{if } a = 0 \\ -1, & \text{if } a < 0 \end{cases} \tag{2.23}$$

Since $\mathrm{sgn}(\, z_{i(i+1)}\,)$ tells whether the grasping force between fingers i and $i+1$ is compression or tension, we can categorize the internal forces by $\boldsymbol{\alpha}$. A fingertip force that satisfies

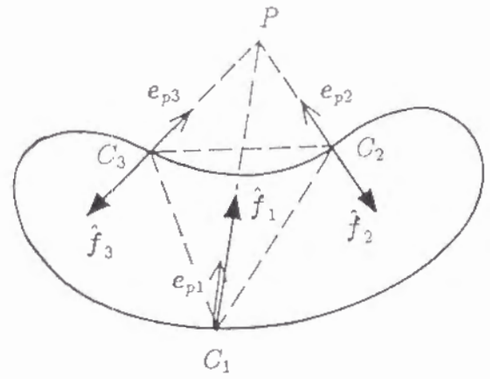

Fig. 2.6. Relation $\hat{f}_i$ and e_{pi}.

Eq. (2.15) will be called the internal force of mode $\boldsymbol{\alpha}$. For example, the internal force in Fig. 2.5 is of mode $[+1,+1,+1]$ and that in Fig. 2.6 is of mode $[-1,+1,+1]$. When $\boldsymbol{F}$ is a grasping force, since this mode is useful for classifying it, $\boldsymbol{\alpha}$ will be called the grasp mode. The variable $\boldsymbol{\alpha}$, and the variables, $\boldsymbol{\beta}$ and $\boldsymbol{\gamma}$, which will be introduced later in this section, will be denoted by the symbols + and − hereafter. For example, $[+1,+1,-1]$ will be expressed as $[+,+,-]$. Figure 2.7 shows the four essentially different grasp modes. For example, the grasp mode in Fig. 2.7(d) is the mode that appears when picking up a plate with a hole by inserting three fingers into the hole and opening them out.

Collecting $\mathrm{sgn}(\boldsymbol{e}_{pi}^{\mathrm{T}}\boldsymbol{a}_i)$, $i = 1,2,3$, which appeared in Eq. (2.20), we define the parameter, $\boldsymbol{\beta}$ by

$$\boldsymbol{\beta} \stackrel{\triangle}{=} [\mathrm{sgn}(\boldsymbol{e}_{p1}^{\mathrm{T}}\boldsymbol{a}_1), \mathrm{sgn}(\boldsymbol{e}_{p2}^{\mathrm{T}}\boldsymbol{a}_2), \mathrm{sgn}(\boldsymbol{e}_{p3}^{\mathrm{T}}\boldsymbol{a}_3)] \tag{2.24}$$

This parameter $\boldsymbol{\beta}$ represents the relation between the location of focus P and the shape of the object. We also define regions *I* through *VII* on plane Q and their code $\boldsymbol{\gamma} = [\gamma_1, \gamma_2, \gamma_3]$ ($\gamma_i = +1$ or -1) as shown in Fig. 2.8. Then for an internal force to be a grasping force, it is necessary for the parameters $\boldsymbol{\alpha}$, $\boldsymbol{\beta}$, and $\boldsymbol{\gamma}$ to satisfy one of the relationships listed in Table 2.1. This can be easily shown by considering the requirements that any internal force should have a focus P (including one at infinity) and that each fingertip force should be in the object's pushing direction. These relationships can further be condensed to the following conditions:

$$\boldsymbol{\beta} = \boldsymbol{\gamma} \ \textit{or} \ -\boldsymbol{\gamma} \tag{2.25}$$

$$\boldsymbol{\alpha} = (\gamma_1 \cdot \gamma_2 \cdot \gamma_3)\boldsymbol{\beta} \tag{2.26}$$

Note that Eq. (2.25) is a condition on the relation between the location of P and the shape of the object with respect to P, and Eq. (2.26) tells the grasp mode realizable under the given location of P and the shape of the object. Relation (2.26) is schematically shown in Fig. 2.9. In the figure, the relation $\boldsymbol{\alpha} = \boldsymbol{\beta}$ should hold if P is in one of the shaded regions

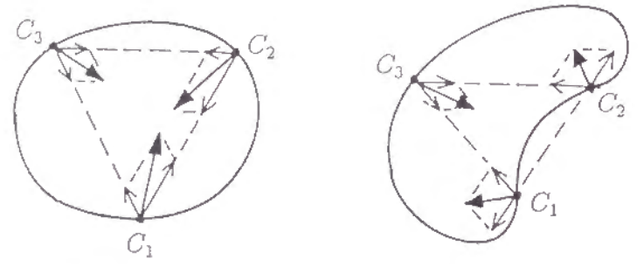

(a) $\alpha = [\,+\;+\;+\,]$

(b) $\alpha = [\,+\;+\;-\,]$

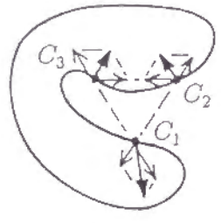

(c) $\alpha = [\,+\;-\;-\,]$

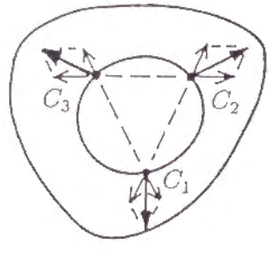

(d) $\alpha = [\,-\;-\;-\,]$

Fig. 2.7. Four grasp modes.

and $\boldsymbol{\alpha} = -\boldsymbol{\beta}$ in other regions. Note also that, due to the introduction of the code of region, $\boldsymbol{\gamma}$ the relationships listed in Table 2.1 have been compactly expressed by Eqs. (2.25) and (2.26).

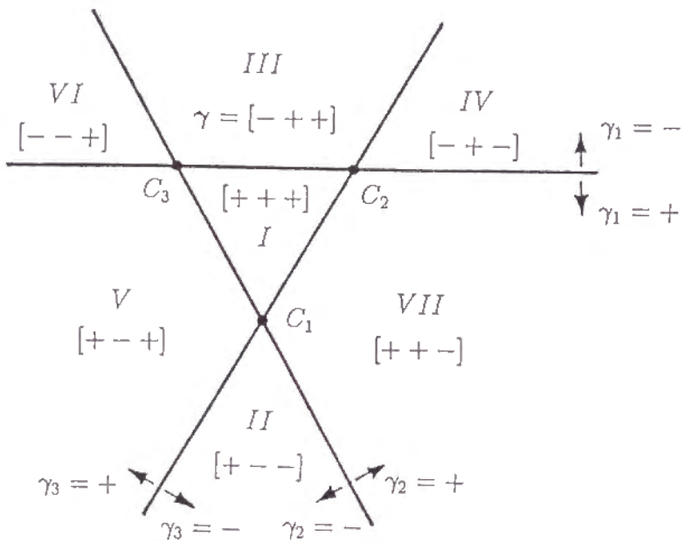

Fig. 2.8. Seven regions on the Plane Q and their codes.

Table 2.1. Relation among α, β, and γ.

Region	γ (Code of Region)	β (Shape of Object)	α (Grasp Mode)
I	$[\,+\;+\;+\,]$	$[\,+\;+\;+\,]$	$[\,+\;+\;+\,]$
		$[\,-\;-\;-\,]$	$[\,-\;-\;-\,]$
II	$[\,+\;-\;-\,]$	$[\,+\;-\;-\,]$	$[\,+\;-\;-\,]$
		$[\,-\;+\;+\,]$	$[\,-\;+\;+\,]$
III	$[\,-\;+\;+\,]$	$[\,-\;+\;+\,]$	$[\,+\;-\;-\,]$
		$[\,+\;-\;-\,]$	$[\,-\;+\;+\,]$
IV	$[\,-\;+\;-\,]$	$[\,-\;+\;-\,]$	$[\,-\;+\;-\,]$
		$[\,+\;-\;+\,]$	$[\,+\;-\;+\,]$
V	$[\,+\;-\;+\,]$	$[\,+\;-\;+\,]$	$[\,-\;+\;-\,]$
		$[\,-\;+\;-\,]$	$[\,+\;-\;+\,]$
VI	$[\,-\;-\;+\,]$	$[\,-\;-\;+\,]$	$[\,-\;-\;+\,]$
		$[\,+\;+\;-\,]$	$[\,+\;+\;-\,]$
VII	$[\,+\;+\;-\,]$	$[\,+\;+\;-\,]$	$[\,-\;-\;+\,]$
		$[\,-\;-\;+\,]$	$[\,+\;+\;-\,]$

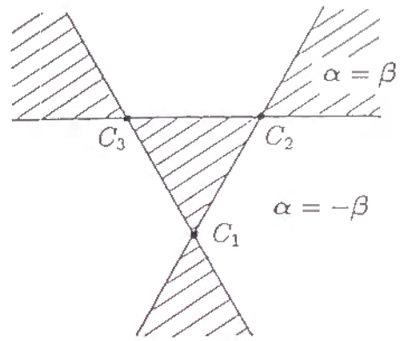

Fig. 2.9. Relation (2.26).

Summarizing the above argument, we have:

Proposition 2: Suppose that the grasping positions $\boldsymbol{r}_i$, the inward normal directions $\boldsymbol{a}_i$, and the static friction coefficients μ_i are given. Then a grasping force can exist if there is a focus P satisfying the following two conditions:

Condition 1: $\boldsymbol{a}_i$, $\boldsymbol{e}_{pi}$, and μ_i satisfy the constraint of Eq. (2.21).

Condition 2: $\boldsymbol{\beta}$ and $\boldsymbol{\gamma}$ satisfy the condition of Eq. (2.25).

By these two conditions, we can obtain the locations of realizable focus P and the realizable grasp modes from the shape of the object, the grasping position, and the friction coefficient of the surface. Note that there are cases where only one grasp mode is possible, where two or more modes are possible, and where no grasping force exists.

Some examples are given in Fig. 2.10. In the figure it is assumed that the object is a cylinder with its axis perpendicular to plane Q, so that vectors a_i are in plane Q. It is also assumed that $\mu_i = 0.4$. Figure 2.10(a) and (b) shows the cases where there are only one mode $\boldsymbol{\alpha} = [+++]$ and $\boldsymbol{\alpha} = [-++]$, respectively. These modes are obtained by checking the conditions for Proposition 2 and using Eq. (2.26). In the case of Fig. 2.10(b), for example, by condition 1 of Proposition 2 the focus P can only exist in the shaded area in Region II ($\boldsymbol{\gamma} = [+--]$), and from Eq. (2.24) we have, $\boldsymbol{\beta} = [-++]$. Hence, condition 2 of Proposition 2 is satisfied and the grasp mode is $\boldsymbol{\alpha} = [-++]$ from Eq. (2.26). Figure 2.10(c) shows the case where two modes $\boldsymbol{\alpha} = [+++]$ and $\boldsymbol{\alpha} = [-++]$ are realizable. Figure 2.10(d) shows the case where no grasping force exists. Note that, in the case of Fig. 2.10(d), by condition 1 of Proposition 2 the focus P can only exist in the shaded area in Region III ($\boldsymbol{\gamma} = [-++]$) and from Eq. (2.24) we have $\boldsymbol{\beta} = [+++]$ for any P in the shaded area, implying that condition 2 does not hold. When there is more than one realizable mode, some additional consideration for selecting one mode will be necessary. This would be a topic for further study.

Once mode α(i.e., the signs of z_{ij}) is determined using Eq. (2.15) for the internal force, an expression of the grasping force $\boldsymbol{F}_g \triangleq [\boldsymbol{f}_{g1}^{\mathrm{T}} \;\; \boldsymbol{f}_{g2}^{\mathrm{T}} \;\; \boldsymbol{f}_{g3}^{\mathrm{T}}] \in \mathrm{R}^9$ is given by

$$\boldsymbol{F}_g = \boldsymbol{B}_g \boldsymbol{h}_g \tag{2.27}$$

where

$$\boldsymbol{B}_g \triangleq \begin{bmatrix} 0 & \hat{\boldsymbol{e}}_{13} & \hat{\boldsymbol{e}}_{12} \\ \hat{\boldsymbol{e}}_{23} & 0 & \hat{\boldsymbol{e}}_{21} \\ \hat{\boldsymbol{e}}_{32} & \hat{\boldsymbol{e}}_{31} & 0 \end{bmatrix} \tag{2.28}$$

$$\hat{\boldsymbol{e}}_{i(i+1)} \triangleq \alpha_{i+2} \cdot \boldsymbol{e}_{i(i+1)}, \quad i = 1, 2, 3 \tag{2.29}$$

$$\hat{\boldsymbol{e}}_{i(i+2)} \triangleq -\hat{\boldsymbol{e}}_{(i+2)i}, \quad i = 1, 2, 3 \tag{2.30}$$

and $\boldsymbol{h}_g$ is an unknown vector satisfying

$$\boldsymbol{h}_g \triangleq [h_{g1} \;\; h_{g2} \;\; h_{g3}]^{\mathrm{T}} \;\; h_{gj} \geq 0. \tag{2.31}$$

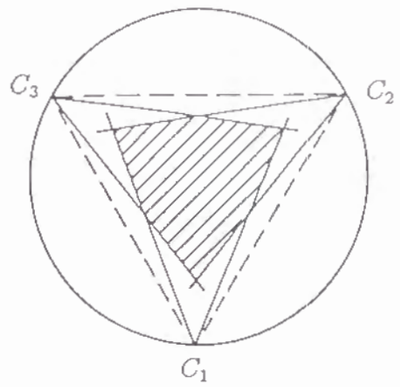

(a) Only $\alpha = [\,+\,+\,+\,]$ is realizable.

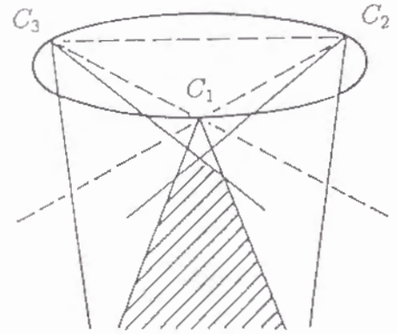

(b) Only $\alpha = [\,-\,+\,+\,]$ in Region II is realizable.

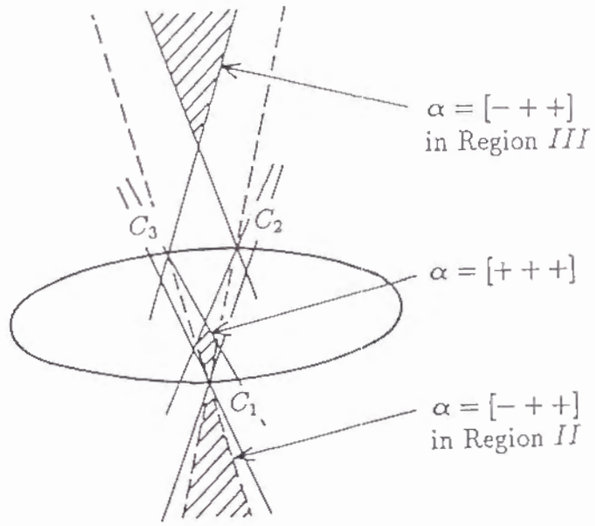

(c) $\alpha = [\,+\,+\,+\,]$ and $\alpha = [\,-\,+\,+\,]$ in Region II and III are realizable.

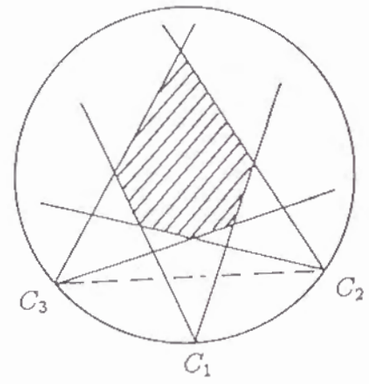

(d) There is no realizable mode.

Fig. 2.10. Example of realizable mode of grasping force. ////: Location of P for realizable grasping force.

The vector $\hat{\boldsymbol{e}}_{ij}$ given by Eqs. (2.29) and (2.30) is the unit vector for the grasping force component at C_i working between fingers i and j. Note that taking mode $\boldsymbol{\alpha}$ into consideration in defining $\hat{\boldsymbol{e}}_{ij}$ makes it possible to assume $h_{gi} \geq 0$. Also note that the condition of Eq. (2.21) must still be satisfied for the existence of the grasping force.

2.5 Manipulating Force for Three-Fingered Hands

The manipulating force is defined for three-fingered hands, and its relation to the grasping force introduced in the previous section is discussed in this section.

Definition 2: For a given resultant force $\boldsymbol{T}$, the fingertip force $\boldsymbol{F} = [\boldsymbol{f}_1^{\mathrm{T}}\ \boldsymbol{f}_2^{\mathrm{T}}\ \boldsymbol{f}_3^{\mathrm{T}}]^{\mathrm{T}}$ is called the manipulating force of mode $\boldsymbol{\alpha}$ if $\boldsymbol{F}$ satisfies the following three conditions:

Condition 1:

$$\boldsymbol{T} = \boldsymbol{A}\boldsymbol{F} \tag{2.32}$$

Condition 2:

$$\boldsymbol{f}_i^{\mathrm{T}}\hat{\boldsymbol{e}}_{ij} \geq 0, \quad i = 1,2,3, j = (i+1),(i+2) \tag{2.33}$$

Condition3:

$$(\boldsymbol{f}_i^{\mathrm{T}}\hat{\boldsymbol{e}}_{i(i+1)})(\boldsymbol{f}_{i+1}^{\mathrm{T}}\hat{\boldsymbol{e}}_{(i+1)i}) = 0, i = 1,2,3. \tag{2.34}$$

Note that the $\hat{\boldsymbol{e}}_{ij}$'s are defined by Eqs. (2.29) and (2.30), and so are dependent on mode $\boldsymbol{\alpha}$. Condition 1 means that $\boldsymbol{F}$ produces the resultant force $\boldsymbol{T}$. Condition 2 implies that the manipulating force is not in the inverse direction of the grasping force. Condition 3 means that $\boldsymbol{F}$ contains no force component that results in compression or tension along the line joining C_1 and C_2, C_2 and C_3, or C_3 and C_1. In other words, $\boldsymbol{F}$ is orthogonal to the grasping force component.

In order to give an explicit expression for the manipulating force, we first introduce the following matrix:

$$\boldsymbol{B}_m \triangleq \begin{bmatrix} 0 & (1-k_2)\bar{\boldsymbol{e}}_{13} & k_3\bar{\boldsymbol{e}}_{12} & \bar{\boldsymbol{e}}_{10} & 0 & 0 \\ k_1\bar{\boldsymbol{e}}_{23} & 0 & (1-k_3)\bar{\boldsymbol{e}}_{21} & 0 & \bar{\boldsymbol{e}}_{20} & 0 \\ (1-k_1)\bar{\boldsymbol{e}}_{32} & k_2\bar{\boldsymbol{e}}_{31} & 0 & 0 & 0 & \bar{\boldsymbol{e}}_{30} \end{bmatrix} \tag{2.35}$$

where

$$\bar{\boldsymbol{e}}_{i0} = \frac{\hat{\boldsymbol{e}}_{i(i+1)} \times \hat{\boldsymbol{e}}_{i(i+2)}}{\|\hat{\boldsymbol{e}}_{i(i+1)} \times \hat{\boldsymbol{e}}_{i(i+2)}\|} \tag{2.36}$$

$$\bar{\boldsymbol{e}}_{i(i+1)} = \bar{\boldsymbol{e}}_{i(i+2)} \times \bar{\boldsymbol{e}}_{i0} \tag{2.37}$$

$$\bar{\boldsymbol{e}}_{i(i+2)} = \bar{\boldsymbol{e}}_{i0} \times \bar{\boldsymbol{e}}_{i(i+1)} \tag{2.38}$$

and k_1, k_2, and k_3 are parameters that can take 1 or 0. The vectors $\bar{\boldsymbol{e}}_{ij}$ given by Eqs. (2.36) $\sim$ (2.38) play the role of basis vectors for the manipulating force.

Figure 2.11 shows the vectors $\hat{\boldsymbol{e}}_{ij}$ and $\bar{\boldsymbol{e}}_{ij}$ schematically for a typical case. Note that $\bar{\boldsymbol{e}}_{i0}$ is normal to the grasp plane Q and

$$\bar{\boldsymbol{e}}_{ij}^{\mathrm{T}}\hat{\boldsymbol{e}}_{ij} \geq 0, \quad i = 1,2,3, j = (i+1),(i+2). \tag{2.39}$$

The matrix $\boldsymbol{B}_m$ is a function of $\boldsymbol{\alpha}$ and $\boldsymbol{k} = [k_1\ k_2\ k_3]^{\mathrm{T}} \in R^3$. The parameter $k_1(k_2, k_3)$ determines which of the two vectors $\{\bar{\boldsymbol{e}}_{23}, \bar{\boldsymbol{e}}_{32}\}$, ($\{\ \bar{\boldsymbol{e}}_{31}, \bar{\boldsymbol{e}}_{13}\ \}$), ($\{\ \bar{\boldsymbol{e}}_{12}, \bar{\boldsymbol{e}}_{21}\ \}$) is included in the matrix $\boldsymbol{B}_m$. With these preparations, we can give the following proposition.

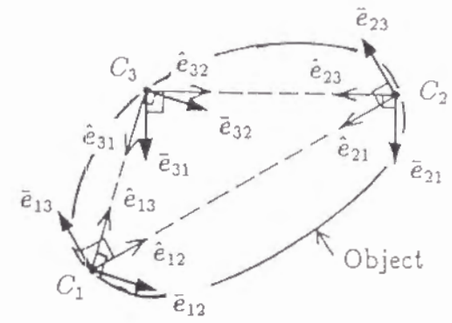

Fig. 2.11. Relation between $\hat{e}_{ij}$ and $\bar{e}_{ij}$ ($\bar{e}_{i0}$: upward and normal to the plane Q).

Proposition 3: A fingertip force $\boldsymbol{F}$, which produces the resultant force $\boldsymbol{T}$, is a manipulating force of mode $\boldsymbol{\alpha}$ if it satisfies

$$\boldsymbol{F} = \boldsymbol{B}_m\boldsymbol{h}_m \tag{2.40}$$

for some $\boldsymbol{\alpha}$, $\boldsymbol{k}$, and $\boldsymbol{h}_m \triangleq [h_{m1}\ h_{m2}\ \cdots h_{m6}]^{\mathrm{T}}$ with $h_{mi} \geq 0, i = 1,2,3$.

Proof: Suppose a fingertip force $\bar{\boldsymbol{F}} \triangleq [\bar{\boldsymbol{f}}_1^{\mathrm{T}}\ \bar{\boldsymbol{f}}_2^{\mathrm{T}}\ \bar{\boldsymbol{f}}_3^{\mathrm{T}}]^{\mathrm{T}}$ satisfies $\boldsymbol{T} = \boldsymbol{A}\bar{\boldsymbol{F}}$ and Eq. (2.40), i.e.,

$$\begin{aligned} \bar{\boldsymbol{f}}_1 &\triangleq k_3h_{m3}\bar{\boldsymbol{e}}_{12} + (1-k_2)h_{m2}\bar{\boldsymbol{e}}_{13} + h_{m4}\bar{\boldsymbol{e}}_{10} \\ \bar{\boldsymbol{f}}_2 &\triangleq k_1h_{m1}\bar{\boldsymbol{e}}_{23} + (1-k_3)h_{m3}\bar{\boldsymbol{e}}_{21} + h_{m5}\bar{\boldsymbol{e}}_{20} \\ \bar{\boldsymbol{f}}_3 &\triangleq k_2h_{m2}\bar{\boldsymbol{e}}_{31} + (1-k_1)h_{m1}\bar{\boldsymbol{e}}_{32} + h_{m6}\bar{\boldsymbol{e}}_{30} \end{aligned} \tag{2.41}$$

It is then enough to show that these $\bar{\boldsymbol{f}}_i$ satisfy Eqs. (2.33) and (2.34). From Eqs. (2.36)$\sim$(2.38) we have

$$\hat{\boldsymbol{e}}_{i(i+1)}^{\mathrm{T}}\bar{\boldsymbol{e}}_{i(i+2)} = \hat{\boldsymbol{e}}_{i(i+1)}^{\mathrm{T}}\bar{\boldsymbol{e}}_{i0} = 0 \tag{2.42}$$

$$\hat{\boldsymbol{e}}_{i(i+2)}^{\mathrm{T}}\bar{\boldsymbol{e}}_{i(i+1)} = \hat{\boldsymbol{e}}_{i(i+2)}^{\mathrm{T}}\bar{\boldsymbol{e}}_{i0} = 0. \tag{2.43}$$

Therefore, from Eqs. (2.41), (2.42), (2.43), and (2.39)

$$\bar{\boldsymbol{f}}_1^{\mathrm{T}}\hat{\boldsymbol{e}}_{12} = k_3h_{m3}\bar{\boldsymbol{e}}_{12}^{\mathrm{T}}\hat{\boldsymbol{e}}_{12} \geq 0 \tag{2.44}$$

$$\bar{\boldsymbol{f}}_1^{\mathrm{T}}\hat{\boldsymbol{e}}_{13} = (1-k_2)h_{m3}\bar{\boldsymbol{e}}_{13}^{\mathrm{T}}\hat{\boldsymbol{e}}_{13} \geq 0 \tag{2.45}$$

and

$$\begin{aligned} (\bar{\boldsymbol{f}}_1^{\mathrm{T}}\hat{\boldsymbol{e}}_{12})(\bar{\boldsymbol{f}}_2^{\mathrm{T}}\hat{\boldsymbol{e}}_{21}) &= k_3(1-k_3)h_{m3}^2(\bar{\boldsymbol{e}}_{12}^{\mathrm{T}}\hat{\boldsymbol{e}}_{12})(\bar{\boldsymbol{e}}_{21}^{\mathrm{T}}\hat{\boldsymbol{e}}_{21}) \\ &= 0. \end{aligned} \tag{2.46}$$

Hence, Eqs. (2.33) and (2.34) for i = 1 are satisfied. It can also be shown by similar arguments that Eqs. (2.33) and (2.34) for i = 2 and 3 are satisfied by $\bar{\boldsymbol{F}}$.

The manipulating force will be expressed by $F_m \triangleq [f_{m1}^{\mathrm{T}}\ f_{m2}^{\mathrm{T}}\ f_{m3}^{\mathrm{T}}]^{\mathrm{T}}$ hereafter. From Proposition 3 a manipulating force F_m of mode α, which produces the resultant force T, satisfies

$$T = AF_m = AB_m h_m. \tag{2.47}$$

Hence, to obtain F_m for a given T, we first calculate $\hat{h}_m \triangleq [\hat{h}_{m1}\ \hat{h}_{m2}\ \cdots \hat{h}_{m6}]^{\mathrm{T}} \in \mathrm{R}^6$ from

$$\hat{h}_m = (AB_m)^{-1}T \tag{2.48}$$

for eight different combinations of k_1, k_2, and $k_3 (k_1, k_2, k_3 = 1$ or 0). We then select the one for which $\hat{h}_{mi} \geq 0$ $(i = 1, 2, 3)$ as the vector h_m. Then $F_m = B_m h_m$ with the above selected values h_m and $k = [k_1\ k_2\ k_3]^{\mathrm{T}}$ is the desired manipulating force. The value k which satisfies $\hat{h}_{mi} \geq 0$ $(i = 1, 2, 3)$ is uniquely determined except for degenerate cases where at least one of the three $\hat{h}_{mi}$ is zero.

A relation between the manipulating and grasping forces is given by the following proposition.

Proposition 4: For any given manipulating force F_m of mode α,

$$||F_m|| \leq ||F_m + F_g|| \tag{2.49}$$

for any grasping force F_g of the same mode α.

Proof: From Eqs. (2.27), (2.28), (2.31), (2.33), and (2.40)

$$F_m^{\mathrm{T}} F_g = \sum_{i=1}^{3} (f_{mi}^{\mathrm{T}} f_{gi}) \geq 0. \tag{2.50}$$

Therefore,

$$\begin{aligned} ||F_m + F_g||^2 &= ||F_m||^2 + 2F_m^{\mathrm{T}} F_g + ||F_g||^2 \\ &\geq ||F_m||^2. \end{aligned} \tag{2.51}$$

2.6 Decomposition of Fingertip Force into Manipulating and Grasping Forces

A method for decomposing a given fingertip force into a manipulating force and a grasping force for three-fingered hands will be given.

Suppose that r_i, a_i, μ_i (i= 1, 2, 3), and a fingertip force F are given, and that this F can be expressed as a sum of manipulating force F_m and a grasping force F_g for some mode α. Then

$$F = F_g + F_m = BH \tag{2.52}$$

where

$$B \triangleq [B_g\ \ B_m] \tag{2.53}$$

$$H \triangleq [h_g^{\mathrm{T}}\ \ h_m^{\mathrm{T}}]^{\mathrm{T}} \tag{2.54}$$

and B_g and B_m are given by Eqs. (2.28) and (2.35). An algorithm for decomposition of F is as follows.

1) Find the set of all realizable modes α from r_i, a_i, μ_i (i= 1,2,3).

2) Pick up one realizable mode α from the set obtained in 1). Calculate $\hat{H} \triangleq [h_g^{\mathrm{T}}\ \ \hat{h}_m^{\mathrm{T}}]^{\mathrm{T}}$ by

$$\hat{H} = B^{-1}F \tag{2.55}$$

for the eight different values of k.

3) Select k for which $h_{gi} \geq 0$ $(i = 1, 2, 3)$ and $\hat{h}_{mi} \geq 0$ $(i = 1, 2, 3)$. Let $\hat{H}$ for this k be H and calculate $F_g = B_g h_g$. Then, if this F_g satisfies the friction constraint, the pair $\{\ F_m = B_m h_m,\ F_g = B_g h_g\ \}$ is a decomposition of F.

4) Repeat steps 2 and 3 until all the realizable modes are checked.

Note that the decomposition may not be unique because of the existence of multiple grasp modes. Also, there are cases where such decomposition does not exist. Note also that whenever a fingertip force F can be decomposed into F_m and F_g, $||F_m|| \leq ||F||$ from Proposition 4.

A simple example of decomposition will be given in the following. The object is a cylinder of radius 5 with its axis coinciding with the z axis of the object coordinate frame Σ_0. Suppose that the three contact points and the fingertip forces are given by

$$\begin{aligned} r_1 &= [0\ \ -5\ \ 0]^{\mathrm{T}} & f_1 &= [1\ \ 8\ \ 0]^{\mathrm{T}} \\ r_2 &= [5\sqrt{3}/2\ \ 5/2\ \ 0] & f_2 &= [-3\ \ -2\ \ 0]^{\mathrm{T}} \\ r_3 &= [-5\sqrt{3}/2\ \ 5/2\ \ 0] & f_3 &= [6\ \ -2\ \ 0]^{\mathrm{T}}. \end{aligned} \tag{2.56}$$

Therefore, the plane Q is given by the x-y plane of Σ_0, and

$$\begin{aligned} a1 &= [0\ \ 1\ \ 0]^{\mathrm{T}} \\ a2 &= [-\sqrt{3}/2\ \ -1/2\ \ 0]^{\mathrm{T}} \\ a3 &= [\sqrt{3}/2\ \ -1/2\ \ 0]^{\mathrm{T}}. \end{aligned} \tag{2.57}$$

Also suppose that $\mu_i = 0.4$, $i = 1, 2, 3$. Then it can be easily shown by using Proposition 2 and Eq. (2.22) that there is only one following manipulating and grasping forces of mode

[+ + +]:

$$\begin{aligned} \boldsymbol{f}_{m1} &= [7/4 \quad 4-3\sqrt{3}/4 \quad 0]^{\mathrm{T}} \\ \boldsymbol{f}_{m2} &= [0 \quad 0 \quad 0]^{\mathrm{T}} \\ \boldsymbol{f}_{m3} &= [9/4 \quad 3\sqrt{3}/4 \quad 0]^{\mathrm{T}} \\ \boldsymbol{f}_{g1} &= [-3/4 \quad 4+3\sqrt{3}/4 \quad 0]^{\mathrm{T}} \\ \boldsymbol{f}_{g2} &= [-3 \quad -2 \quad 0]^{\mathrm{T}} \\ \boldsymbol{f}_{g3} &= [15/4 \quad -2-3\sqrt{3}/4 \quad 0]^{\mathrm{T}} \end{aligned} \tag{2.58}$$

This is shown in Fig. 2.12. It can be easily seen that these forces satisfy Definitions 1 and 2.

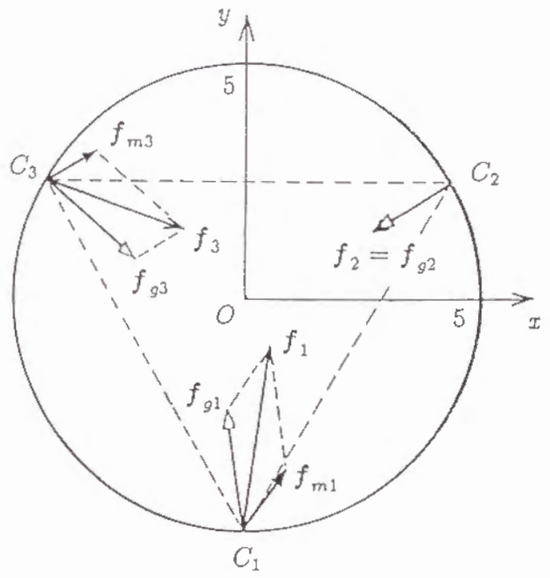

Fig. 2.12. Example of decomposition of fingertip force into manipulating and grasping forces (the scale of forces is × 0.5).

In the following section, it will be shown that similar discussions can also be presented for two other types of hands, i.e., two-fingered hands with planar motion and four-fingered hands.

2.7 Other Types of Hands

2.7.1 Two-Fingered Hands with Planar Motion

We consider a two-fingered hand grasping an object as shown in Fig. 2.13. Assume that each finger has two degrees of freedom and can move its fingertip in a plane. Assume also the two fingertips make point contacts with friction with a grasped object. Hence, the hand can force the object to make a planar motion. Similar to the case of three-fingered hands, we consider an object coordinate frame $\Sigma_O(\mathrm{O}-xy)$. Let $\boldsymbol{f}_i = [f_{ix} \quad f_{iy}]^{\mathrm{T}} \in \mathrm{R}^2$ denote the force applied by the i-th finger $(i = 1, 2)$ on the object in the $x-y$ plane, and let $\boldsymbol{r}_i = [r_{ix} \quad r_{iy}]^{\mathrm{T}} \in \mathrm{R}^2$ denote the position of contact point C_i, of the i-th finger. We assume that no force works in the direction normal to the plane $x-y$. The resultant force $\boldsymbol{f} \in \mathrm{R}^2$ and the resultant moment $n \in \mathrm{R}^1$ due to $\{f_1, f_2\}$ are given by

$$\boldsymbol{f} = \sum_{i=1}^{2} \boldsymbol{f}_i \tag{2.59}$$

$$n = \sum_{i=1}^{2} (r_{ix} f_{iy} - r_{iy} f_{ix}). \tag{2.60}$$

Then the relation between the total fingertip force $\boldsymbol{F} = [\boldsymbol{f}_1^{\mathrm{T}} \quad \boldsymbol{f}_2^{\mathrm{T}}]^{\mathrm{T}} \in \mathrm{R}^4$ and the total resultant force $\boldsymbol{T} = [f_x, f_y, n]^{\mathrm{T}} \in \mathrm{R}^3$ is expressed as

$$\boldsymbol{T} = \boldsymbol{A}\boldsymbol{F} \tag{2.61}$$

where

$$\boldsymbol{A} = \left[\begin{array}{cc|cc} \boldsymbol{E}_2 & & \boldsymbol{E}_2 & \\ \hline -r_{1y} & r_{1x} & -r_{2y} & r_{2x} \end{array}\right] \in \mathrm{R}^{3\times 4} \tag{2.62}$$

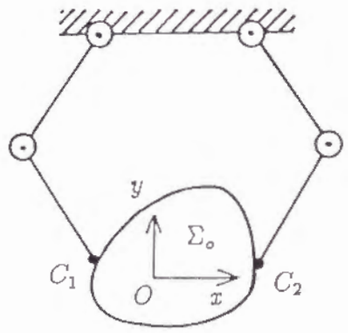

Fig. 2.13. Two-fingered hand with planar motion.

By a similar argument to that in the preceding sections, we can show that the grasping force and the manipulating force are given as follows. Let $\boldsymbol{e}_{12} \in \mathrm{R}^2$ denote the unit vector

directing from C_1 to C_2 and let $\boldsymbol{e}_{21} = -\boldsymbol{e}_{12}$. Then the grasping force $\boldsymbol{F}_g = [\boldsymbol{f}_{g1}^{\mathrm{T}}, \boldsymbol{f}_{g2}^{\mathrm{T}}]^{\mathrm{T}} \in \mathrm{R}^2$ is given by

$$\boldsymbol{F}_g = \boldsymbol{B}_g \boldsymbol{h}_g \tag{2.63}$$

where h_g is an arbitrary scalar satisfying $h_g \geq 0$, and

$$\boldsymbol{B}_g = \begin{bmatrix} \hat{\boldsymbol{e}}_{12} \\ \hat{\boldsymbol{e}}_{21} \end{bmatrix}. \tag{2.64}$$

Here, $\hat{\boldsymbol{e}}_{12} = \alpha \boldsymbol{e}_{l2}$, and α is a scalar taking a value of $+1$ or -1. There are two grasp modes represented by $\alpha = +1$ and $\alpha = -1$, which are shown in Fig. 2.14. Note that the grasping force must also satisfy the friction constraint similar to Eq. (2.18) imposing a restriction on the shape of object and the location of contact points on the object. Let $\hat{\boldsymbol{e}}_{12} = [\hat{e}_{12x}, \hat{e}_{12y}]^{\mathrm{T}}$, then the manipulating force $\boldsymbol{F}_m \in \mathrm{R}^4$ is given by

$$\boldsymbol{F}_m = \boldsymbol{B}_m \boldsymbol{h}_m \tag{2.65}$$

where

$$\boldsymbol{B}_m = \begin{bmatrix} k\hat{\boldsymbol{e}}_{12} & \bar{\boldsymbol{e}}_{10} & \boldsymbol{0} \\ (1-k)\hat{\boldsymbol{e}}_{21} & \boldsymbol{0} & \bar{\boldsymbol{e}}_{20} \end{bmatrix} \in \mathrm{R}^{4\times 3} \tag{2.66}$$

$$\bar{\boldsymbol{e}}_{10} = [-\hat{e}_{12y}, \hat{e}_{12x}]^{\mathrm{T}}, \quad \bar{\boldsymbol{e}}_{20} = -\bar{\boldsymbol{e}}_{10} \tag{2.67}$$

and $\boldsymbol{h}_m = [h_{m1} \;\; h_{m2} \;\; h_{m3}]^{\mathrm{T}}$ with $h_{m1} \geq 0$. Unit vectors $\bar{\boldsymbol{e}}_{10}$ and $\bar{\boldsymbol{e}}_{20}$ are also shown in Fig. 2.14. Using Eqs. (2.63) and (2.65) we can decompose a total fingertip force into the grasping and manipulating forces as in Section 2.6. For example, consider the case shown in Fig. 2.15 where

$$\begin{aligned} &\boldsymbol{r}_1 = [-2 \;\; 0]^{\mathrm{T}} \quad \boldsymbol{r}_2 = [2 \;\; 0]^{\mathrm{T}} \\ &\boldsymbol{a}_1 = [1 \;\; 0]^{\mathrm{T}} \quad \boldsymbol{a}_2 = [-1 \;\; 0]^{\mathrm{T}} \\ &\mu_1 = \mu_2 = 0.6. \end{aligned} \tag{2.68}$$

Then the fingertip force given by

$$\boldsymbol{f}_1 = [1.5 \;\; -0.7]^{\mathrm{T}} \quad \boldsymbol{f}_2 = [-1 \;\; 0.5]^{\mathrm{T}} \tag{2.69}$$

is decomposed into

$$\begin{aligned} &\boldsymbol{f}_{g1} = [1 \;\; 0]^{\mathrm{T}} \quad &&\boldsymbol{f}_{g2} = [-1 \;\; 0]^{\mathrm{T}} \\ &\boldsymbol{f}_{m1} = [0.5 \;\; -0.7]^{\mathrm{T}} \quad &&\boldsymbol{f}_{m2} = [0 \;\; 0.5]^{\mathrm{T}} \end{aligned} \tag{2.70}$$

This decomposition is also shown in Fig. 2.15.

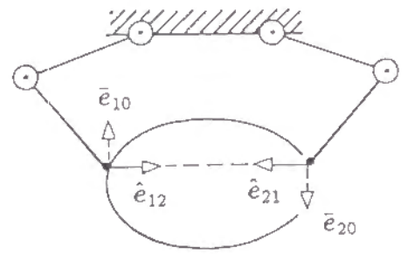

(a) $\alpha = +1$

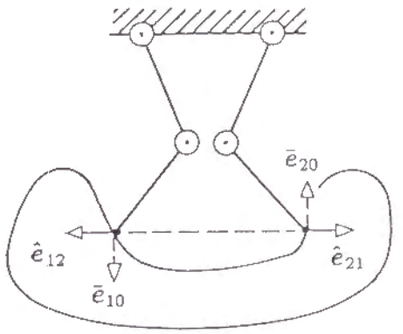

(b) $\alpha = -1$

Fig. 2.14. Grasp mode of two-fingered hands with planar motion.

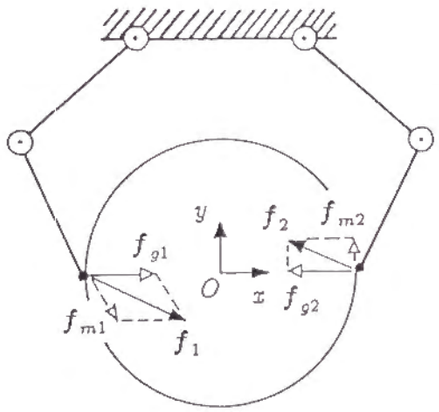

Fig. 2.15. Example of decomposition of fingertip force into manipulating and grasping forces.

Note that a similar argument can also be developed for two-fingered hands with linear motion treated in Section 2.2, and it can be shown that there are two grasp modes corresponding to those in Fig. 2.14.

2.7.2 Four-Fingered Hands

We can define the grasping and manipulating forces also for four-fingered hands as shown in Fig. 2.16. Since the arguments are quite similar to those for three-fingered hands, we will just give the expressions of these forces corresponding to Eqs. (2.27) and (2.40).

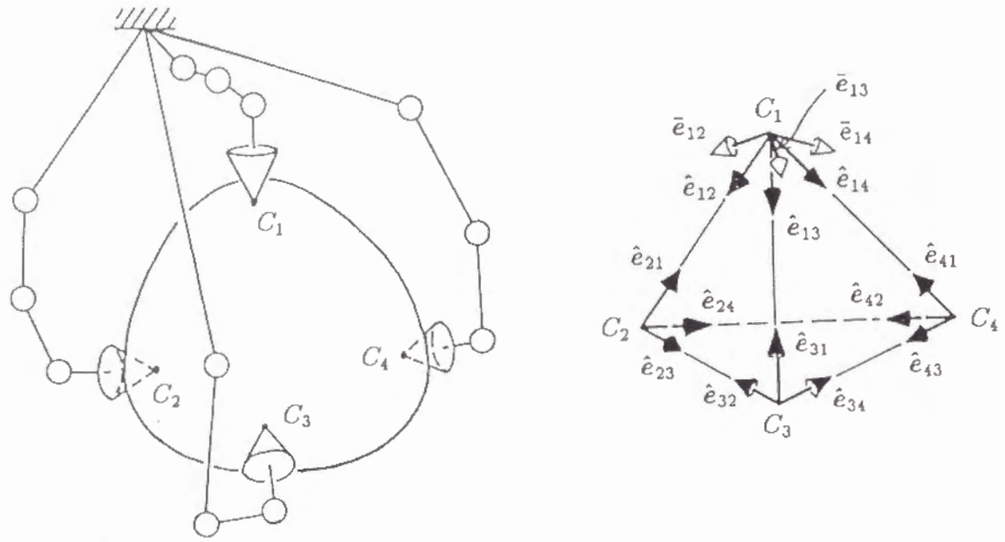

(a) Hand and an object

(b) Unit vectors $\hat{e}_{ij}$ for grasping force and $\bar{e}_{ij}$ for manipulating force ($\bar{e}_{2j}$,$\bar{e}_{3j}$,$\bar{e}_{4j}$ are not shown)

Fig. 2.16. Four-fingered hands.

Let $\boldsymbol{e}_{ij} \in \mathrm{R}^3$ denote the unit vector directing from the i-th contact point C_i to the j-th contact point C_j, $i, j = 1, 2, 3, 4$; $i \neq j$. Also let $\hat{\boldsymbol{e}}_{ij} = z_{ij}\boldsymbol{e}_{ij}$, where $z_{ij} \in \mathrm{R}^1$ satisfies $z_{ij} = z_{ji}$, and $\boldsymbol{\alpha} = [\mathrm{sgn}(z_{23}), \mathrm{sgn}(z_{13}), \mathrm{sgn}(z_{12}), \mathrm{sgn}(z_{14}), \mathrm{sgn}(z_{24}), \mathrm{sgn}(z_{34})] \in \mathrm{R}^6$ represents the grasp mode. Then the grasping force $\boldsymbol{F}_g = [\boldsymbol{f}_{g1}^{\mathrm{T}} \ \boldsymbol{f}_{g2}^{\mathrm{T}} \ \boldsymbol{f}_{g3}^{\mathrm{T}} \ \boldsymbol{f}_{g4}^{\mathrm{T}}]^{\mathrm{T}} \in \mathrm{R}^{12}$ is given by

$$\boldsymbol{F}_g = B_g \boldsymbol{h}_g \tag{2.71}$$

where

$$\boldsymbol{h}_g = [h_{g1} \cdots h_{g6}]^{\mathrm{T}} \in \mathrm{R}^6, \quad h_{gi} \geq 0, i = 1, 2, \cdots, 6 \tag{2.72}$$

$$B_g = \begin{bmatrix} 0 & \hat{e}_{13} & \hat{e}_{12} & \hat{e}_{14} & 0 & 0 \\ \hat{e}_{23} & 0 & \hat{e}_{21} & 0 & \hat{e}_{24} & 0 \\ \hat{e}_{32} & \hat{e}_{31} & 0 & 0 & 0 & \hat{e}_{34} \\ 0 & 0 & 0 & \hat{e}_{41} & \hat{e}_{42} & \hat{e}_{43} \end{bmatrix}. \tag{2.73}$$

Note that the essential degree of arbitrariness of the internal force (or grasping force) is six in the present case because we are supposed to adjust the six-dimensional resultant force vector $\boldsymbol{T}$ by using the twelve-dimensional fingertip force vector $\boldsymbol{F}$. In Eq. (2.73), the expression of the grasping force, this arbitrariness is represented by the six pairs $\{\hat{e}_{ij}, \hat{e}_{ji}\}$ of unit force vectors along the six edges of the tetrahedron formed by the four contact points C_i as shown in Fig. 2.16(b) by black arrows. On the other hand, the manipulating force is given by

$$\boldsymbol{F}_m = B_m \boldsymbol{h}_m \tag{2.74}$$

where

$$\boldsymbol{h}_m = [h_{m1} \cdots h_{m6}]^{\mathrm{T}} \in \mathrm{R}^6, \quad h_{mi} \geq 0, \ i = 1, 2, \ldots, 6 \tag{2.75}$$

$$B_m = \begin{bmatrix} 0 & (1-k_2)\bar{e}_{13} & k_3\bar{e}_{12} & k_4\bar{e}_{14} & 0 & 0 \\ k_1\bar{e}_{23} & 0 & (1-k_3)\bar{e}_{21} & 0 & k_5\bar{e}_{24} & 0 \\ (1-k_1)\bar{e}_{32} & k_2\bar{e}_{31} & 0 & 0 & 0 & k_6\bar{e}_{34} \\ 0 & 0 & 0 & (1-k_4)\bar{e}_{41} & (1-k_5)\bar{e}_{42} & (1-k_6)\bar{e}_{43} \end{bmatrix} \tag{2.76}$$

and $\hat{\boldsymbol{e}}_{ij}$ is the unit vector normal to the plane including the three contact points other than C_j and satisfies $\bar{\boldsymbol{e}}_{ij}^{\mathrm{T}}\hat{\boldsymbol{e}}_{ij} > 0$. An example of the set $\bar{\boldsymbol{e}}_{ij}$ is shown by white arrows in Fig. 2.16(b) for $i = 1$. Note that, for example, $\bar{\boldsymbol{e}}_{14}$ is perpendicular to $\hat{\boldsymbol{e}}_{12}$,$\hat{\boldsymbol{e}}_{23}$ and $\hat{\boldsymbol{e}}_{31}$, which are unit vectors for grasping force components between C_1 and C_2, C_2 and C_3, and C_3 and C_1. Hence, when the location of contact points C_i ($i = 1, 2, 3, 4$), friction coefficients μ_i ($i = 1, 2, 3, 4$), and the grasp mode $\boldsymbol{\alpha}$ are given, the decomposition of a given fingertip force $\boldsymbol{F}$ into grasping force $\boldsymbol{F}_g$ and manipulating force $\boldsymbol{F}_m$ can be done by a procedure similar to that in Section 2.6. Note, however, that the concept of the focus of the internal force introduced for three-fingered hands cannot be directly extended to the case of four-fingered hands. Hence, there is no direct extension of Proposition 2 on the existence of grasping force. Obtaining conditions for the existence of a grasping force for four-fingered hands will be a topic for future research.

For hands with more than four fingers, we have not succeeded in defining the grasping and manipulating forces. This will also be a topic for future research.

2.8 Application to the Synthesis of Fingertip Force

A simple application of the concepts of grasping and manipulating forces to the synthesis of fingertip force for a given task of manipulation will be presented in this section.

Consider a two-fingered hand with planar motion and a cylindrical object with a radius of 0.05[m], a mass of 1kg, and friction coefficient $\mu = 0.5$ as shown in Fig. 2.17. Suppose that the given task is to carry the object following a circular trajectory. First we define the object frame Σ_O, its origin at the center of the cylinder. We assume that the contact points are given by $\boldsymbol{r}_1 = [-0.05 \ \ 0]^{\mathrm{T}}$ and $\boldsymbol{r}_2 = [0.05 \ \ 0]^{\mathrm{T}}$. The desired trajectory of the

origin of Σ_O is assumed to be given by a half circle with a radius of 0.05m starting from p_0 of the reference frame Σ_R shown in Fig. 2.17, going through p_1, p_2, and p_3, and reaching p_4.

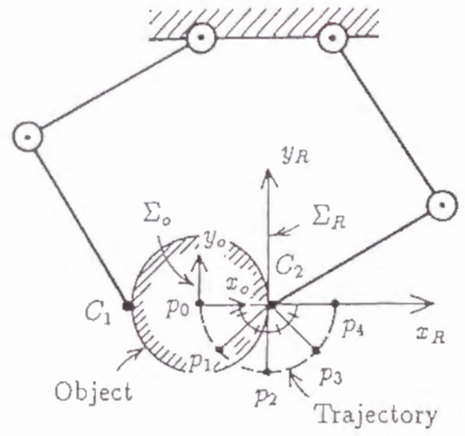

Fig. 2.17. Example of synthesis of fingertip force.

The trajectory accelerates by 5m/s^2 during the path (p_0, p_1), goes with constant speed during(p_1, p_3), and decelerates by -5m/s^2 during (p_3, p_4). The orientation of the object is assumed to be fixed. Then for the case of no gravitational effect, the time history $\boldsymbol{f}(t)$(N) of the desired total resultant force to be applied to the origin of the object is given in Fig. 2.18. Noticing that the realizable grasp mode is given by $\alpha = +1$ and using Eq. (2.66) with $k = 1$ for the path (p_0, p_2) and $k = -1$ for the path (p_2, p_4), the manipulating force $\boldsymbol{F}_m(t) = [\boldsymbol{f}_{m1}^{\mathrm{T}}(t) \;\; \boldsymbol{f}_{m2}^{\mathrm{T}}(t)]^{\mathrm{T}}$ is given in Fig. 2.19.

Now we consider the selection of the grasping force $\boldsymbol{F}_g$, the general form of $\boldsymbol{F}_g$ in this case is $\boldsymbol{F}_g = [1 \;\; 0 \;\; -1 \;\; 0]^{\mathrm{T}}\boldsymbol{h}_g$ from Eq. (2.63), the fingertip force $\boldsymbol{F}(t) = [\boldsymbol{f}_1^{\mathrm{T}}(t) \;\; \boldsymbol{f}_2^{\mathrm{T}}(t)]^{\mathrm{T}}$ for a fixed $\boldsymbol{h}_g$ is given in Fig. 2.20. Therefore, if we select a grasping force satisfying $h_g \geq 2.5\pi[\mathrm{N}] \simeq 7.9[\mathrm{N}]$, then the given task can be achieved without slipping. If the object is under gravitational effect, $\boldsymbol{F}_m(t)$ is given as in Fig. 2.21, and $h_g \geq (2.5\pi + g)[\mathrm{N}] \simeq 17.7[\mathrm{N}]$ (g is the gravity constant) is necessary for achieving the task without slipping. Further, if some external disturbance force $\boldsymbol{f}_e(t)$ such that $\|\boldsymbol{f}_e(t)\| < 2[\mathrm{N}]$ is expected to work at the origin of Σ_0 and should be canceled out by the fingertip force, then the time history of $\boldsymbol{f}(t)$ may deviate within the shaded region shown in Fig. 2.22. Obtaining the corresponding region of the manipulating force shown in Fig. 2.23, we find that it is enough to select a grasping force satisfying $h_g \geq 2.5\pi + 2[\mathrm{N}] \simeq 9.9[\mathrm{N}]$ to achieve the task.

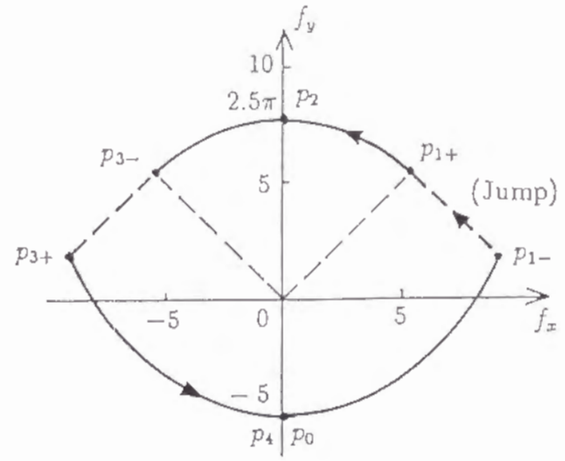

Fig. 2.18. Trajectory of the total resultant force $T = [\; f_x \;\; f_y \;\; 0 \;]^{\mathrm{T}}$ [N] for the object trajectory $p_0 - p_4$ in Fig. 2.17.

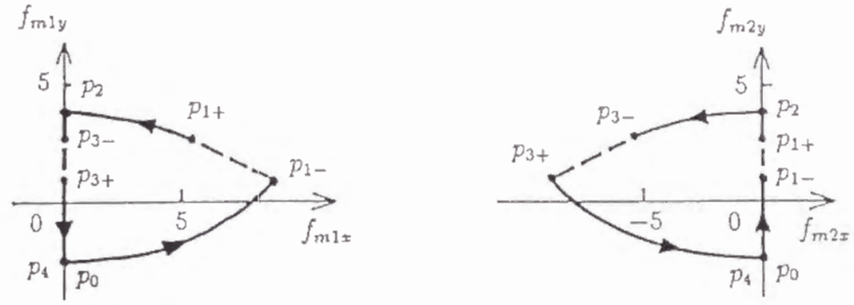

(a) $f_{m1}(t)$ (b) $f_{m2}(t)$

Fig. 2.19. Trajectory of manipulating force $F_m(t)$ [N].

These simple selections of grasping force can usually be done off-line for each given task, reducing the necessary real-time computation for synthesizing the fingertip forces. If the given task is more complicated and just one selection of the grasping force is not appropriate, we can decompose the task into several sequential subtasks and determine a suitable grasping force for each subtask.

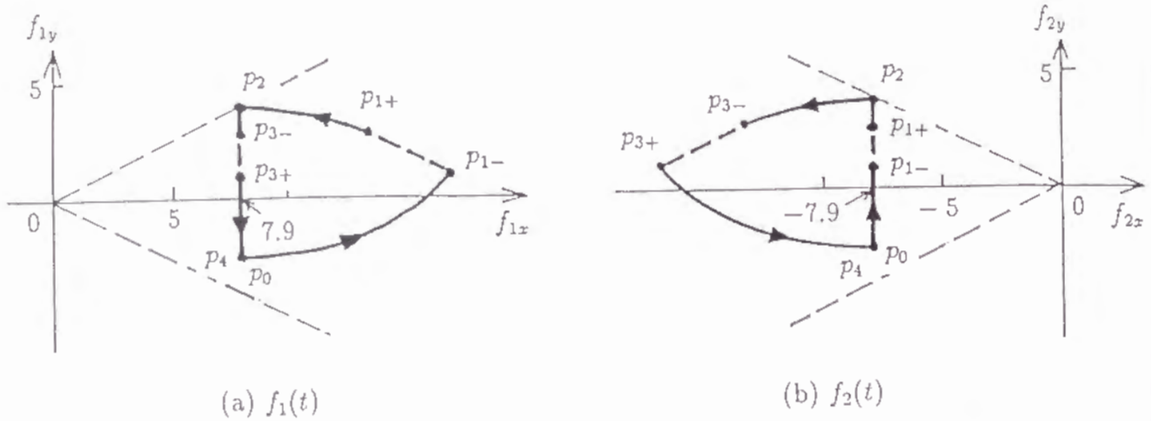

(a) $f_1(t)$ (b) $f_2(t)$

Fig. 2.20. Trajectory of fingertip force $F(t) = [\ f_1(t)\ \ f_2(t)\ ]^{\mathrm{T}}$ [N] for $h_g = 7.9$ [N]. - - -: Frictional limit.

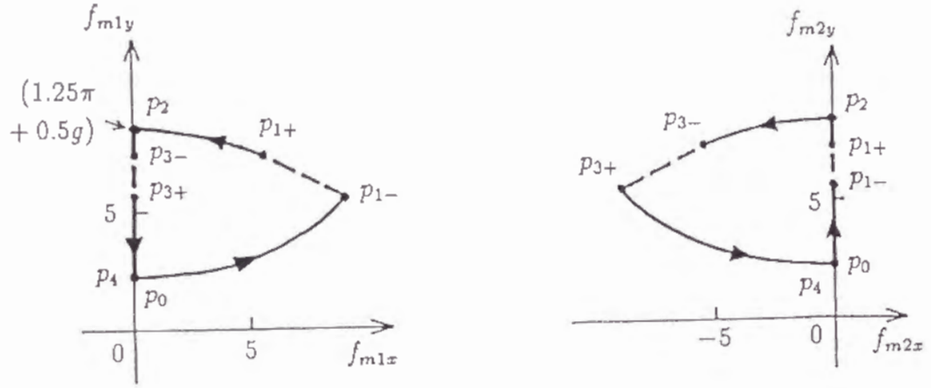

(a) $f_{m1}(t)$ (b) $f_{m2}(t)$

Fig. 2.21. Trajectory fingertip force $F_m(t)$ [N] under gravity in minus y direction.

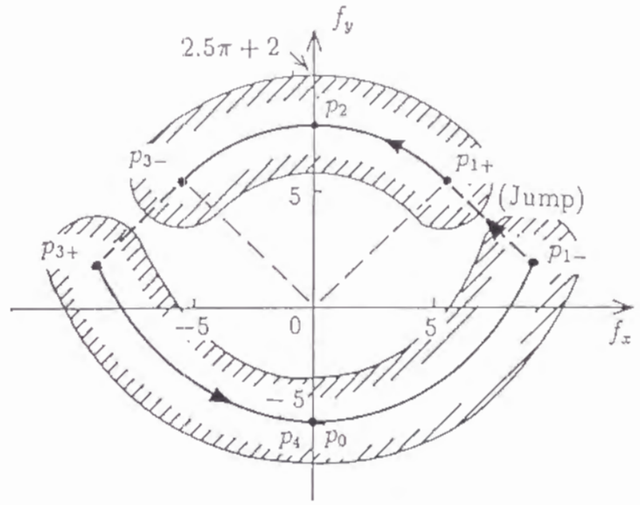

Fig. 2.22. Region of possible trajectory of the total resultant force $T = [\ f_x\ \ f_y\ \ 0\ ]^{\mathrm{T}}$ [N] for the object trajectory $p_0 - p_4$ in Fig. 2.17 and external disturbance $f_e(t)$ such that $||f_e(t)|| < 2$[N].

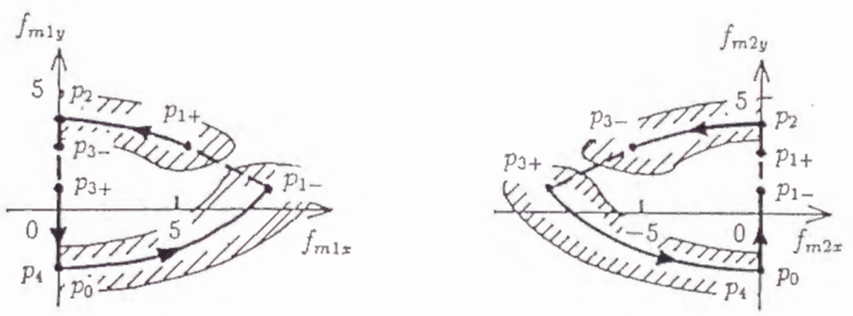

(a) Region of $f_{m1}(t)$ (b) Region of $f_{m2}(t)$

Fig. 2.23. Trajectory of manipulating force $F_m(t) = [\ f_{m1}^{\mathrm{T}}(t)\ \ f_{m2}^{\mathrm{T}}(t)\ ]^{\mathrm{T}}$[N] for the resultant force in Fig. 2.22.

2.9 Conclusion

The concepts of the manipulating force and grasping force, which have sometimes been used intuitively for describing some force components involved in manipulation of objects by

human hands, have been studied for multifingered robot hands. The main results obtained in this thesis are summarized as follows.

1) The grasping and manipulating forces for two-fingered hands with linear motion have been discussed to explain the motivation and the main idea of this thesis.

2) Three-fingered hands have been studied in detail. First, the grasping force has been defined as an internal force that satisfies the static friction constraint. The concept of grasp mode has been introduced. Then the manipulating force has been defined as a fingertip force satisfying the following three conditions: a) It produces the specified resultant force. b) It is not in the inverse direction of the grasping force. c) It is orthogonal to the grasping force component. An explicit expression of the manipulating force has been given. An algorithm for decomposing a given fingertip force into manipulating and grasping forces has also been given.

3) It has been shown that similar arguments can be developed for two-fingered hands with planar motion and four-fingered hands.

4) To show the usefulness of the concepts of grasping and manipulating forces, a simple problem of synthesizing the fingertip force of a two-fingered hand with planar motion for a given task of manipulating a cylindrical object has been discussed. It has been shown that the grasping force can be determined off-line, implying that the load of real-time computation is reduced.

These results will be useful for developing control algorithms for multifingered robot hands and cooperated manipulation of objects by multiple robots. In particular, the concepts of grasping force and grasp mode would be helpful for securely grasping objects with various shapes. In applying these results to on-line control, however, we will have to pay attention to the rather large computational amount for calculating grasping and manipulating forces.

Chapter 3

Dynamic Manipulation / Grasping Control of Multifingered Robot Hands

3.1 Introduction

One important research topic in the field of multifingered hands involves the determination and control of the internal forces. Indeed in multiple manipulator and parallel manipulator systems also entail the same problem. However, for multifingered hands it is necessary that the fingertip forces satisfy the static frictional constraint in order to have the non-slip grasping.

For the determination of the internal forces, Kerr and Roth approximate the static frictional constraint and the joint torque constraint by means of linearization, and determine the internal forces. Consequently the fingertip force satisfies the linearized constraint [21]. Nakamura et al. formulate the determination problem of the internal force into quadratic programing, and obtain the internal forces which make the Euclid norm of the fingertip force the minimum value [34],[35]. However, the method is not suitable for real time control because it requires a great deal of time to solve the non-linear programing.

On the other hand, several control algorithms have been proposed [49], [30], [59]. Li et al. consider the dynamics of the fingers and the object, and propose the control algorithm which includes both the position control of the object and the internal force control [30]. This controller is based on the dynamic coordinative manipulation [35], and a main characteristic of this is to have a servo controller for the internal force control. However, it is not very clear how to choose the controlled variables. That is, the number of controlled variables of the internal force control by Li's method is nine when considering a three-fingered hand with frictional point contact, and it is not identical to the number of

dimensions of internal force. On the other hand, it is have proven in Chapter 2 that the number of dimensions of the above case is three. Since the internal force among the fingers is the constraint force caused by the constant spans between the contact points, we think that the set of variables with the same number of elements as the dimensions of the internal force should be used for the force control, based on the hybrid position/force control [42], [57].

In this chapter, a dynamic manipulation/grasping controller of multifingered robot hands based on the dynamic control and the position/force hybrid control is proposed and discussed in this paper. This controller, using the manipulating and grasping forces introduced in Chapter 2, consists of a compensator which linearizes the whole grasping system and a servo controller for the linearized system. It makes the hand manipulate an object by means of position control and grasp it by means of force control. The distinctive features of the proposed controller are : 1) It uses a grasp parameter having the same number of elements as the internal force. 2) It decomposes the total force required to apply the grasped object into the manipulating force which is a part of fingertip force.

In Section 2, the kinematical constraint among the fingers and the motion equations of the fingers and the object are presented as basic equations. In Section 3, the dynamic manipulation/grasping controller is proposed, and the position of the object and the grasp parameter are found to be the controlled variables for the manipulation and the grasping, respectively. Then, in Section 4 simulation results are shown to investigate the validity of the proposed controller. Finally, Section 5 considers the advantages of this controller over another type of controller method used for the load distribution problem of multiple manipulators.

3.2 Basic Equations

3.2.1 Kinematical Constraint

Three-fingered hands with frictional point contacts are discussed in this chapter assuming the same conditions as in Chapter 2. A three-fingered hand and an object under consideration are shown in Fig. 3.1. In the figure, Σ_b is the base coordinate frame fixed at an arbitrary position on the object. $\boldsymbol{r}_p$ is the position vector of the origin of Σ_o from the origin of Σ_b. $\boldsymbol{p}_i$ $(i = 1, 2, 3)$ is the position vector of the contact point C_i of the i-th finger from the origin of Σ_o, and $\boldsymbol{f}_i$ is the i-th fingertip force.

Each fingertip has to follow the contact point on the object during manipulation for non-slip grasping. Consequently, the velocity of the object $\boldsymbol{v} = [\dot{\boldsymbol{r}}_p^{\mathrm{T}} \ \boldsymbol{\omega}^{\mathrm{T}}]^{\mathrm{T}}$ and the velocity of the joint variable $\dot{\boldsymbol{q}} = [\dot{\boldsymbol{q}}_1^{\mathrm{T}} \dot{\boldsymbol{q}}_2^{\mathrm{T}} \dot{\boldsymbol{q}}_3^{\mathrm{T}}]^{\mathrm{T}} \in \mathrm{R}^n$ consisting of that of the i-th finger $\dot{\boldsymbol{q}}_i \in \mathrm{R}^{ni}$ $(n = n_1 + n_2 + n_3)$ have the following kinematical constraint.

$$\boldsymbol{J}_o \boldsymbol{v} = \boldsymbol{J}_f \dot{\boldsymbol{q}} \tag{3.1}$$

where,

$$\boldsymbol{J}_o = \begin{bmatrix} \boldsymbol{J}_{o1} \\ \boldsymbol{J}_{o2} \\ \boldsymbol{J}_{o3} \end{bmatrix}, \quad \boldsymbol{J}_{oi} = [\boldsymbol{E}_3 \quad -\boldsymbol{P}_i] \in \mathrm{R}^{3\times 6}, \quad i = 1, 2, 3$$

$$\boldsymbol{P}_i = \begin{bmatrix} 0 & -p_{iz} & p_{iy} \\ p_{iz} & 0 & -p_{ix} \\ -p_{iy} & p_{ix} & 0 \end{bmatrix}, \quad \boldsymbol{p}_i = [p_{ix} \quad p_{iy} \quad p_{iz}]^{\mathrm{T}}, \quad i = 1, 2, 3$$

$$\boldsymbol{J}_f = \begin{bmatrix} \boldsymbol{J}_{f1} & \boldsymbol{0} & \boldsymbol{0} \\ \boldsymbol{0} & \boldsymbol{J}_{f2} & \boldsymbol{0} \\ \boldsymbol{0} & \boldsymbol{0} & \boldsymbol{J}_{f3} \end{bmatrix} \in \mathrm{R}^{9\times n}$$

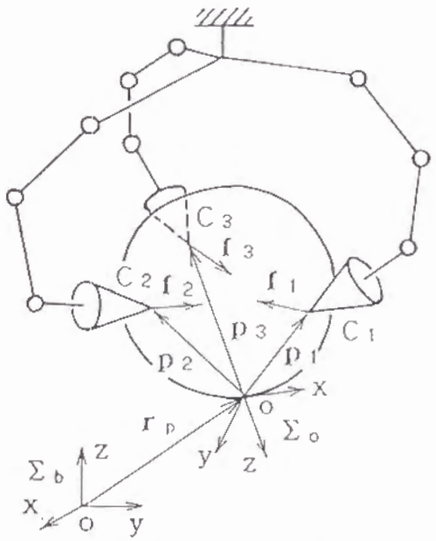

Fig. 3.1. Three-fingered hand and object.

The velocity of the object can also be expressed by using a set of rotational velocities around three axes. Let this velocity vector be $\dot{\boldsymbol{r}} = [\dot{\boldsymbol{r}}_p^{\mathrm{T}} \dot{\boldsymbol{\phi}}^{\mathrm{T}}]^{\mathrm{T}} \in \mathrm{R}^6$, then the relation between $\boldsymbol{v}$ and $\dot{\boldsymbol{r}}$ can be expressed as follows.

$$\boldsymbol{v} = \boldsymbol{W} \dot{\boldsymbol{r}} \tag{3.2}$$

3.2.2 Motion Equation of Fingers and Object

The motion equation of the three fingered hand can be expressed as the following equation.

$$\boldsymbol{M}_f \ddot{\boldsymbol{q}} + \boldsymbol{h}_f + \boldsymbol{J}_f^{\mathrm{T}} \boldsymbol{F} = \boldsymbol{\tau} \tag{3.3}$$

where, $\boldsymbol{\tau} = [\boldsymbol{\tau}_1^{\mathrm{T}}\ \boldsymbol{\tau}_2^{\mathrm{T}}\ \boldsymbol{\tau}_3^{\mathrm{T}}]^{\mathrm{T}} \in \mathrm{R}^9$ represents the joint torque vector and $\boldsymbol{F} = [\boldsymbol{f}_1^{\mathrm{T}}\ \ \boldsymbol{f}_2^{\mathrm{T}}\ \ \boldsymbol{f}_3^{\mathrm{T}}]^{\mathrm{T}} \in \mathrm{R}^9$ represents the fingertip force, $\boldsymbol{M}_f$ represents the inertia matrix, and $\boldsymbol{h}_f$ represents the centrifugal force, the Coriolis forces, and the gravity force.

On the other hand, the motion equation of the object can be expressed as the following equation.

$$\boldsymbol{M}_o\ddot{\boldsymbol{r}} + \boldsymbol{h}_o = \boldsymbol{T} \tag{3.4}$$

$$\boldsymbol{T} = \boldsymbol{J}_o^{\mathrm{T}}\boldsymbol{F} \tag{3.5}$$

where $\boldsymbol{T} = [\boldsymbol{f}^{\mathrm{T}}\boldsymbol{N}^{\mathrm{T}}]^{\mathrm{T}} \in \mathrm{R}^6$ represents the total force applied to the object by the fingers, $\boldsymbol{M}_o$ represents the inertia matrix, $\boldsymbol{h}_o$ represents the centrifugal force, the Coriolis forces, and gravity force.

3.3 Manipulation and Grasping Control Using Manipulating and Grasping Forces

3.3.1 Manipulating and Grasping Forces

The manipulating and grasping forces are defined as the components of the fingertip force in order to discuss the total force required for desired manipulation and the internal force for non-slip grasping as the fingertip force.

The grasping force $\boldsymbol{F}_g = [\boldsymbol{f}_{g1}^{\mathrm{T}}\boldsymbol{f}_{g2}^{\mathrm{T}}\boldsymbol{f}_{g3}^{\mathrm{T}}]^{\mathrm{T}} \in \mathrm{R}^9$ is defined as the fingertip force that satisfies the following two conditions: 1) It produces no resultant force. 2) It satisfies the static friction constraint at the contact points. The manipulating force $\boldsymbol{F}_m = [\boldsymbol{f}_{m1}^{\mathrm{T}}\boldsymbol{f}_{m2}^{\mathrm{T}}\boldsymbol{f}_{m3}^{\mathrm{T}}]^{\mathrm{T}} \in \mathrm{R}^9$ is then defined as the fingertip force that satisfies the following three conditions: 1) It produces the specified total force. 2) It is not in the inverse direction of the grasping force. 3) It is orthogonal to the grasping force component. The grasping force and the manipulating force can be expressed by the following equations.

$$\boldsymbol{F} = \boldsymbol{F}_g + \boldsymbol{F}_m \tag{3.6}$$

$$\boldsymbol{F}_g = \boldsymbol{B}_g\boldsymbol{h}_g \tag{3.7}$$

$$\boldsymbol{h}_g = [h_{g1}\ \ h_{g2}\ \ h_{g3}]^{\mathrm{T}},\ h_{gi} \geq 0, i = 1,2,3$$

$$\boldsymbol{F}_m = \boldsymbol{B}_m\boldsymbol{h}_m,\quad \boldsymbol{B}_m \in \mathrm{R}^{9\times 6} \tag{3.8}$$

$$\boldsymbol{h}_m = [h_{m1}\ldots h_{m6}]^{\mathrm{T}}, h_{mi} \geq 0, i = 1,2,3$$

where $\boldsymbol{B}_g$ determined by a set of contact point locations is as follows.

$$\boldsymbol{B}_g = \begin{bmatrix} 0 & \hat{\boldsymbol{e}}_{13} & \hat{\boldsymbol{e}}_{12} \\ \hat{\boldsymbol{e}}_{23} & 0 & \hat{\boldsymbol{e}}_{21} \\ \hat{\boldsymbol{e}}_{32} & \hat{\boldsymbol{e}}_{31} & 0 \end{bmatrix} \in \mathrm{R}^{9\times 3} \tag{3.9}$$

$$\hat{\boldsymbol{e}}_{i(i+1)} = \alpha_{i+2}\boldsymbol{e}_{i(i+1)},\quad i = 1,2,3 \tag{3.10}$$

$$\boldsymbol{e}_{i(i+1)} = \frac{\boldsymbol{p}_{i+1} - \boldsymbol{p}_i}{||\boldsymbol{p}_{i+1} - \boldsymbol{p}_i||},\quad i = 1,2,3 \tag{3.11}$$

$$\hat{\boldsymbol{e}}_{i(i+2)} = -\hat{\boldsymbol{e}}_{(i+2)i},\quad i = 1,2,3 \tag{3.12}$$

$\alpha = [\alpha_1, \alpha_2, \alpha_3]$, $\alpha_i = +1$ or -1, is a set of parameters which should be determined according to the shape of the object. $\alpha_i = +1$ and $\alpha_i = -1$ mean that elements of the grasping force between C_{i+1} and C_{i+2} are inward and outward, respectively, so we refer to this α as the grasp mode. In addition, we refer to $\boldsymbol{h}_g$ as the grasp parameter, because the grasping force is determined uniquely by Eq. (3.7) when a set of contact points and a grasp mode are given. Figure 3.2 shows an example of the grasping force when $\alpha = [+1,\ +1,\ +1]$.

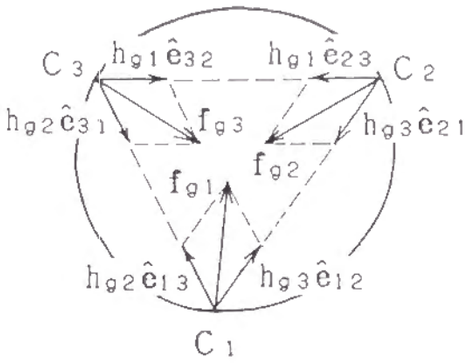

Fig. 3.2. Grasping force.

To obtain the manipulating force $\boldsymbol{F}_m$ for a given total force $\boldsymbol{T}$, we first calculate $\boldsymbol{h}_m$ which satisfies $h_{mi} \geq 0$ $(i = 1,2,3)$ from

$$\boldsymbol{h}_m = (\boldsymbol{J}_o^{\mathrm{T}}\boldsymbol{B}_m)^{-1}\boldsymbol{T} \tag{3.13}$$

by using Eqs. (3.5) and (3.8). Then we calculate $\boldsymbol{F}_m$ from

$$\boldsymbol{F}_m = \boldsymbol{B}_m(\boldsymbol{J}_o^{\mathrm{T}}\boldsymbol{B}_m)^{-1}\boldsymbol{T} \tag{3.14}$$

by substituting Eq. (3.13) into Eq. (3.8).

3.3.2 Dynamic Manipulation/Grasping Controller

In this section, the dynamic manipulation/grasping controller is proposed.

First, a linearization of the system by means of state feedback is presented. The joint torque calculated by the following equations can linearize the fingers/object system expressed in Section 2.

$$
\begin{aligned}
\boldsymbol{\tau}_c &= \boldsymbol{\tau}_o + \boldsymbol{\tau}_f && (3.15)\\
\boldsymbol{\tau}_o &= \boldsymbol{J}_f^{\mathrm{T}} \boldsymbol{F}_d && (3.16)\\
\boldsymbol{F}_d &= \boldsymbol{F}_{md} + \boldsymbol{F}_{gd} && (3.17)\\
\boldsymbol{F}_{md} &= \boldsymbol{B}_m (\boldsymbol{J}_o^{\mathrm{T}} \boldsymbol{B}_m)^{-1} \boldsymbol{T}_d && (3.18)\\
\boldsymbol{T}_d &= \boldsymbol{M}_o \dot{\boldsymbol{v}}_d + \boldsymbol{h}_o && (3.19)\\
\dot{\boldsymbol{v}}_d &= \boldsymbol{W} \boldsymbol{u}_1 + \dot{\boldsymbol{W}} \dot{\boldsymbol{r}} && (3.20)\\
\boldsymbol{F}_{gd} &= \boldsymbol{B}_g \boldsymbol{u}_2 && (3.21)\\
\boldsymbol{\tau}_f &= \boldsymbol{M}_f \ddot{\boldsymbol{q}}_d + \boldsymbol{h}_f && (3.22)\\
\ddot{\boldsymbol{q}}_d &= \boldsymbol{J}_f^{\dagger} (\boldsymbol{J}_o \dot{\boldsymbol{v}}_d + \dot{\boldsymbol{J}}_o \boldsymbol{v} - \dot{\boldsymbol{J}}_f \dot{\boldsymbol{q}}) + (\boldsymbol{E}_n - \boldsymbol{J}_f^{\dagger} \boldsymbol{J}_f) \boldsymbol{y} && (3.23)
\end{aligned}
$$

where, $\boldsymbol{u}_1 \in \mathrm{R}^6$, $\boldsymbol{u}_2 \in \mathrm{R}^3$ are the control inputs to the linearized system, and $M^{\dagger}$ represents the pseudo-inverse matrix of a matrix $\boldsymbol{M}$. Then the system, which consists of the fingers and the object, can be linearized as follows.

$$
\begin{aligned}
\ddot{\boldsymbol{r}} &= \boldsymbol{u}_1 && (3.24)\\
\boldsymbol{h}_g &= \boldsymbol{u}_2 && (3.25)
\end{aligned}
$$

And the acceleration of the joint variables satisfies

$$
\ddot{\boldsymbol{q}} = \ddot{\boldsymbol{q}}_d \qquad (3.26)
$$

Note that linearization is applied to the grasp parameter for grasping. This linearization allows us to specify the desired manipulation as $\boldsymbol{r}_d$ and the desired grasping as $\boldsymbol{h}_{gd}$ independently. The proof of this linearization is described in Appendix A.

Even if we use the compensator for the linearization, a servo compensator is required because of the modeling error in the real system. Here we use two degrees of freedom controller[48]. This compensator expressed as the following equations is used to calculate the control inputs $\boldsymbol{u}_1$ and $\boldsymbol{u}_2$ for the linearized system.

$$
\begin{aligned}
\boldsymbol{u}_1 &= \ddot{\boldsymbol{r}}_d + \boldsymbol{K}_P \boldsymbol{e} + \boldsymbol{K}_I \int \boldsymbol{e} dt + \boldsymbol{K}_D \dot{\boldsymbol{e}} && (3.27)\\
\boldsymbol{e} &= \boldsymbol{r}_d - \boldsymbol{r} && (3.28)\\
\boldsymbol{u}_2 &= \boldsymbol{h}_{gd2} + \boldsymbol{K}_F \int (\boldsymbol{h}_{gd2} - \boldsymbol{h}_g) dt && (3.29)\\
\boldsymbol{h}_{gd2} &= \boldsymbol{h}_{g2} - T_C \dot{\boldsymbol{h}}_{gd2} && (3.30)
\end{aligned}
$$

where $\boldsymbol{r}_d$ represents the desired trajectory of the object, $\boldsymbol{h}_{gd}$ represents the desired trajectory of the grasp parameter, and T_C is the time constant in the first order lag for the desired response of the grasp parameter. The block diagram of the proposed controller is shown in Fig. 3.3

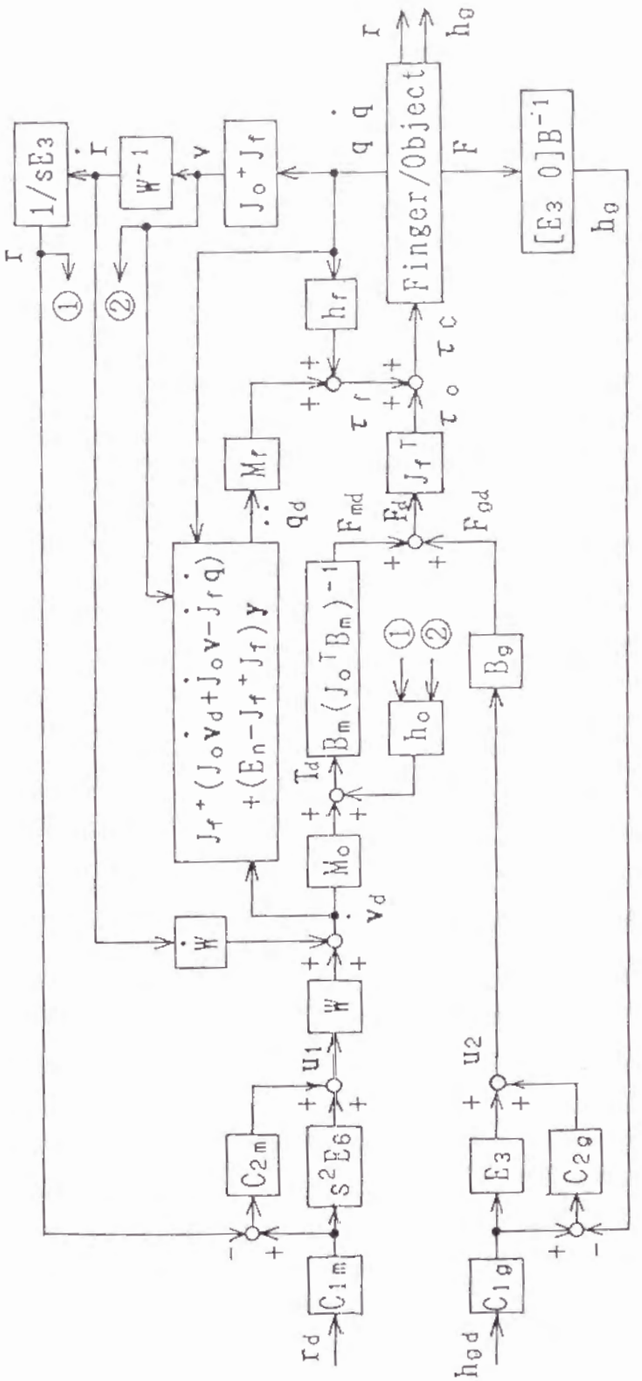

Fig. 3.3. Dynamic manipulation/grasping controller.

3.3.3 Consideration on the controlled variable for the grasping

In this section, the controlled variable for grasping is discussed.

In the case of a three-fingered with frictional point contact, the number of controlled variables of internal force control by Li's method is nine, and this is not the same as the number of dimensions of internal force. It is investigated the dimensions of the internal force and proved that number of the dimensions of the above case is three, described in Chapter 2. Since the internal force among the fingers is the constraint force caused by the constant spans between the contact points, we think that the set of variables with the same number of elements as the dimensions of internal force should be used for the force control, based on the hybrid position/force control [42], [57].

The grasp parameter has the same number of elements as the dimension of the internal force, and it corresponds to the grasping force uniquely with a clear relation to the direction of the grasping force. Therefore this parameter representation makes it easy for fingertip force to satisfy the constraint of static friction. So, it is suitable to use the grasp parameter for grasping control, and the proposed controller seems to be an improved one compared to the control method of Li et al.

3.4 Simulation

Figure 3.4 shows the three-fingered hand used in the simulation to investigate the validity of the controller proposed in Section 3. Table 3.1 shows the length ℓ_{ij}, the mass m_{fij}, and the principal moment of the inertia around the center of gravity $I_{fijk}(k = 1, 2, 3)$ of the j-th link of the i-th finger. The object shown in Table 3.2 represents a cylinder with a diameter of 0.1[m], a height of 0.1[m], a mass of m_o and a principal moment of inertia of I_{ok} $(k = 1, 2, 3)$. Three contact points are located as $\boldsymbol{p}_1 = [0.05 \;\; 0 \;\; -0.025]^{\mathrm{T}}$, $\boldsymbol{p}_2 = [0 \;\; 0.05 \;\; -0.025]^{\mathrm{T}}$[m], $\boldsymbol{p}_3 = [0 \;\; -0.05 \;\; -0.025]^{\mathrm{T}}$[m], where $\boldsymbol{p}_i$ is described on Σ_o and the origin of Σ_o is located in the center of the object and the initial roll-pitch-yaw of Σ_o, ϕ is $[0 \;\; 0 \;\; 180]^{\mathrm{T}}$[deg]. In this simulation, $\alpha = [+1, \;\; +1, \;\; +1]$.

Table 3.1. Parameters of finger.

j	ℓ_{ij} [m]	m_{fij} [kg]	$I_{fijk}(\times 10^{-4}[\mathrm{kg \cdot m^2}])$		
1	0	2.00×10^{-1}	0.13	0.13	0.13
2	9.00×10^{-1}	2.00×10^{-1}	0.13	5.47	5.47
3	7.50×10^{-1}	2.00×10^{-1}	0.13	3.82	3.82

Table 3.2. Parameters of object.

m_o [kg]	$I_{ok}(\times 10^{-4}[\mathrm{kg \cdot m^2}])$		
2.00×10^{-1}	2.92	2.92	2.92

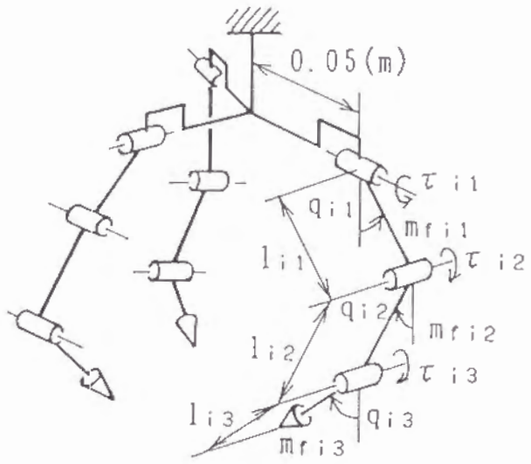

Fig. 3.4. Three-fingered hand for simulation.

The desired trajectory of the manipulation is given as the position of the object on the circle with radius 0.05[m]; the orientation of the trajectory is constant. During the first one second of the simulation, the object is assumed to be supported with a table at the initial position and orientation. Sampling time is 1[ms] and the step-size of the numerical integration is 0.1[ms]. The position of the object $\boldsymbol{r}$ is calculated by using $\dot{\boldsymbol{q}}$ in the following equations:

$$\boldsymbol{r} = \boldsymbol{r}_o + \int \dot{\boldsymbol{r}} dt \tag{3.31}$$

$$\dot{\boldsymbol{r}} = \boldsymbol{W}^{-1} \boldsymbol{v} \tag{3.32}$$

$$\boldsymbol{v} = \boldsymbol{J}_o^{\dagger} \boldsymbol{J}_f \dot{\boldsymbol{q}} \tag{3.33}$$

$$\boldsymbol{J}_o^{\dagger} = (\boldsymbol{J}_o^{\mathrm{T}} \boldsymbol{J}_o)^{-1} \boldsymbol{J}_o^{\mathrm{T}}$$

The gains and the time constant in the servo compensator expressed by Eqs. (3.27) $\sim$ (3.30) are as follows: $\boldsymbol{K}_P = \mathrm{diag.}(4000, \cdots, 4000)$, $\boldsymbol{K}_I = \mathrm{diag.}(8000, \cdots, 8000)$, $\boldsymbol{K}_D = \mathrm{diag.}(200, \cdots, 200)$, and $\boldsymbol{K}_F = \mathrm{diag.}(100, \cdots, 100)$, and $T_c = 0.05$[s].

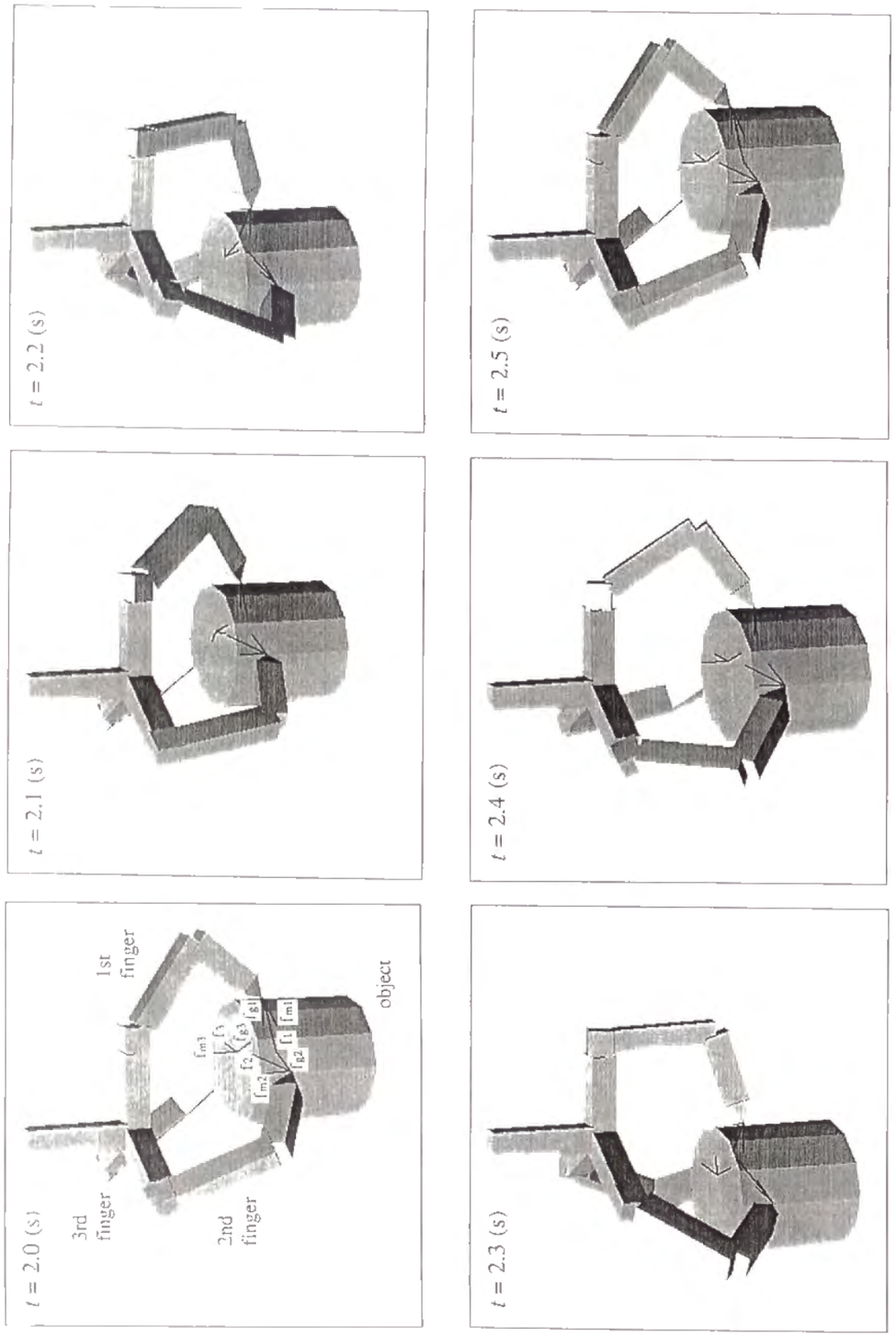

Fig. 3.5. Manipulation by three-fingered hand.

Figure 3.5 shows the posture of the hand when $t = 2.0 \sim 2.5$[s]. Figures 3.6 and 3.7 show the position and orientation responses by the solid line and the error by the dotted line, and Fig. 3.8 shows the reference and the response of the grasp parameter. In the simulation, the nominal values of the parameters of the fingers and the object dynamics are assumed to be in error, and all the nominal values of the mass and the inertia are 80 percent of the real ones. Figures 3.6 and 3.7 show that the maximum translational error of the position is about 5×10^{-4}[m], and the maximum rotational error is 5×10^{-2} degrees, so the desired manipulation is carried out. On the other hand, Figure 3.8 shows that the object is grasped with the desired grasping force during the manipulation.

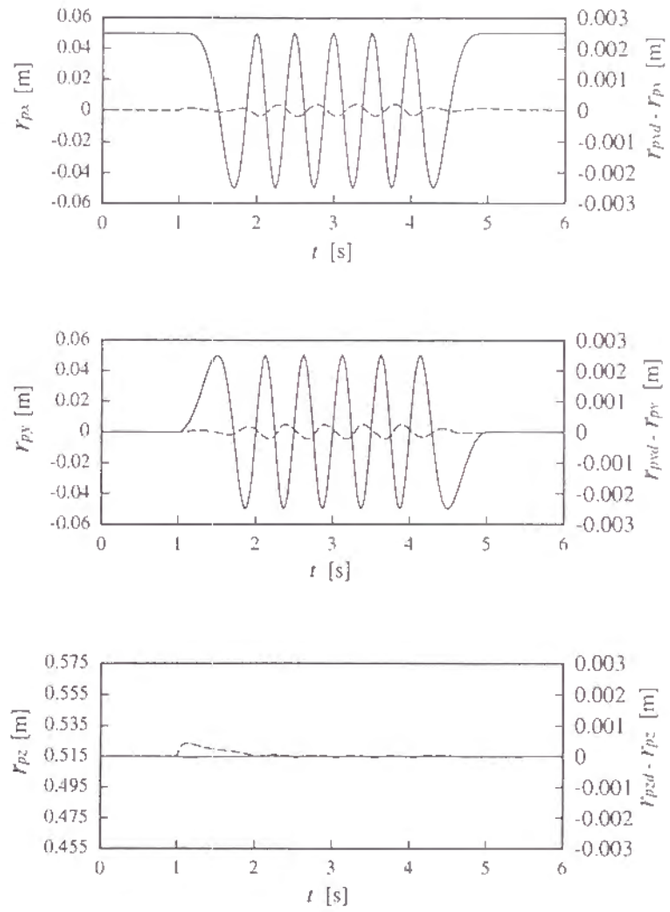

Fig. 3.6. Simulation results of manipulation (position).

Figure 3.9 shows the angle θ_i between the i-th fingertip force and the inward normal vector at C_i. In the figure, the dotted line means the maximum value of μ_i when the coefficient of the static friction at C_i is 1.0, so manipulation without slipping is accomplished

in this case. The desired value of h_{g1} is changed to 2.0[N] after three seconds, then we find it produces the margin of θ_i.

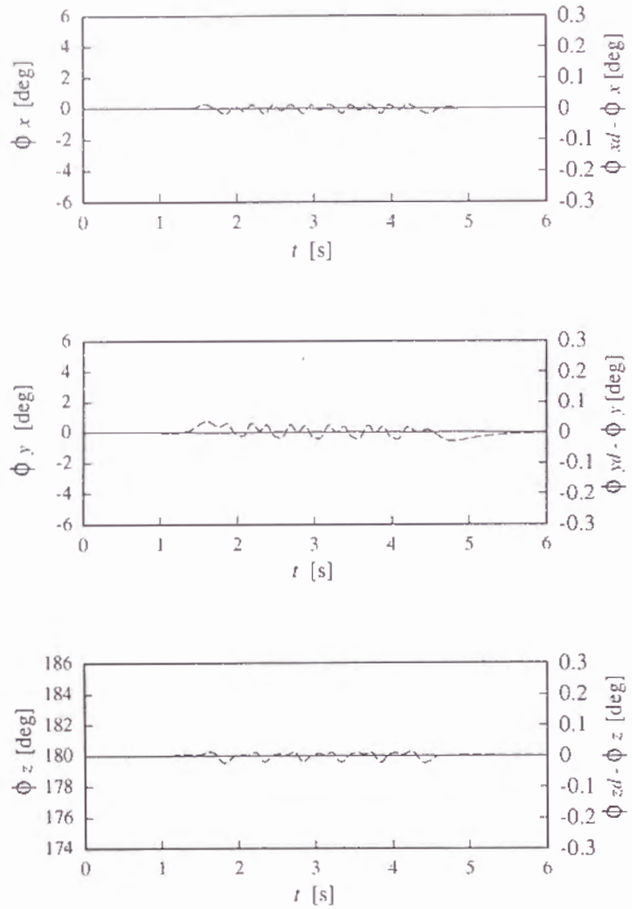

Fig. 3.7. Simulation results of manipulation (orientation).

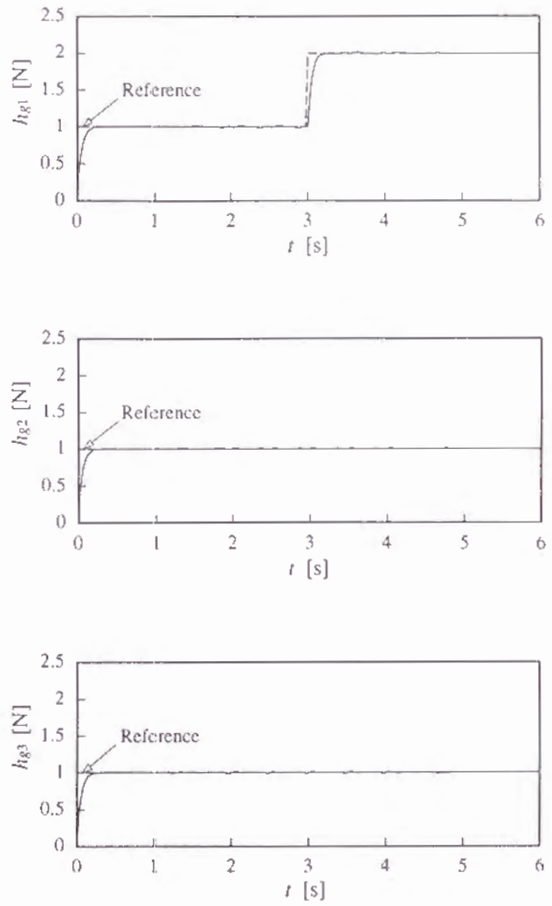

Fig. 3.8. Simulation results of grasping.

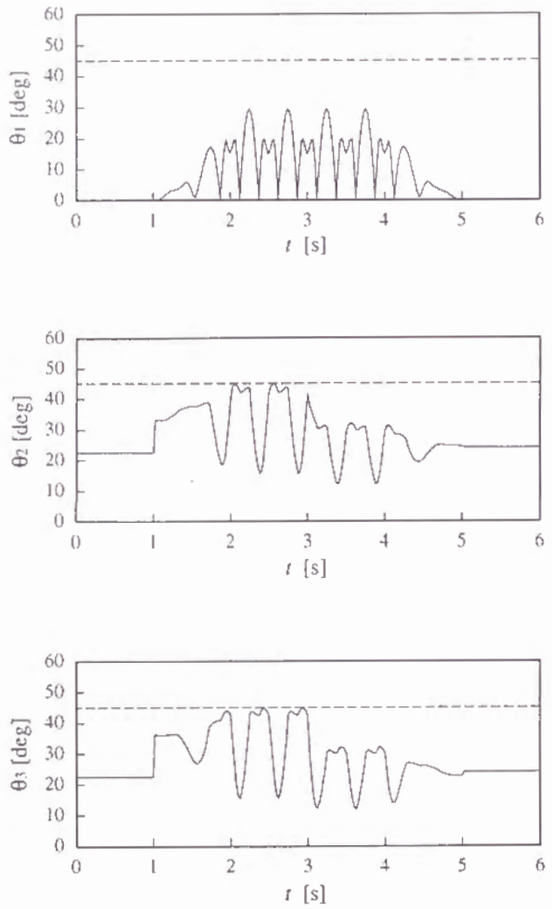

Fig. 3.9. Direction of fingertip force.

3.5 Discussion on Direction of Fingertip Force

In this section, the decomposition of the total force, which is required by the manipulation into the component of the fingertip force, is discussed. Then the validity of using the manipulating force is described.

The relation between the total force and the fingertip force is expressed in Eq. (3.5), with $\boldsymbol{T}$ and $\boldsymbol{F}$ being six elements and nine elements, respectively. Therefore, the internal force exists, and the decomposition of a given total force into a fingertip force can not be determined uniquely. In the proposed controller, the total force is decomposed into the manipulating force $\boldsymbol{F}_m$ by Eq. (3.18). This manipulating force defined in Chapter 2 satisfies the following equations,

$$\boldsymbol{f}_{mi}^{\mathrm{T}} \boldsymbol{f}_{gi} \geq 0, \quad i = 1, 2, 3 \tag{3.34}$$

On the other hand, there exists another method to decompose a given total force, namely, using the pseudo inverse of $\boldsymbol{J}_o^{\mathrm{T}}$, solve Eq. (3.5) for $\boldsymbol{F}$. Thus,

$$\tilde{\boldsymbol{F}}_m = (\boldsymbol{J}_o^{\mathrm{T}})^{\dagger} \boldsymbol{T} \tag{3.35}$$

This decomposition method is used for the force distribution problem of multiple manipulators handling one object[2]. In the case of multifingered hands, $\tilde{\boldsymbol{F}}_m$ can not be used as the fingertip force because the direction of $\boldsymbol{f}_i$ is restricted by the constraint of the static friction. In order to make $\boldsymbol{f}_i$ satisfy that constraint, we can add the internal force $\boldsymbol{F}_I$ as follows,

$$\tilde{\boldsymbol{F}} = \boldsymbol{F}_m + \boldsymbol{F}_I \tag{3.36}$$

Now, Fig. 3.10 shows $\boldsymbol{F}_m$ and $\tilde{\boldsymbol{F}}_m$, in a case of a two-fingered hand, are obtained for the same total force $\boldsymbol{T}$. In this case,

$$\boldsymbol{F}_m = \begin{bmatrix} f_x \\ \frac{f_y}{2} - \frac{N}{a} \\ 0 \\ \frac{f_y}{2} - \frac{N}{a} \end{bmatrix} \tag{3.37}$$

$$\tilde{\boldsymbol{F}}_m = \begin{bmatrix} \frac{f_x}{2} \\ \frac{f_y}{2} - \frac{N}{a} \\ \frac{f_x}{2} \\ \frac{f_y}{2} + \frac{N}{a} \end{bmatrix} \tag{3.38}$$

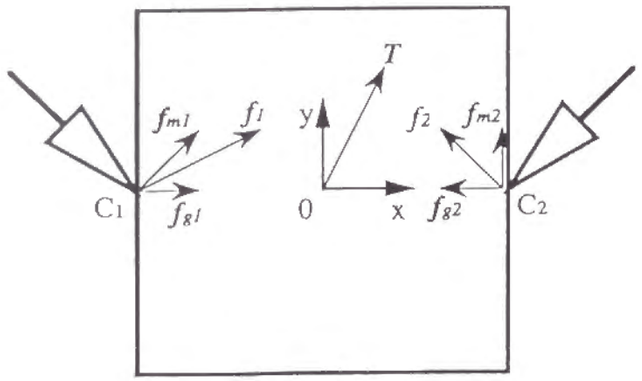

(a) proposed method

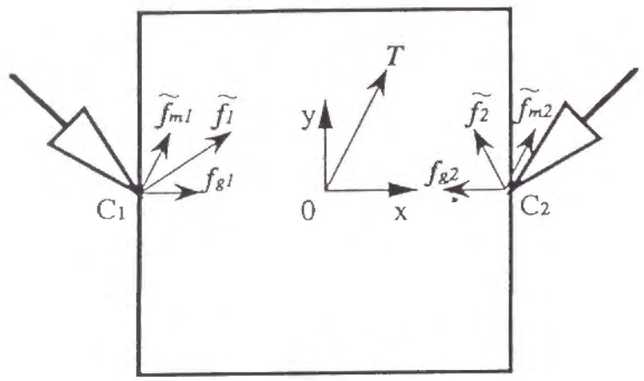

(b) method by Eqs. (3.35) and (3.36)

Fig. 3.10. Comparison of fingertip force.

where a is the width of the object and $\boldsymbol{T} = [f_x \quad f_y \quad N]^{\mathrm{T}}$, and $\boldsymbol{F}_I = \boldsymbol{F}_g$. The difference can be seen with respect to the x components. That is, the direction determined by C_1 and C_2, and the angle θ_2 becomes larger than those of $\boldsymbol{f}_2$. This means that $\boldsymbol{F}_I$ should be changed according to the total force $\boldsymbol{T}$ in the case of the decomposition by Eq. (3.35). On the other hand, the manipulating force by Eq. (3.18) does not disturb the grasping, because it satisfies Eq. (3.34).

Figure 3.11 shows the angle θ_i when the decomposition by Eq. (3.35) is used in the simulation. We can notice that the θ_i in Fig. 3.11 is larger than that in Fig. 3.9, and that the proposed method is suitable for non-slip grasping with the constant grasping force.

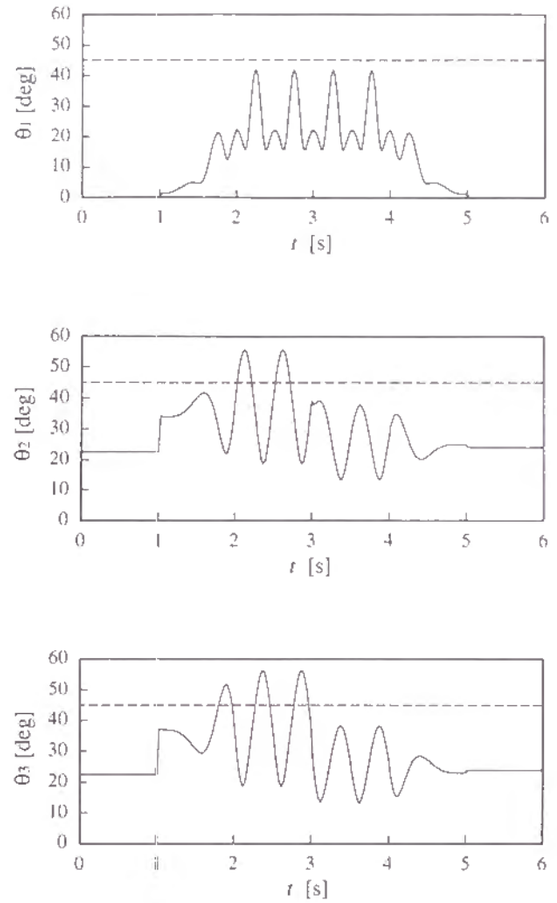

Fig. 3.11. Direction of fingertip force in method by Eqs. (3.35) and (3.36).

3.6 Conclusion

A dynamic manipulation/grasping controller using the manipulating and grasping forces of multifingered hands has been discussed. The main results obtained in this chapter are summarized as follows.

1) The basic configuration of the dynamic manipulation/grasping controller for three-fingered hands has been presented. The controller consists of a linearization of the system and a servo compensator, and its remarkable characteristic is that the grasp parameter, which has the same number of elements as that of the essential dimensions of the internal force, is used as the controlled variable of the grasping.

2) The validity of the proposed controller is shown by simulation results, and the manipulating force is shown to be available to minimize the angle of the fingertip force.

The manipulating and grasping forces can be defined not only for three-fingered hands but also for two-fingered or four-fingered hands, described in chapter 2, and the same controller can be constructed for those cases.

Appendix A The proof of the Linearization

By using Eqs. (3.1) $\sim$ (3.8), the whole dynamics of the system is derived as following equation:

$$\begin{bmatrix} M_f & J_f^{\mathrm{T}} B_m (J_o^{\mathrm{T}} B_m)^{-1} M_o W & J_f^{\mathrm{T}} B_g \\ -J_f & J_o W & 0 \end{bmatrix} \begin{bmatrix} \ddot{\boldsymbol{q}} \\ \ddot{\boldsymbol{r}} \\ \boldsymbol{h}_g \end{bmatrix} + \begin{bmatrix} \boldsymbol{h}_f + J_f^{\mathrm{T}} B_m (J_o^{\mathrm{T}} B_m)^{-1} (M_o \dot{W} \dot{\boldsymbol{r}} + \boldsymbol{h}_o) \\ -\dot{J}_f \dot{\boldsymbol{q}} + J_o \dot{W} \dot{\boldsymbol{r}} + J_o W \dot{\boldsymbol{r}} \end{bmatrix} = \begin{bmatrix} \boldsymbol{\tau} \\ 0 \end{bmatrix} \tag{3.a}$$

On the other hand, the control law described in Eqs. (3.15) $\sim$ (3.23) are summarized as following equation:

$$\begin{bmatrix} \boldsymbol{\tau} \\ 0 \end{bmatrix} = \begin{bmatrix} M_f & J_f^{\mathrm{T}} B_m (J_o^{\mathrm{T}} B_m)^{-1} M_o W & J_f^{\mathrm{T}} B_g \\ -J_f & J_o W & 0 \end{bmatrix} \begin{bmatrix} \ddot{\boldsymbol{q}}_d \\ \boldsymbol{u}_1 \\ \boldsymbol{u}_2 \end{bmatrix} + \begin{bmatrix} \boldsymbol{h}_f + J_f^{\mathrm{T}} B_m (J_o^{\mathrm{T}} B_m)^{-1} (M_o \dot{W} \dot{\boldsymbol{r}} + \boldsymbol{h}_o) \\ -\dot{J}_f \dot{\boldsymbol{q}} + J_o \dot{W} \dot{\boldsymbol{r}} + \dot{J}_o W \dot{\boldsymbol{r}} \end{bmatrix} \tag{3.b}$$

By substituting Eq. (3.b) into Eq. (3.a), we derive:

$$\begin{bmatrix} M_f & J_f^{\mathrm{T}} B_m (J_o^{\mathrm{T}} B_m)^{-1} M_o W & J_f^{\mathrm{T}} B_g \\ -J_f & J_o W & 0 \end{bmatrix} \begin{bmatrix} \ddot{\boldsymbol{q}} - \ddot{\boldsymbol{q}}_d \\ \ddot{\boldsymbol{r}} - \ddot{\boldsymbol{u}}_1 \\ \boldsymbol{h}_g - \boldsymbol{u}_2 \end{bmatrix} = 0 \tag{3.c}$$

Now let D be,

$$D = \begin{bmatrix} M_f & J_f B_m \left(J_o^{\mathrm{T}} B_m\right)^{-1} M_o W & J_f^{\mathrm{T}} B_g \\ -J_f & J_o W & 0 \end{bmatrix}$$

Then,

$$\mathrm{rank}(D)$$

$$\begin{aligned} &= \mathrm{rank}\left(D \begin{bmatrix} E_n & 0 & 0 \\ 0 & W^{-1} M_o^{-1} (J_o^{\mathrm{T}} B_m) & 0 \\ 0 & \cdot & 0 \\ & & E_3 \end{bmatrix} \right) \\ &= \mathrm{rank} \begin{bmatrix} M_f & J_f^{\mathrm{T}} B_m & J_f^{\mathrm{T}} B_g \\ -J_f & J_o M_o^{-1} (J_o^{\mathrm{T}} B_m) & 0 \end{bmatrix} \\ &= \mathrm{rank} \begin{bmatrix} M_f & J_f^{\mathrm{T}} B_m & J_f^{\mathrm{T}} B_g \\ 0 & (J_f M_f^{-1} J_f^{\mathrm{T}} + J_o M_o^{-1} J_o^{\mathrm{T}}) B_m & J_f M_f^{-1} J_f^{\mathrm{T}} B_g \end{bmatrix} \\ &= n + \mathrm{rank} \Big[(J_f M_f^{-1} J_f^{\mathrm{T}} + J_o M_o^{-1} J_o^{\mathrm{T}}) B_m \\ &\quad (J_f M_f^{-1} J_f^{\mathrm{T}} + J_o M_o^{-1} J_o^{\mathrm{T}}) B_g \Big] \\ &= n + \mathrm{rank} \left(\begin{bmatrix} J_f & J_o \end{bmatrix} \begin{bmatrix} M_f^{-1} & 0 \\ 0 & M_o^{-1} \end{bmatrix} \begin{bmatrix} J_f & J_o \end{bmatrix}^{\mathrm{T}} \begin{bmatrix} B_m & B_g \end{bmatrix} \right) \\ &= n + 9 \end{aligned} \tag{3.d}$$

Equation (3.d) means rank of D is full rank. Then Eqs. (3.24) $\sim$ (3.26) are derived by using Eqs. (3.c) and (3.d).

Chapter 4

Adaptive Grasping by Multifingered Hands

4.1 Introduction

There are two meanings of stability regarding grasping and manipulation described in Chapter 1. That is, *stability of motion* and *stability of contact*. Stability of motion means the ability to return a grasped object to the static equilibrium position when some changes in the position occur. On the other hand, stability of contact means the ability to maintain contact against any disturbance of external forces on an object.

Regarding research on stability of motion, that is on manipulation, Hanafusa and Asada[12] discussed it looking at the potential energy of the system. Fearing[11], Cutkosky and Kao[9], Kitagawa et al.[24], and Kaneko et al.[19], discussed the resultant compliance on an object produced by a compliance of each finger. This type of research was mainly on static stability of the grasped object.

On the other hand, stability of contact, that is grasping, is discussed as a problem of internal force. It's well known that internal force is an important factor in the analysis and synthesis of fingertip forces for grasping and manipulation. Kerr and Roth[21] proposed to determine the optimal internal force as that with the minimum norm under an approximated frictional constraint. Nakamura[36] discussed the stability of contact by using the equivalent mass characteristics at the fingertips. The small grasping force is considered to be suitable as regards these types of research. However, there can be another concept in which a big grasping force is considered to be suitable[58].

Non-slip grasping is important for their multifingered hands to continue the required manipulation. It is not always desirable to grasp an object using big fingertip force, because the joint torque to produce fingertip force is limited for real multifingered hands. In such a case, to find a suitable grasping force is necessary for not only grasping but also

manipulation, since the joint torque is used not only for grasping but also for manipulation.

In this chapter, adaptive grasping is discussed for two-fingered hands with constraints of static friction and joint torque, under repeated manipulation. In Section 4.2, the dynamics manipulation/grasping controller of two-fingered hands is described briefly. One of the special features of the controller is that a grasp parameter can be determined independently of manipulation as a desired valuable for grasping. In Section 4.3, scalar functions are defined for evaluation of grasping and manipulation, and the effects on them are discussed. Then, an algorithm for adaptive grasping which uses these functions is proposed. This algorithm realizes the desired manipulation without any slip of the fingertips, adjusting the grasp parameter to the repeated manipulation tasks. In Section 4.5, the effectiveness of the proposed algorithm is shown using several experiments.

4.2 Grasping and Manipulation by Two-fingered Hands

4.2.1 Basic Equations

In this chapter, grasping and manipulation by two-fingered hands are deal with, where the assumptions are same as those in previous chapters. A two-fingered hand and an object are shown in Fig. 4.1. Where Σ_B is the base coordinate frame, Σ_o the object coordinate frame, $\boldsymbol{r}_p = [r_{px} \quad r_{py}]^{\mathrm{T}}$ the position vector of the origin of Σ_o from the origin of Σ_B, and θ the orientation of the object. $\boldsymbol{p}_i = [p_{ix} \quad p_{iy}]^{\mathrm{T}}$ is the position vector of the contact point C_i of the i-th fingertip force.

The kinematical constraint among the fingertips, as mentioned in the previous chapter, is represented by the following equation.

$$\boldsymbol{J}_o \dot{\boldsymbol{r}} = \boldsymbol{J}_f \dot{\boldsymbol{q}} \tag{4.1}$$

where $\dot{\boldsymbol{r}} = [\dot{\boldsymbol{r}}_p^{\mathrm{T}} \quad \dot{\theta}]^{\mathrm{T}} \in \mathrm{R}^3$ is the velocity of the object, $\dot{\boldsymbol{q}} = [\dot{\boldsymbol{q}}_1^{\mathrm{T}} \quad \dot{\boldsymbol{q}}_2^{\mathrm{T}}]^{\mathrm{T}} \in \mathrm{R}^4$ the velocity of the joint variable, $\boldsymbol{J}_o$ is

$$\boldsymbol{J}_o = \begin{bmatrix} \boldsymbol{J}_{o1} \\ \boldsymbol{J}_{o2} \end{bmatrix}, \quad \boldsymbol{J}_{oi} = \begin{bmatrix} \boldsymbol{E}_2 & \begin{matrix} -p_{iy} \\ p_{ix} \end{matrix} \end{bmatrix}$$

$\boldsymbol{E}_n$ denotes the unity matrix, and $\boldsymbol{J}_f$ represents the Jacobian matrix which has the Jacobian matrix of each finger as diagonal element.

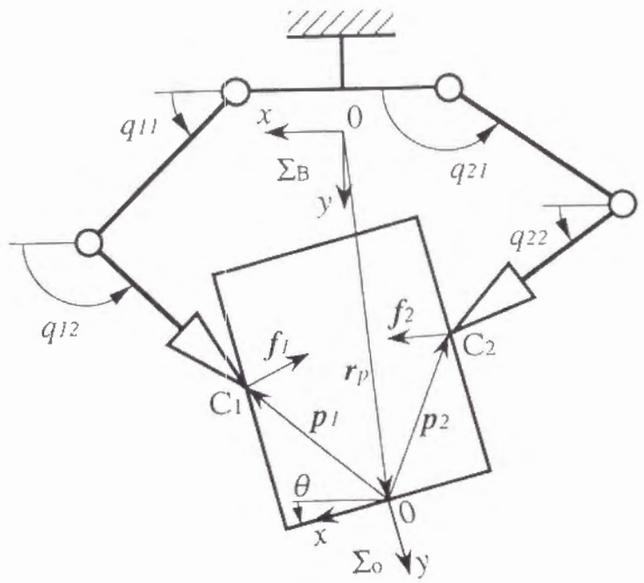

Fig. 4.1. Two-fingered hand and object.

The equation of motion of the two fingered hand can be expressed by the following equation.

$$\boldsymbol{M}_f \ddot{\boldsymbol{q}} + \boldsymbol{h}_f + \boldsymbol{J}_f^{\mathrm{T}} \boldsymbol{F} = \boldsymbol{\tau} \tag{4.2}$$

where $\boldsymbol{\tau} = [\boldsymbol{\tau}_1^{\mathrm{T}} \quad \boldsymbol{\tau}_2^{\mathrm{T}}]^{\mathrm{T}} \in \mathrm{R}^4$ represents the joint torque vector, $\boldsymbol{F} = [\boldsymbol{f}_1^{\mathrm{T}} \quad \boldsymbol{f}_2^{\mathrm{T}}]^{\mathrm{T}} \in \mathrm{R}^4$ represents the fingertip force, $\boldsymbol{M}_f$ the inertia matrix of the fingers, and $\boldsymbol{h}_f$ the centrifugal force, Coriolis force and the gravity force.

In this chapter, the maximum joint torque is assumed to be limited by the following equation.

$$|\tau_{ij}| \leq \tau_{ij\max} \tag{4.3}$$

where τ_{ij} is the joint torque of the j-th joint of the i-th finger, and $\tau_{ij\max}$ is the constant determined by the actuator and the reduction system.

The equation of motion of the object can be expressed by the following equation.

$$\boldsymbol{M}_o \ddot{\boldsymbol{r}} + \boldsymbol{h}_o = \boldsymbol{T} \tag{4.4}$$

$$\boldsymbol{T} = \boldsymbol{J}_o^{\mathrm{T}} \boldsymbol{F} \tag{4.5}$$

where $\boldsymbol{T} = [\boldsymbol{f}^{\mathrm{T}} \quad N]^{\mathrm{T}} \in \mathrm{R}^3$ represents a total force applied to the object, $\boldsymbol{M}_o$ the inertia matrix of the object, $\boldsymbol{h}_o$ the centrifugal fore, the Coriolis force, and the gravity force.

4.3 Dynamic Manipulation/Grasping Controller of Two-fingered Hands

In this section, the dynamic manipulation/grasping controller of two-fingered hands with planar motion is described briefly.

The grasping force $F_g = [f_{g1}^{\mathrm{T}} \ f_{g2}^{\mathrm{T}}]^{\mathrm{T}} \in \mathrm{R}^4$ and the manipulating force $F_m = [f_{m1}^{\mathrm{T}} \ f_{m2}^{\mathrm{T}}]^{\mathrm{T}}$ of two-fingered hands are expressed by the following equations.

$$
\begin{aligned}
F &= F_g + F_m && (4.6)\\
F_g &= B_g h_g, \quad B_g \in \mathrm{R}^{4\times 1} && (4.7)\\
h_g &\geq 0 && (4.8)\\
F_m &= B_m h_m, \quad B_m \in \mathrm{R}^{4\times 3} && (4.9)\\
h_m &= [h_{m1} \ h_{m2} \ h_{m3}]^{\mathrm{T}}, \quad h_{m1} \geq 0 && (4.10)
\end{aligned}
$$

An example of the manipulating and grasping forces is shown in Fig. 4.2. h_g in Eq. (4.8) is called the grasp parameter and determines f_{g1} and f_{g2}.

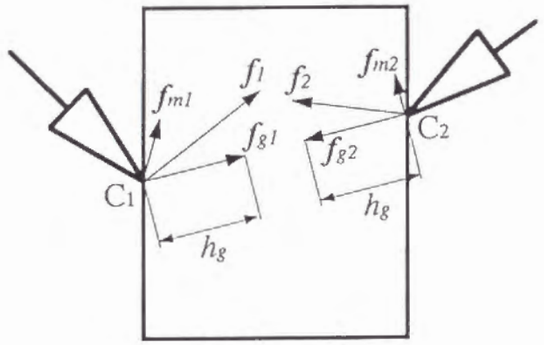

Fig. 4.2. Manipulating and grasping forces.

In planar motion, the orientation of the object is expressed by the angle around the normal axis to the plane, so it is not necessary to use two types of variables for orientation like in Chapter 3. In this case, the joint torque which linearizes the system is calculated by the following equations.

$$
\begin{aligned}
\tau_c &= \tau_o + \tau_f && (4.11)\\
\tau_o &= J_f^{\mathrm{T}} F_d && (4.12)\\
F_d &= F_{md} + F_{gd} && (4.13)\\
F_{md} &= B_m (J_o^{\mathrm{T}} B_m)^{-1} (M_o u_1 + h_o) && (4.14)
\end{aligned}
$$

$$
\begin{aligned}
F_{gd} &= B_g u_2 && (4.15)\\
\tau_f &= M_f \ddot{q}_d + h_f && (4.16)\\
\ddot{q}_d &= J_f^{-1} (J_o u_1 + \dot{J}_o \dot{r} - \dot{J}_f \dot{q}) && (4.17)
\end{aligned}
$$

where $u_1 \in \mathrm{R}^3$ and $u_2 \in \mathrm{R}^1$ are the control inputs to the linearize system. Then, the system is linearized as follows.

$$
\begin{aligned}
\ddot{r} &= u_1 && (4.18)\\
h_g &= u_2 && (4.19)
\end{aligned}
$$

On the other hand, the servo compensator is just same as that in Chapter 3.

$$
\begin{aligned}
u_1 &= \ddot{r}_d + K_P e + K_I \int e dt + K_D \dot{e} && (4.20)\\
e &= r_d - r && (4.21)\\
u_2 &= h_{gd2} + K_F \int (h_{gd2} - h_g) dt && (4.22)\\
h_{gd2} &= h_{gd} - T_c \dot{h}_{gd2} && (4.23)
\end{aligned}
$$

where r_d is the desired trajectory of the object, h_{gd} the desired trajectory of the grasp parameter, and T_c the time constant in the first order lag for the desired response of the grasp parameter.

4.4 Adaptive Grasping

4.4.1 Evaluation of Grasping and Manipulation

In this section, scalar indexes for evaluation of grasping and manipulation are defined and a method of adaptive grasping, which changes the grasping force according to a given task, is proposed.

Firstly scalar indexes of manipulation and grasping are defined as follows.

Index of Manipulation:

$$
\begin{aligned}
J_m &= \frac{1}{t_2 - t_1} \int_{t1}^{t2} ||e_m||^2 dt && (4.24)\\
e_m &= L^{-1} (r_d - r)\\
L &= \mathrm{diag.}(r_{prs}, \ r_{pys}, \ \theta_s)
\end{aligned}
$$

Index of Grasping :

$$
\begin{aligned}
J_g &= \frac{1}{t_2 - t_1} \int_{t1}^{t2} ||e_g||^2 dt && (4.25)\\
e_g &= [e_{g1} \quad e_{g2}]^{\mathrm{T}}\\
e_{gi} &= \frac{|\theta_i|}{\theta_{i\max} - |\theta_i|}\\
\theta_{i\max} &= \tan^{-1}(\mu_i)
\end{aligned}
$$

where t_1 and t_2 represent the starting and ending times of the evaluation. L shows the matrix to normalize the error, θ_i the angle between the fingertip force $\boldsymbol{f}_i$ and an inward normal vector of the contact plane on the object, μ_i shows a maximum coefficient value of static friction, $\theta_{i\max}$ the maximum value of θ_i dependent on μ_i. Index J_m means the tracking performance of manipulation and index J_g probability of non-slip grasping. e_{gi} in Eq. (4.25) is introduced to evaluate probability of non-slip grasping of i-th finger, shown in Fig. 4.3. J_m and J_g are defined as those having small values when manipulation and grasping are well carried out.

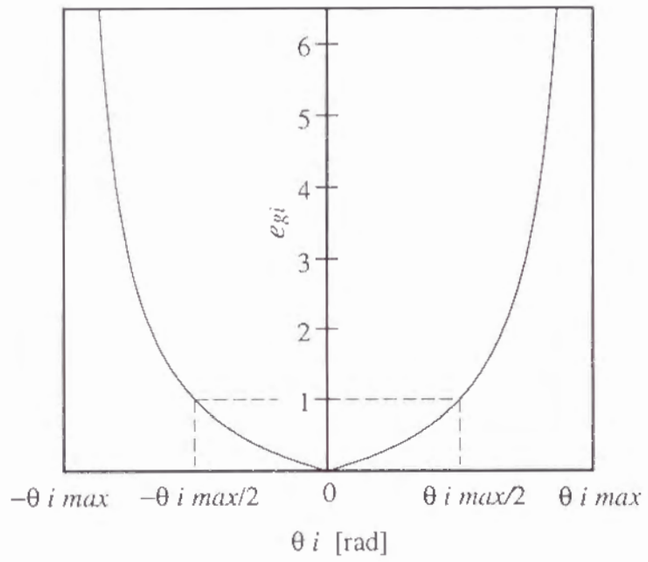

Fig. 4.3. Value of e_{gi}.

Following paragraphs describes that J_m and J_g change according to not only control schemes and manipulation tasks but also grasping situation determined by the desired value of grasp parameter h_{gd}.

First, it is shown that J_g is affected by h_{gd} intuitively. When h_{gd} is determined to have a small value, θ_i has a big value because the grasping force is small and the direction of the fingertip force is dominated by that of the manipulating force. Then, J_g has a big value. In this case, if θ_i becomes $\theta_{i\max}$, J_g becomes infinity. On the other hand, when h_{gd} is determined to have a big value, θ_i has a small value because the direction of the fingertip force is dominated by that of the grasping force. Then, J_g has a small value.

Second, it is shown that J_m is affected by h_{gd}. The joint torque consists of τ_f which is required for motion of the fingers, $\boldsymbol{J}_f^{\mathrm{T}}\boldsymbol{F}_{md}$ which is required for manipulation of the object, and $\boldsymbol{J}_f^{\mathrm{T}}\boldsymbol{F}_{gd}$ which is required to produce the grasping force. Therefore, when $\tau_f + \boldsymbol{J}_f^{\mathrm{T}}\boldsymbol{F}_{md} + \boldsymbol{J}_f^{\mathrm{T}}\boldsymbol{F}_{gd}$ exceeds the limited value because of a big h_{gd}, the joint torque which is required for motion of the fingers and the manipulation, $\tau_f + \boldsymbol{J}_F^{\mathrm{T}}\boldsymbol{F}_{md}$, can not be produced. That is, J_m becomes to have a bigger value in comparison with the case when h_{gd} and the grasping force are small.

The grasping force in this paper is the internal force which always produces no resultant force. Consequently, any stiffness of the system will not be affected by the grasping force. Hanafusa et al. defined the internal force in another way, and discussed the changes of stiffness of the system by that internal force[15].

4.4.2 Determination of Grasping Force by Adaptive Grasping

In this section, an algorithm of adaptive grasping is proposed.

For adaptive grasping, both manipulation and grasping must be considered. Consequently, scalar index J is defined as follows:

$$J = wJ_m + J_g \tag{4.26}$$

where $w > 0$ is the weighting parameter. Considering the characteristics of J_m and J_g, J becomes a big value when h_{gd} is a small value and when h_{gd} is a big value. Furthermore, J seems to have a minimum value when h_{gd} has a certain value, then a set of situations of grasping and manipulation becomes the best.

The following procedure is a proposed algorithm for adaptive grasping, which determines the grasping force. In the algorithm, $h_{gd}(n)$ and $J(n)$ mean the values of h_{gd} and J in the n-th trial, respectively.

Algorithm of adaptive grasping

Step 1: Set $\omega > 0$, $k < 0$, $\varepsilon > 0$

Step 2: Set realizable $h_{gd}(0)$ and manipulate an object with $h_{gd} = h_{gd}(0)$. Calculate J by Eq. (4.26) and $J(0) = J$.

Step 3: Set realizable $h_{gd}(1)(\neq h_{gd}(0))$.
set trial number n as $n = 1$.

Step 4: Manipulate the object with $h_{gd} = h_{gd}(n)$.
calculate J and $J(n) = J$.

Step 5: Calculate the change of J, $\Delta J(n)$, by means of the following equation.

$$\Delta J(n) = J(n) - J(n-1) \tag{4.27}$$

If $\Delta J(n) \leq \varepsilon$, go to Step 8.
If $\Delta J(n) > \varepsilon$, go to Step 6.

Step 6: Calculate $h_{gd}(n+1)$ by means of the following equation.

$$h_{gd}(n+1) = h_{gd}(n) + k\frac{\Delta J(n)}{\Delta h_{gd}(n)} \quad (4.28)$$

$$\Delta h_{gd}(n) = h_{gd}(n) - h_{gd}(n-1) \quad (4.29)$$

Step 7: $n \leftarrow n+1$. Go to Step 4.

Step 8: End.

This algorithm is expected to minimize J with a suitable h_{gd}, that is to improve grasping and manipulation. ε introduced in Step 5 is dependent on the scattering of J caused by the noise of detected data like the fingertip force. This ε, which is set to have a small positive value, determines the terminal condition.

4.5 Experiment

In this section, experimental results illustrate the validity of the proposed algorithm.

The two-fingered hand and the object used in the experiment are shown in Fig. 4.4 and Fig. 4.5. Table 4.1 shows length ℓ_{ik}, mass m_{ik}, and the principal moment of the inertia around the centers of gravity I_{ik} of the k-th link of the i-th finger, where the center of gravity are assumed to be center of each link. A DC servo motor with a power of 50[W] is used as the actuator for each joint, and the reduction ratio is 1/5. The span between the first joint of two fingers is 0.30[m]. Σ_B is located as the origin of it is at the middle of the first joints of the fingers, and as the directions of the axes are shown in the figure.

Table 4.1. Parameters of the finger.

k	ℓ_{ik}[m]	m_{ik}[kg]	I_{ik}[kg · m^2]
1	0.30	0.40	0.49×10^{-3}
2	0.15	0.26	3.00×10^{-3}
3	0.30	0.40	3.00×10^{-3}
4	0.45	0.58	9.79×10^{-3}

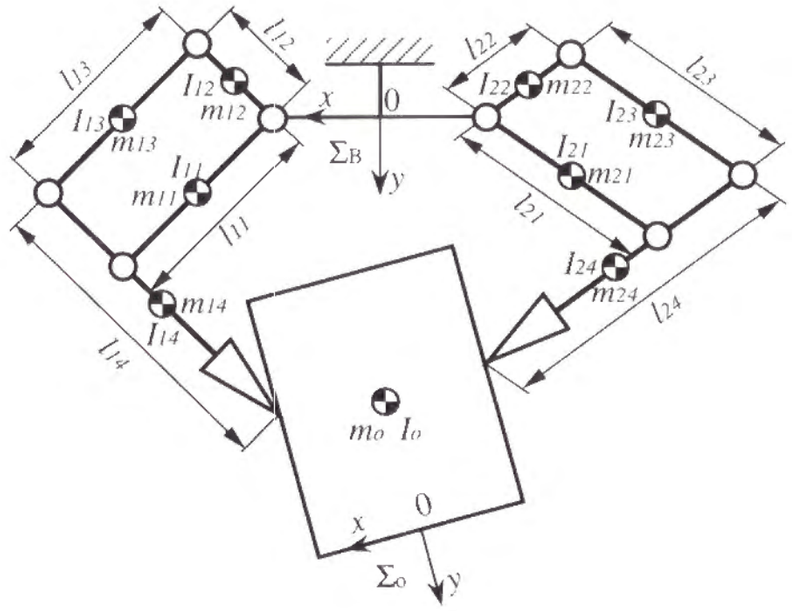

Fig. 4.4. Two-fingered hand and object.

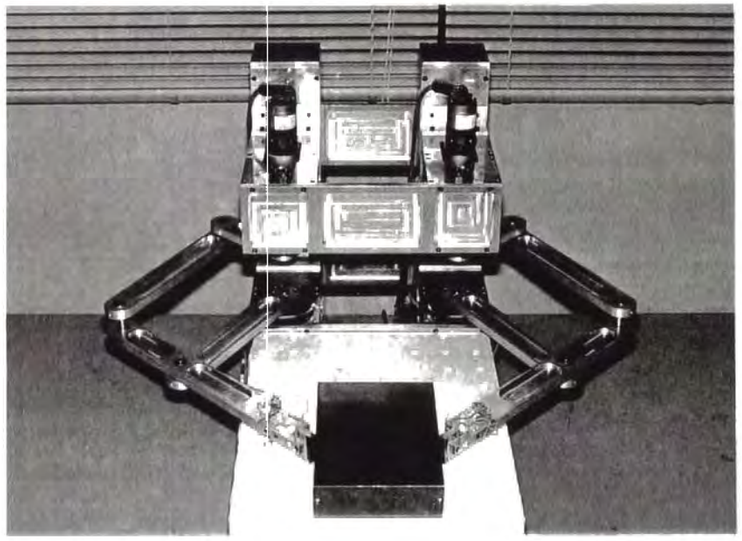

Fig. 4.5. Experimental setup.

The object is rectangular with a width of 0.17[m], and a length of 0.25[m]. Table 4.2 shows mass m_o and the principal moment of the inertia around the center on gravity I_o of the object. Two contact points are located at the center of both sides.

Table 4.2. Parameters of the object.

m_O[kg]	I_O[kg · m^2]
0.35	2.67×10^{-3}

As a preparation of the experiments, the characteristics of friction, which are required in the linearization of the system, are identified based on the method of identification[41]. Table 4.3 shows the motion friction forces of the joint torque along the plus and the minus direction, τ^{+}_{mij} and τ^{-}_{mij}, and the viscous frictional coefficient, V_{ij}.

Table 4.3. Parameters of friction.

ij	τ^{+}_{mij}[Nm]	τ^{-}_{mij}[Nm]	V_{ij}[Nm/(rad/s)]
11	0.169	-0.120	0.102
12	0.178	-0.251	0.065
21	0.205	-0.157	0.113
22	0.196	-0.146	0.081

The desired trajectory of the manipulation is given as the position of the object on the circle with a radius of 0.05[m], and as the orientation constant, $\theta = 0$. During the first 1[s] of the experiment, the object is assumed to be supported by a table at the initial position and orientation, because it is necessary to realize a secure grasp before manipulation. The desired velocity is determined by ω_{max}, which is the maximum frequency of the circular motion.

A coefficient of static friction is treated as $\mu_i = 1/\sqrt{3}$, that means $\theta_{\mathrm{imax}} = 30$[deg]. The limitation of the joint torque is assumed by the following equation:

$$\tau_{ij\mathrm{max}} = 2 \ [\mathrm{Nm}] \tag{4.30}$$

Indeed this limitation appears as saturation of the driver amplifier, however, it is reasonable to treat this limitation as Eq. (4.3) so as to discuss its effect clearly.

The gains and time constant in the servo compensator are $\boldsymbol{K}_P = \mathrm{diag.}(100, 100, 100)$, $\boldsymbol{K}_I = \mathrm{diag.}(50, 50, 50)$, $\boldsymbol{K}_D = \mathrm{diag.}(8, 8, 8)$, and $T_c = 0.05$[s]. Sampling time is 3.7[ms]. First, the relation of the value of the indexes and responses of manipulation and grasping are investigated. Figures 4.6 $\sim$ 4.9 show the results of manipulation and grasping, respectively, in the case of $\omega_{max} = 1.0$[Hz], where $h_{gd} = 2.5$[N] and $h_{gd} = 6.0$[N]. In the case of $h_{gd} = 2.5$[N], these results show that a response of manipulation is better, but the response of grasping is worse. Note that the response of grasping should be evaluated not by h_g but by θ_i. On the other hand, in the case of $h_{gd} = 6.0$[N], these results show that a response of manipulation is worse, but a response of grasping is better.

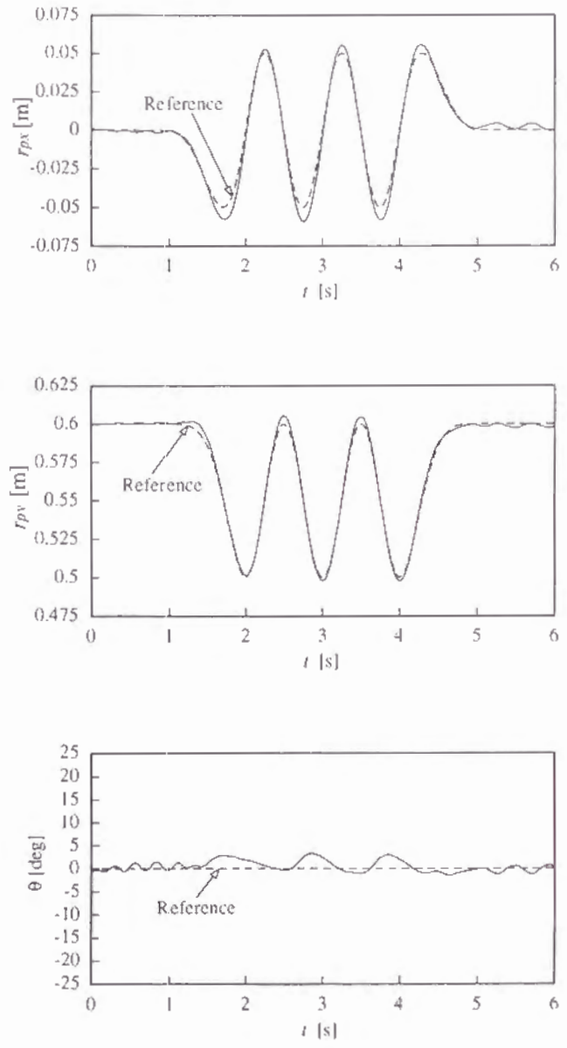

Fig. 4.6. Experimental results of manipulation ($h_{gd} = 2.5$[N]).

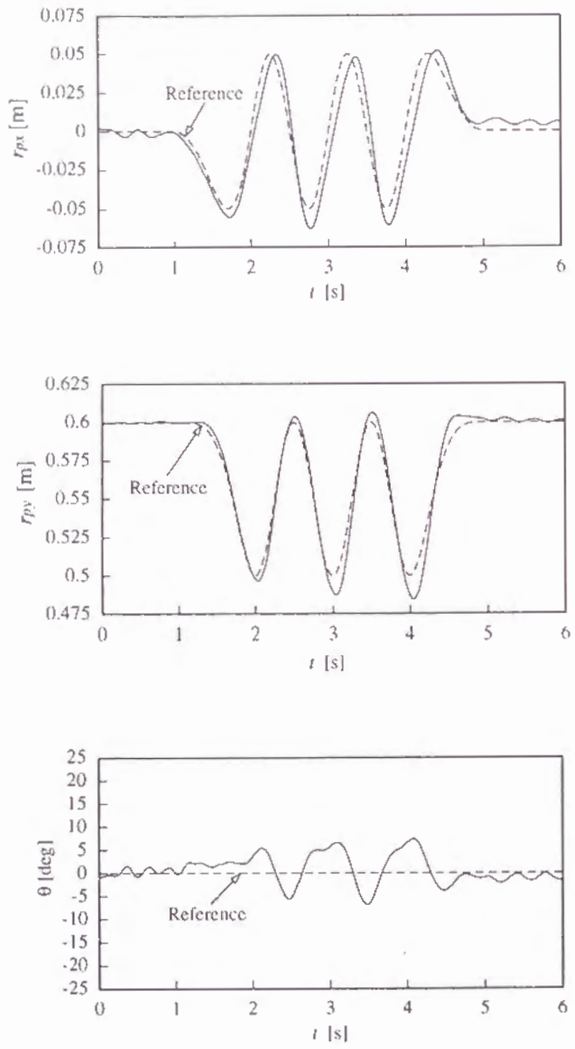

Fig. 4.7. Experimental results of manipulation (h_{gd}=6.0[N]).

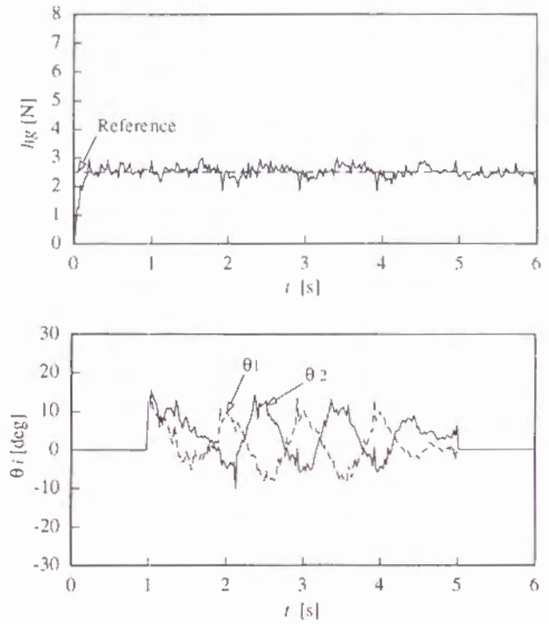

Fig. 4.8. Experimental results of grasping (h_{gd} = 2.5[N]).

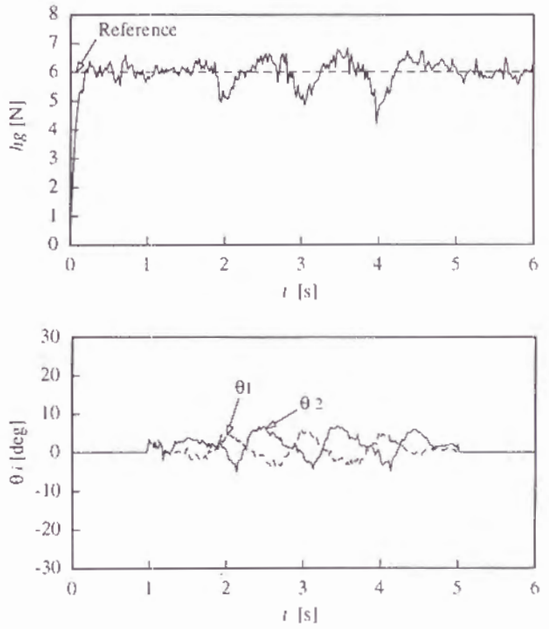

Fig. 4.9. Experimental results of grasping (h_{gd}=6.0[N]).

The reasons why these trials are tested in the cases of $h_{gd} = 2.5$[N] and $h_{gd} = 6.0$[N] are as follows: In the case of $h_{gd} = 2.0$[N], slipping occurs during manipulation. Also, in the case that h_{gd} has an exceedingly value, the manipulation can not be continued due to a big orientational error.

Figure 4.10 shows the changes in joint torque. In the case of $h_{gd} = 6.0$[N], the required joint torque can not be obtained because of its limitation.

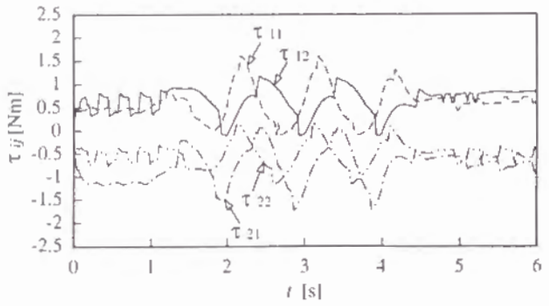

(a) $h_{gd} = 2.5$[N]

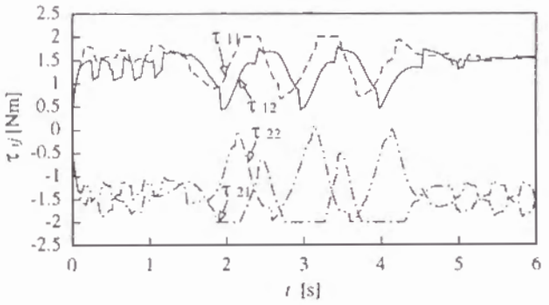

(b) h_{gd}=6.0[N]

Fig. 4.10. Experimental results of joint torques.

Figure 4.11 shows the changes in the indexes J_m, J_g and J according to the changes in h_{gd}, in the cases of $\omega_{max} = 1.0$[Hz], 1.1[Hz], and 1.2[Hz]. To change the value of ω_{max} means to change the manipulation task. The parameters are as follows: $t_1 = 1$[s], $t_2 = 5$[s], $r_{pxs} = r_{pys} = 1$, $\theta_s = 0.085$ considering the width of the object and $\omega = 200$.

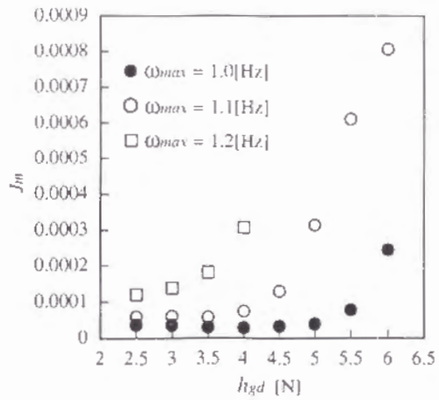

(a) J_m for manipulation

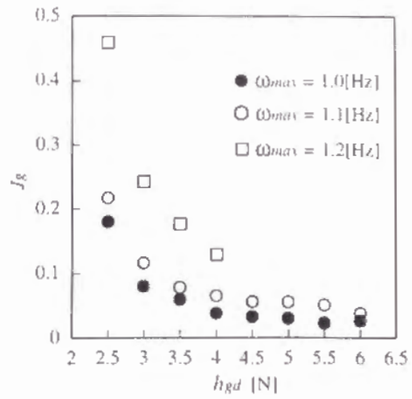

(b) J_g for grasping

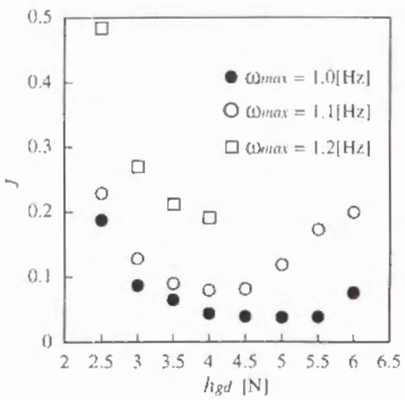

(c) J for manipulation and grasping

Fig. 4.11. Scalar functions for manipulation and grasping.

If ω_{max} becomes bigger, J generally becomes bigger as well. Especially, in the case of $\omega_{max} = 1.0$[Hz] and 1.1[Hz], J has the minimum value, that is there exist an optimal combination of grasping and manipulation. In the case of $\omega_{max} = 1.2$[Hz], the manipulation can not be continued where $h_{gd} \geq 4.5$[N], and J does not have a minimum value. However, it seems possible that J has a minimum value with a suitable ω. h_{gd}, with the minimum value of J, has a smaller value when $\omega_{max} = 1.1$[Hz] comparing with the case when $\omega_{max} = 1.0$[Hz]. This means that the effect of the limitation of the joint torque appears strong, because the required joint torque for the manipulation is bigger when ω_{max} is bigger.

Second, the proposed algorithm is tested to investigate its validity, in the case of $\omega_{max} = 1.0$[Hz], where $\omega = 200$, $k = -10$, $\varepsilon = 0.002$. Figure 4.12 shows the changes in J and h_{gd}, where $h_{gd}(0) = 2.5$[N], $h_{gd}(1) = 3.0$[N] in Case I, and $h_{gd}(0) = 6.0$[N], $h_{gd}(1) = 5.5$[N] in Case II.

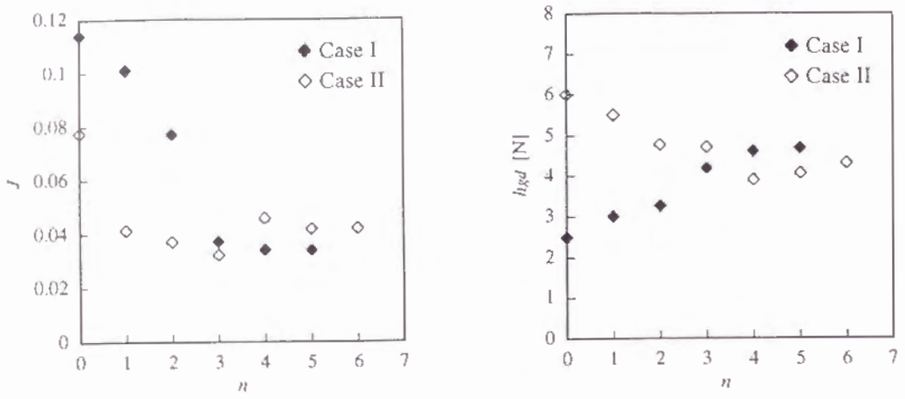

(a) Change of J (b) Adaptation of h_{gd}

Fig. 4.12. Experimental results of adaptive grasping.

The final values of J are $J(5) = 0.0338$ in Case I and $J(6) = 0.0420$ in Case II. The final values of h_{gd} are $h_{gd}(5) = 4.69$[N] in Case I and $h_{gd}(6) = 4.31$[N] in Case II. The reason why the two values of h_{gd} are different seems to be due to the scattering of J. Indeed, in Fig. 4.11(c), J has a similar value near the minimum one, that is the optimum one, with a certain value of h_{gd} between $h_{gd} = 4.0$ and $h_{gd} = 5.5$.

Figures 4.13, Fig. 4.14 and 4.15 show the results of manipulation, grasping and the produced joint torques respectively. The response of manipulation in Fig. 4.13 is better than that of Fig. 4.7, and the response of grasping in Fig. 4.14 is better than that of Fig. 4.8, although the produced torque was not enough in Fig. 4.15. These results show the validity of the proposed algorithm.

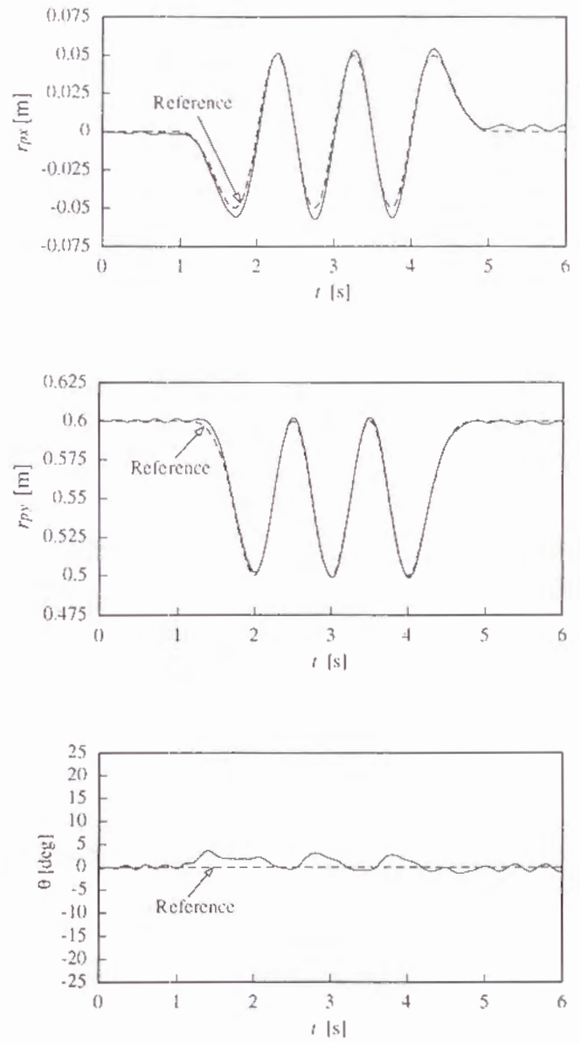

Fig. 4.13. Experimental results of manipulation with suitable h_{gd}.

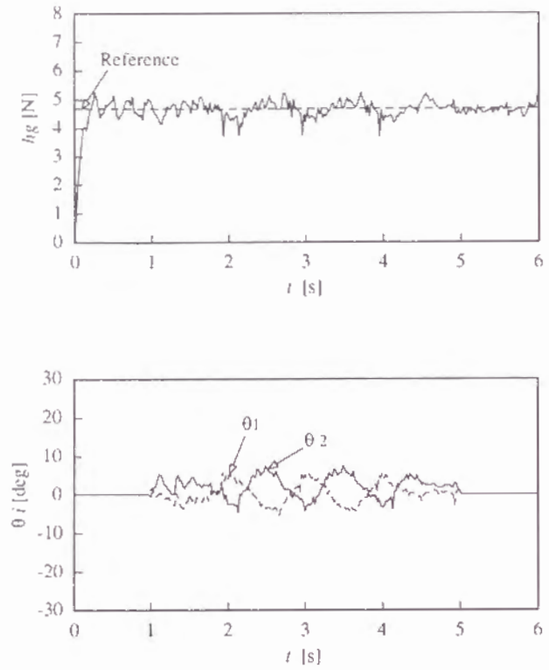

Fig. 4.14. Experimental results of grasping with suitable h_{gd}.

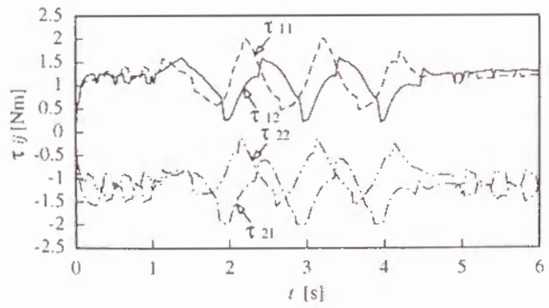

Fig. 4.15. Experimental results of joint torques with suitable h_{gd}.

4.6 Conclusion

The major results obtained in this chapter are summarized as follows.

1) An algorithm of adaptive grasping for two-fingered hands is proposed. This algorithm is valid for repeated manipulation tasks with the constraints of static friction of fingertip and joint torque.

2) The validity of the proposed algorithm is shown using experimental results.

The proposed algorithm seems to be valid to change the grasping force suitable

Chapter 5

Impedance Control of Redundant Macro-Micro Manipulators

5.1 Introduction

Macro-micro manipulator systems have been proposed to improve the capability of position and force control[23], [46], [60]. Khatib has pointed out that the inertia of the endpoint of manipulator can be decreased [23]. Sharon et al. have shown that the bandwidth of the position and force controllers can be expanded[46]. Yoshikawa et al. have proposed to use a rigid micro manipulator attached to a flexible manipulator in order to improve the tracking capability of the endpoint[60].

Macro-micro manipulators often have redundancy. To the problem of redundancy Hanafusa et al. have proposed a method of utilization of redundancy from the kinematical point of view[13]. Yokoi et al. have proposed to control not only the compliance of the endpoint but also the compliance of the joints according to the degrees of redundancy[55]. However, since these controllers are based on the kinematics and stiffness, the dynamic behavior of the manipulators has not been mentioned. Therefore they may not be effective for control of macro-micro manipulators when external forces are applied to the endpoint of the manipulator.

In this chapter, an impedance control scheme of redundant macro-micro manipulators is proposed. By using this control scheme, we can specify not only the desired mechanical impedance of the end effector, but also that of the macro manipulator by considering the internal force applied at the tip of the macro manipulator. This control scheme can utilize both merits of the macro and micro manipulators. That is, by specifying a suitable set of the desired mechanical impedance, a compliant motion can be realized without any excessive joint torque of the macro manipulator, and a wide motion range of the macro manipulator can be used effectively to compensate a small motion range of the micro manipulator. In Section 5.2, basic equations are described. In Section 5.3, an impedance

controller for redundant macro-micro manipulators is proposed. In Section 5.4, a method for specification of stiffness of the macro manipulator for realizing the desired position of the micro manipulator is presented. In Section 5.5, simulation results are given to show the validity of the proposed controller.

5.2 Basic Equations

A redundant macro-micro manipulator discussed in this chapter is shown in Fig. 5.1. It is assumed to move in three dimensional space and both of the macro and micro manipulators are assumed to have 6 degrees of freedom. In the figure, $\Sigma_{\rm b}$, $\Sigma_{\rm M}$, and $\Sigma_{\rm m}$ mean the base coordinate frame, the macro coordinate frame, and the micro coordinate frame, respectively. The origin of $\Sigma_{\rm M}$ is located at the tip of the macro manipulator, and the origin of $\Sigma_{\rm m}$ is located at the endpoint of the manipulator. $\boldsymbol{T}_{ext}$ is the external force, and $\boldsymbol{T}_M$ is the internal force applied at the tip of the macro manipulator by the micro manipulator. $\dot{\boldsymbol{r}} \in {\rm R}^6$ is the velocity of the endpoint of the manipulator, and $\dot{\boldsymbol{r}}_M \in {\rm R}^6$ is the velocity of the macro manipulator. $\dot{\boldsymbol{r}}$ is expressed by a set of the translational and rotational velocity of $\Sigma_{\rm m}$, and $\dot{\boldsymbol{r}}_M$ is expressed by that of $\Sigma_{\rm M}$. To express three elements of the orientation, for example, a set of roll-pitch-yaw can be used.

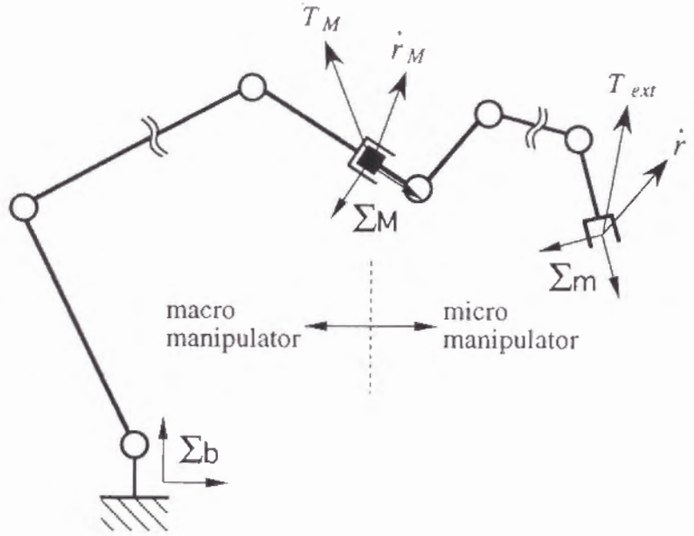

Fig. 5.1. Redundant macro-micro manipulator.

However, the position and orientation are described independently at first, because the

relation between $\dot{\boldsymbol{r}}$ and $\dot{\boldsymbol{r}}_M$ should be clear.

$\boldsymbol{r}_p \in {\rm R}^3$ and $\boldsymbol{r}_{Mp} \in {\rm R}^3$ are the position vectors of the origin of $\Sigma_{\rm m}$ and $\Sigma_{\rm M}$ from the origin of $\Sigma_{\rm b}$, respectively. For the micro manipulator, $\boldsymbol{r}_{mp} \in {\rm R}^3$ is used as the position vector of the origin of $\Sigma_{\rm m}$ from the origin of $\Sigma_{\rm M}$. $\boldsymbol{r}_{mp}$ is expressed as ${}^M\boldsymbol{r}_{mp}$, when $\boldsymbol{r}_{mp}$ is described in $\Sigma_{\rm M}$.

On the other hand, ${}^b\boldsymbol{A}_m \in {\rm R}^{3\times3}$, ${}^b\boldsymbol{A}_M \in {\rm R}^{3\times3}$, and ${}^M\boldsymbol{A}_m \in {\rm R}^{3\times3}$ are the transformation matrices of the orientation. ${}^b\boldsymbol{A}_m$ and ${}^b\boldsymbol{A}_M$ express the orientation of $\Sigma_{\rm m}$ and $\Sigma_{\rm M}$ described in $\Sigma_{\rm b}$, respectively. Superscript b on left side means $\Sigma_{\rm b}$, and may be neglected when it is obvious. ${}^M\boldsymbol{A}_m$ expresses the orientation of $\Sigma_{\rm m}$ described in $\Sigma_{\rm M}$.

The position of the endpoint can be expressed by Eq. (5.1) and the orientation of it can be expressed by Eq. (5.2), when the position and orientation of the macro and micro manipulators are given:

$$\boldsymbol{r}_p = \boldsymbol{r}_{Mp} + {}^b\boldsymbol{A}_M\,{}^M\boldsymbol{r}_{mp} \tag{5.1}$$

$${}^b\boldsymbol{A}_m = {}^b\boldsymbol{A}_M\,{}^M\boldsymbol{A}_m \tag{5.2}$$

where the position and orientation of the micro manipulator are assumed to be given in $\Sigma_{\rm M}$ at first. A set of three elements of the orientation can be derived by the transformation matrices of the orientation, and $\boldsymbol{r}$, $\boldsymbol{r}_M$, and $\boldsymbol{r}_m \in {\rm R}^6$ with it are used when it is necessary.

The velocity of the macro manipulator $\dot{\boldsymbol{r}}_M$ and the velocity of the micro manipulator $\dot{\boldsymbol{r}}_m \in {\rm R}^6$ in $\Sigma_{\rm M}$ can be expressed as follows:

$$\dot{\boldsymbol{r}}_M = \boldsymbol{J}_M \dot{\boldsymbol{q}}_M \tag{5.3}$$

$${}^M\dot{\boldsymbol{r}}_m = {}^M\boldsymbol{J}_m \dot{\boldsymbol{q}}_m \tag{5.4}$$

where $\dot{\boldsymbol{q}}_M \in {\rm R}^6$ and $\dot{\boldsymbol{q}}_m \in {\rm R}^6$ are the joint velocities of the macro and micro manipulators, respectively, and $\boldsymbol{J}_M$ and ${}^M\boldsymbol{J}_m$ are the Jacobian matrices. Then the velocity of the endpoint of manipulator can be expressed by,

$$\dot{\boldsymbol{r}} = \boldsymbol{J}_{Mm}\dot{\boldsymbol{r}}_M + {}^b\boldsymbol{R}_M\,{}^M\dot{\boldsymbol{r}}_m \tag{5.5}$$

where

$$\boldsymbol{J}_{Mm} = \begin{bmatrix} \boldsymbol{E}_3 & -\boldsymbol{P} \\ 0 & \boldsymbol{E}_3 \end{bmatrix} \tag{5.6}$$

$$\boldsymbol{P} = \begin{bmatrix} 0 & -p_z & p_y \\ p_z & 0 & -p_x \\ -p_y & p_x & 0 \end{bmatrix}$$

$$\boldsymbol{p} = [p_x\ p_y\ p_z]^{\rm T} = {}^b\boldsymbol{A}_M\,{}^M\boldsymbol{r}_{mp} \tag{5.7}$$

$${}^b\boldsymbol{R}_M = \begin{bmatrix} {}^b\boldsymbol{A}_M & 0 \\ 0 & {}^b\boldsymbol{A}_M \end{bmatrix}$$

and E_3 means the three dimensional unit matrix. By substituting Eqs. (5.3) and (5.4) to Eq. (5.5), we can get the following equation,

$$\dot{r} = J\dot{q} \tag{5.8}$$

where $\dot{q} = \left[\dot{q}_M^{\mathrm{T}} \quad \dot{q}_m^{\mathrm{T}}\right]^{\mathrm{T}}$ is the joint velocity of the whole manipulator and

$$J = \left[\begin{array}{cc} J_{Mm}J_M & {}^bR_M{}^MJ_m \end{array}\right]$$

is the Jacobian matrix of it.

The equation of motion of redundant macro-micro manipulator, to which an external force T_{ext} is applied at the endpoint, can be expressed like the case of ordinary manipulator as follows,

$$M_q\ddot{q} + h_q = \tau + J^{\mathrm{T}}T_{ext} \tag{5.9}$$

where $\tau = \left[\begin{array}{cc} \tau_M^{\mathrm{T}} & \tau_m^{\mathrm{T}} \end{array}\right]^{\mathrm{T}} \in \mathrm{R}^{2n}$ represents the joint torques, M_q represents the inertia matrix, h_q represents the non-linear term which includes the centrifugal, the Coriolis, and the gravity forces.

5.3 Control Law

The mechanical impedance is specified only for endpoint in the case of ordinary impedance control [16]. In the case of the proposed controller, the mechanical impedances are specified not only at the endpoint but also at the tip of the macro manipulator:

$$M_{rd}\ddot{r} + D_{rd}\dot{r}_e + K_{rd}r_e = T_{ext} \tag{5.10}$$

$$M_{Md}\ddot{r}_M + D_{Md}\dot{r}_{Me} + K_{Md}r_{Me} = T_M \tag{5.11}$$

where M_{rd}, D_{rd}, and K_{rd} are the desired matrices of inertia, coefficient of viscous friction, and stiffness of the endpoint; M_{Md}, D_{Md}, and K_{Md} are the desired matrices of inertia, coefficient of viscous friction, and stiffness of the macro manipulator, respectively; $r_e(= r - r_d)$ and $r_{Me}(= r_M - r_{Md})$ are position errors of the endpoint and macro manipulator; r_d, $r_{Md}(= r_d - r_{md})$, and r_{md} are the desired position of the endpoint, the macro manipulator, and the micro manipulator, respectively.

Note that the specification of the desired mechanical impedance of the endpoint is not for macro manipulator only but for the whole manipulator. Moreover, note that the internal force T_M is used in specifying the desired mechanical impedance. By considering this T_M, macro manipulator can be moved in order to compensate the small motion range of the micro manipulator.

Equations (5.10) and (5.11) can be combined as follows,

$$M_d\begin{bmatrix}\ddot{r}_M \\ \ddot{r}\end{bmatrix} + D_d\begin{bmatrix}\dot{r}_{Me} \\ \dot{r}_e\end{bmatrix} + K_d\begin{bmatrix}r_{Me} \\ r_e\end{bmatrix} = \begin{bmatrix}T_M \\ T_{ext}\end{bmatrix} \tag{5.12}$$

where M_d, D_d, and K_d are determined as follows.

$$M_d = \begin{bmatrix} M_{Md} & 0 \\ 0 & M_{rd} \end{bmatrix},\ D_d = \begin{bmatrix} D_{Md} & 0 \\ 0 & D_{rd} \end{bmatrix}$$

$$K_d = \begin{bmatrix} K_{Md} & 0 \\ 0 & K_{rd} \end{bmatrix}$$

Based on the above preparation, we can derive the following control law, which makes the redundant macro-micro manipulator expressed in Eq. (5.9) have the desired dynamics (5.12).

$$\begin{aligned}\tau = {} & M_q\tilde{J}^{-1}\left[M_d^{-1}\left\{\begin{bmatrix}T_M \\ T_{ext}\end{bmatrix} - D_d\begin{bmatrix}\dot{r}_{Me} \\ \dot{r}_e\end{bmatrix}\right.\right. \\ & \left.\left. -K_d\begin{bmatrix}r_{Me} \\ r_e\end{bmatrix}\right\} - \dot{\tilde{J}}\dot{q}\right] + h_q - J^{\mathrm{T}}T_{ext}\end{aligned} \tag{5.13}$$

where

$$\tilde{J} = \begin{bmatrix} J_M & 0 \\ J_{Mm}J_M & {}^bR_M{}^MJ_m \end{bmatrix}$$

5.4 Specification of Stiffness of Macro Manipulator

In this section, how to specify the stiffness of the macro manipulator is discussed, which makes the position and orientation of the micro manipulator converge toward their desired values, ${}^Mr_{mpd}$ and ${}^MA_{md}$, when a constant external force is applied at the endpoint.

As the preparation for this section, the desired value of J_{Mm}, J_{Mmd}, is derived previously. The desired position and orientation of the endpoint, r_{pd} and ${}^MA_{md}$, are assumed to be given by the specified task. Then the desired position and orientation of macro manipulator, r_{Mpd} and ${}^bA_{Md}$, are determined by Eqs. (5.1) and (5.2) as follows,

$$r_{Mpd} = r_{pd} - {}^bA_{Md}{}^Mr_{mpd} \tag{5.14}$$

$${}^bA_{Md} = {}^bA_{md}{}^MA_{md}{}^{-1} \tag{5.15}$$

Then, J_{Mm} becomes the following J_{Mmd},

$$J_{Mmd} = \begin{bmatrix} E_3 & -P_d \\ 0 & E_3 \end{bmatrix} \tag{5.16}$$

$$P_d = \begin{bmatrix} 0 & -p_{zd} & p_{yd} \\ p_{zd} & 0 & -p_{xd} \\ -p_{yd} & p_{xd} & 0 \end{bmatrix}$$

$$\boldsymbol{p}_d = [p_{xd}\ p_{yd}\ p_{zd}]^{\mathrm{T}} = {}^b\boldsymbol{A}_{Md}{}^M\boldsymbol{r}_{mpd} \tag{5.17}$$

Now, let's consider the manipulator in a state of rest,

$$\begin{bmatrix} \ddot{\boldsymbol{r}}_M \\ \ddot{\boldsymbol{r}} \end{bmatrix} = \begin{bmatrix} 0 \\ 0 \end{bmatrix}, \begin{bmatrix} \dot{\boldsymbol{r}}_M \\ \dot{\boldsymbol{r}} \end{bmatrix} = \begin{bmatrix} 0 \\ 0 \end{bmatrix} \tag{5.18}$$

So, the following equations are derived by substituting Eq. (5.18) to Eq. (5.12).

$$\boldsymbol{K}_{Md}\boldsymbol{r}_{Me} = \boldsymbol{T}_M \tag{5.19}$$

$$\boldsymbol{K}_{rd}\boldsymbol{r}_{re} = \boldsymbol{T}_{ext} \tag{5.20}$$

When the micro manipulator converges to the desired position and orientation, the following equations hold.

$$\boldsymbol{r}_e = \boldsymbol{J}_{Mmd}\boldsymbol{r}_{Me} \tag{5.21}$$

$$\boldsymbol{T}_M = \boldsymbol{J}_{Mmd}^{\mathrm{T}}\boldsymbol{T}_{ext} \tag{5.22}$$

where $\boldsymbol{J}_{Mmd}$ is expressed by Eq. (5.16).

Then, eliminating $\boldsymbol{T}_M$, $\boldsymbol{T}_{ext}$, and $\boldsymbol{r}_e$ from Eqs. (5.19) $\sim$ (5.22), we can get the following equation,

$$\begin{aligned} \boldsymbol{K}_{Md}\boldsymbol{r}_{Me} &= \boldsymbol{J}_{Mmd}^{\mathrm{T}}\boldsymbol{T}_{ext} \\ &= \boldsymbol{J}_{Mmd}^{\mathrm{T}}\boldsymbol{K}_{rd}\boldsymbol{r}_e \\ &= \boldsymbol{J}_{Mmd}^{\mathrm{T}}\boldsymbol{K}_{rd}\boldsymbol{J}_{Mmd}\boldsymbol{r}_{Me} \end{aligned} \tag{5.23}$$

That is, the desired position and orientation can be realized by specifying the stiffness of the macro manipulator by using the following equation, when $\boldsymbol{K}_{rd}$ is given by the specified task.

$$\boldsymbol{K}_{Md} = \boldsymbol{J}_{Mmd}^{\mathrm{T}}\boldsymbol{K}_{rd}\boldsymbol{J}_{Mmd} \tag{5.24}$$

5.5 Simulation

In this section, a redundant macro-micro manipulator moving in two dimension is used for simulation in order to investigate the validity of the proposed controller.

The macro and micro manipulators are assumed to have three joints. The parameters of the macro and micro manipulators are shown in Table 5.1. The motion ranges in joint space are assumed as follows.

$$\begin{aligned} 0 &\le q_{M1} \le \pi \\ -\pi &\le q_{M2} \le 0 \\ -\pi &\le q_{M3} \le 0 \\ 0 &\le q_{m1} \le \pi \\ -\pi &\le q_{m2} \le 0 \\ -\pi &\le q_{m3} \le 0 \end{aligned}$$

Of course, the motion range of endpoint of the micro in this case is small because the lengths of links of the micro manipulator are shorter than those of the macro.

Table 5.1. Parameters of macro-micro manipulator

(a) macro manipulator

link No.	1	2	3
length L_{Mi}[m]	1	1	0.2
mass m_{Mi}[kg]	10	10	2

(b) micro manipulator

link No.	1	2	3
length L_{mi}[m]	0.1	0.1	0.1
mass m_{mi}[kg]	0.1	0.1	0.1

Initial position and orientation of the manipulator, shown in Fig. 5.2, are given by initial joint angle, $\boldsymbol{q}_M(0)$ and $\boldsymbol{q}_m(0)$.

$$\boldsymbol{q}_M(0) = [3\pi/4\ \ -\pi/2\ \ -\pi/4]^{\mathrm{T}}$$
$$\boldsymbol{q}_m(0) = [3\pi/4\ \ -\pi/2\ \ -\pi/4]^{\mathrm{T}}$$

The desired position and orientation are assumed to be the same as the initial values. Initial velocity is assumed to be zero.

The desired mechanical impedances are specified as follows.

$$\boldsymbol{M}_{Md} = \mathrm{diag.}[10, 10, 0.2]$$
$$\boldsymbol{D}_{Md} = \mathrm{diag.}[200, 200, 4]$$
$$\boldsymbol{K}_{Md} = \mathrm{diag.}[1000, 1000, 20]$$

$$\boldsymbol{M}_{rd} = \mathrm{diag.}[0.1, 0.1, 0.002]$$
$$\boldsymbol{D}_{rd} = \mathrm{diag.}[200, 200, 0.4]$$
$$\boldsymbol{K}_{rd} = \mathrm{diag.}[1000, 1000, 20]$$

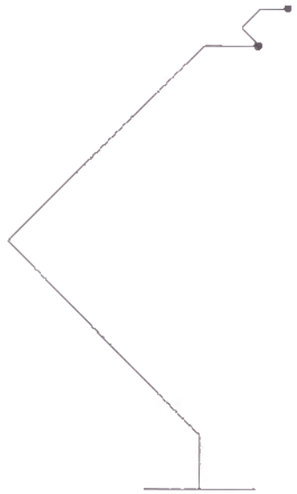

Fig. 5.2. Initial posture of redundant macro-micro manipulator for simulation.

To specify the above parameters, the following guidelines are considered.

1) The inertia of macro manipulator M_{Md} should not be made small because the original value of it is not small.

2) K_{Md} should be specified by Eq. (5.24) for making the position and orientation of micro manipulator go to the desired position and orientation.

3) D_{Md} and D_{rd} should be specified adequately by considering the damping factor of the second order system determined by Eqs. (5.10) and (5.11).

In this simulation, $\boldsymbol{D}_{Md}$ and $\boldsymbol{D}_{rd}$ are specified to make the damping factor be 1 by the following relations.

$$\frac{D_{Mdii}}{2\sqrt{M_{Mdii}K_{Mdii}}} = 1.0,\ ii = 11, 22, 33$$
$$\frac{D_{rdii}}{2\sqrt{M_{rdii}K_{rdii}}} = 1.0,\ ii = 11, 22, 33$$

Firstly, position response is investigated when the constant external force along x axis, $\boldsymbol{T}_{ext} = [\ 150[\mathrm{N}], 0[\mathrm{N}], 0[\mathrm{Nm}]\ ]^{\mathrm{T}}$, is applied. Figure 5.3(a) shows that the deviation of the endpoint $\boldsymbol{r}_e$ appears faster than that of the macro manipulator $\boldsymbol{r}_{Me}$, so that of the micro manipulator appears faster as the result. The reason for these motions are that the natural frequencies as the second order systems of the macro manipulator and the endpoint are,

$$\sqrt{\frac{K_{Mdii}}{M_{Mdii}}} = 10\ [\mathrm{rad/s}],\ ii = 11, 22, 33$$
$$\sqrt{\frac{K_{rdii}}{M_{rdii}}} \doteq 100\ [\mathrm{rad/s}],\ ii = 11, 22, 33$$

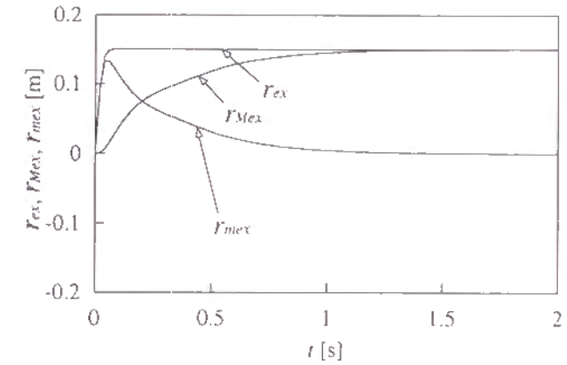

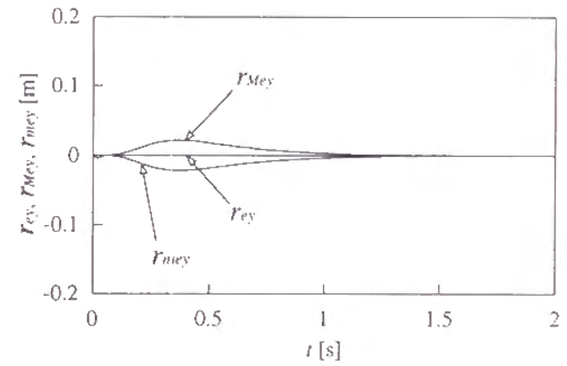

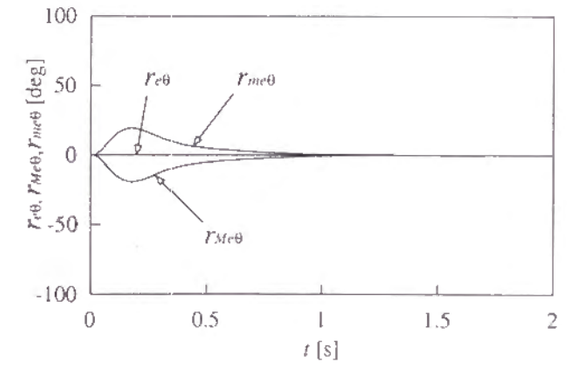

(a) deviation

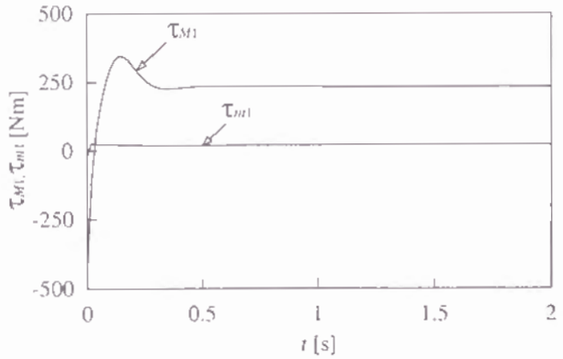

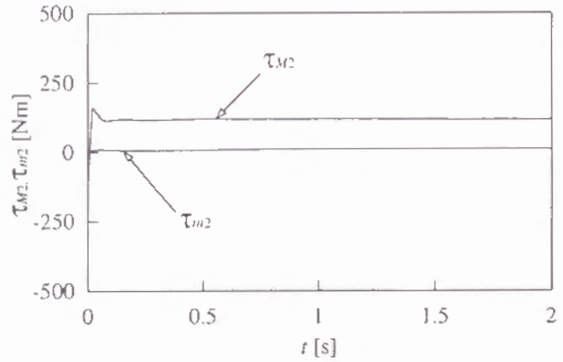

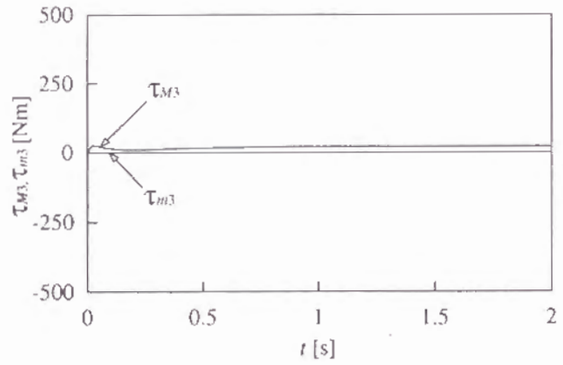

(b) joint torque

Fig. 5.3. Simulation results when external force is constant and $K_{Md} = J_{Mmd}^{\mathrm{T}} K_{rd} J_{Mmd}$.

Figure 5.3(b) shows the joint torques are not excessive because of the guideline 1). If this guideline is neglected, the joint torques must be excessive for changing the mass characteristics. Furthermore, the deviation of the micro manipulator r_{me} goes to be zero, even when the x element of $\boldsymbol{r}_e$ is 150[N]/1000[N/m]=0.15[m]. Therefore, the proposed controller

utilizes the small motion range of the micro manipulator effectively, against additional external forces.

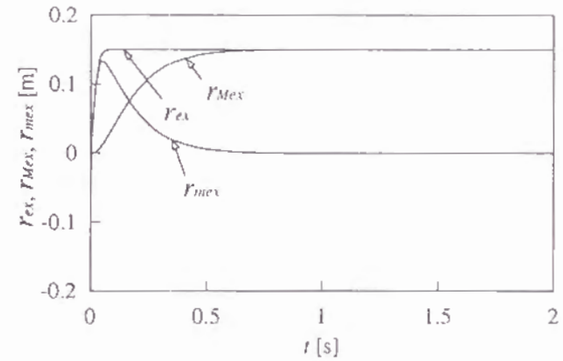

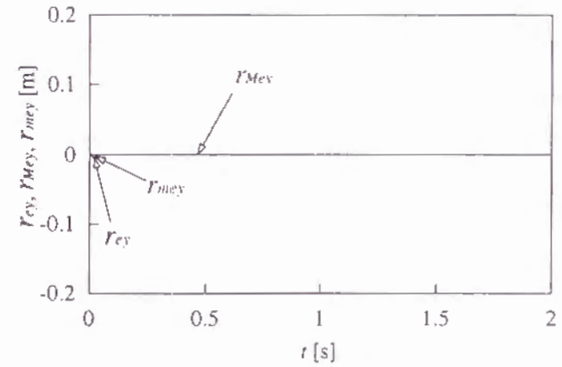

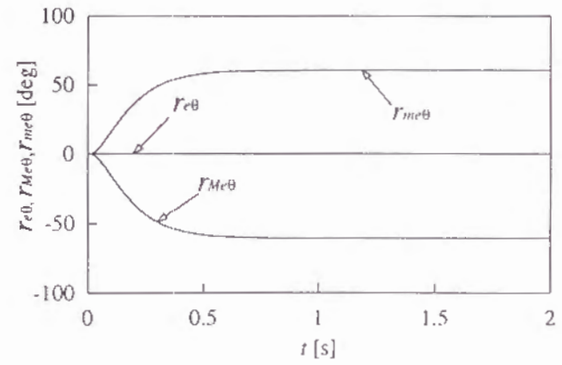

(a) deviation

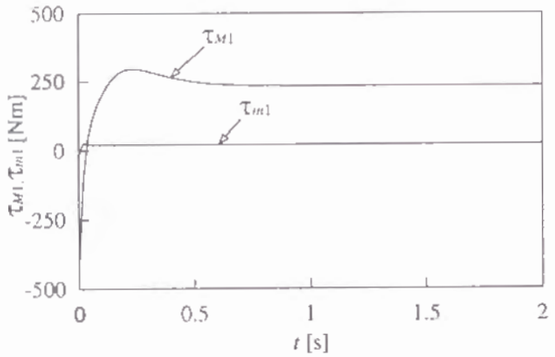

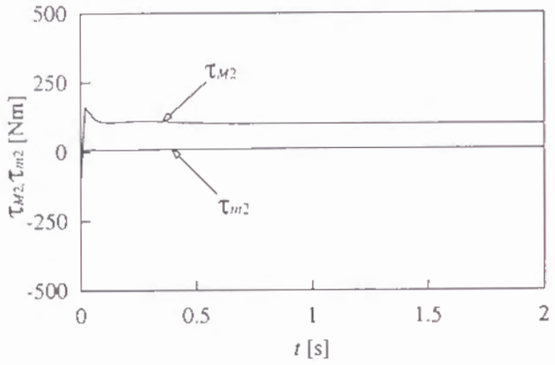

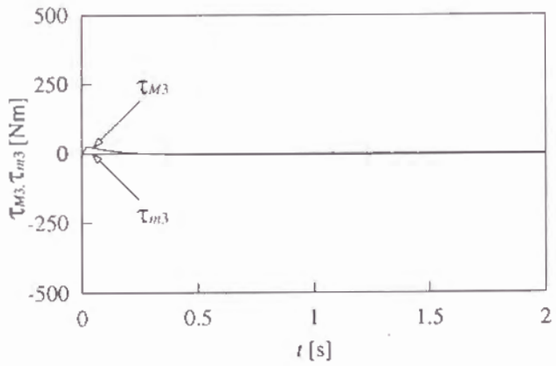

(b) joint torque

Fig. 5.4. Simulation results when external force is constant and $K_{Md} = K_{rd}$.

Secondly, to investigate the result of Section 5.4, that is Eq. (5.24), a similar situation is tested except $K_{Md} = K_{rd}$. Even Fig. 5.4(b) shows that the joint torques are not large, and, Fig. 5.4(a) shows that the $\boldsymbol{r}_{me}$ does not go to zero. Therefore, the first joint angle of the micro manipulator comes out of the motion range, as shown in Fig. 5.5.

Finally, the external force of the combined sine wave expressed by the following equation is applied.

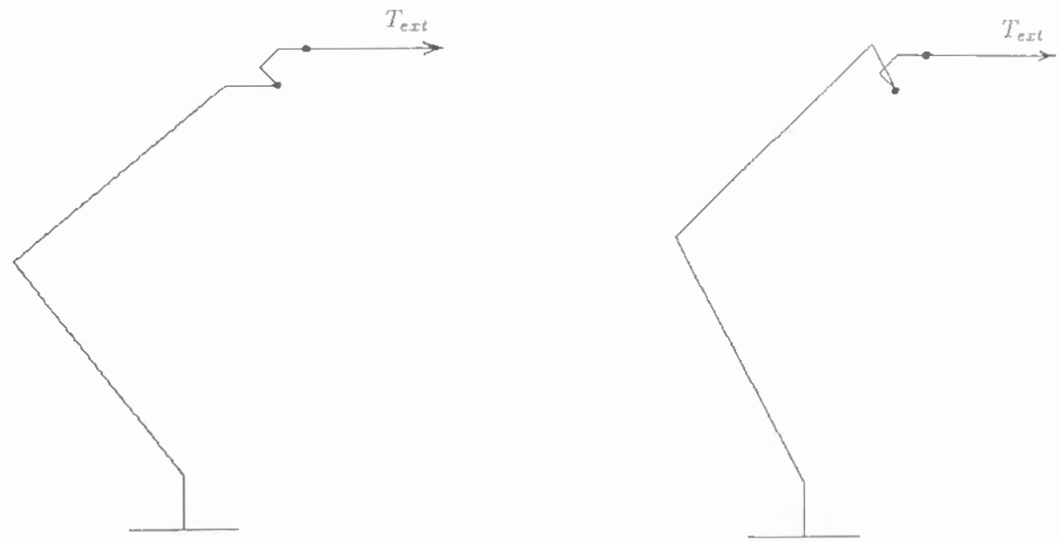

(a) $K_{Md} = J_{Mmd}^{\mathrm{T}} K_{rd} J_{Mmd}$ (b) $K_{Md} = K_{rd}$

Fig. 5.5. Final posture of macro-micro manipulator.

$$\boldsymbol{T}_{ext} = \begin{bmatrix} a_1(\cos(2\pi f_{r1}t) - 1) + a_2(\cos(2\pi f_{r2}t) - 1) \\ a_1 \sin(2\pi f_{r1}t) + a_2 \sin(2\pi f_{r2}t) \\ 0 \end{bmatrix} \tag{5.25}$$

where a_1, a_2 mean the amplitudes, f_{r1}, f_{r2} mean the values of frequency. Here the case of a_1=50[N], a_2=25[N], f_{r1}=0.25[Hz], f_{r2}=4.0[Hz] are tested and shown in Fig. 5.6(a). Figure 5.6(b) shows that the macro manipulator moves according to the lower frequency element of the external force, on the other hand, the micro manipulator moves according to its higher frequency element. Figure 5.6(c) shows the joint torques are not excessive. The results of this simulation mean that the proposed controller lets the macro-micro manipulator share the load by the external force. Then, a motion control which utilizes both of the merits, the wide motion range of the macro manipulator and the high capability of compliant motion of the micro manipulator, can be available by the proposed controller.

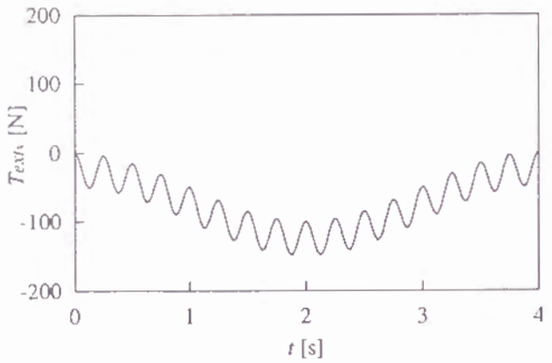

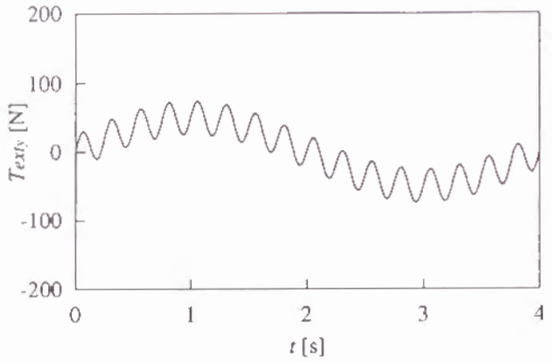

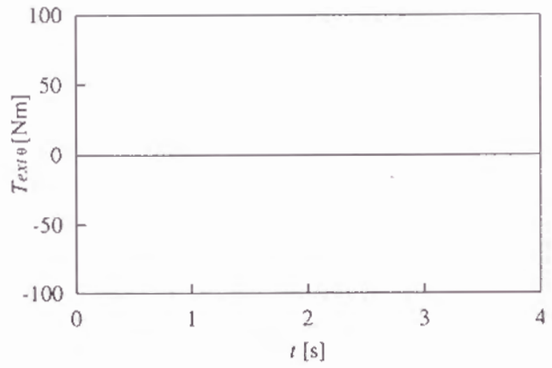

(a) external force

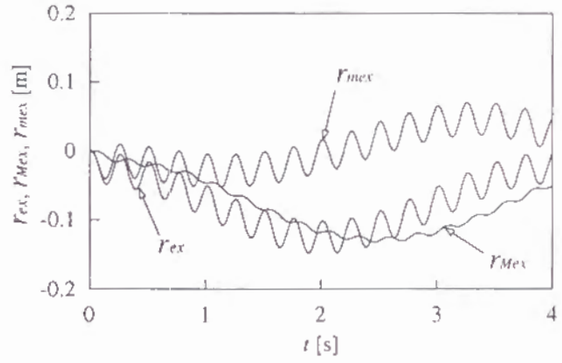

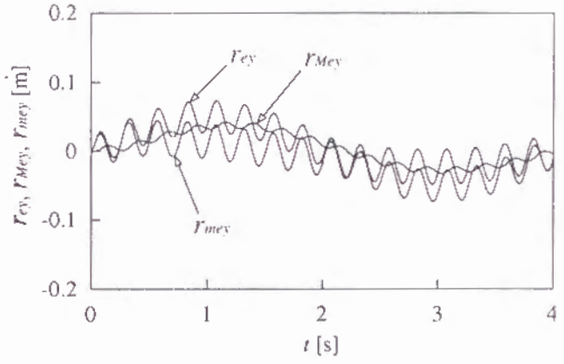

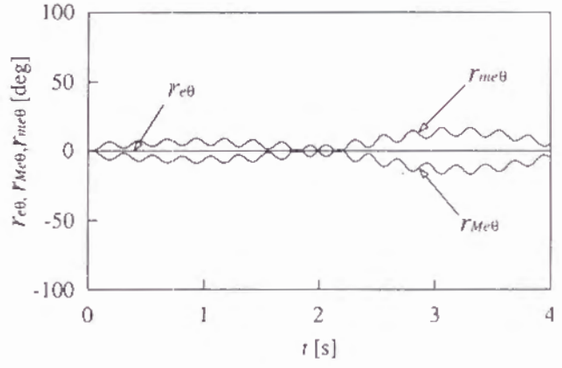

(b) deviation

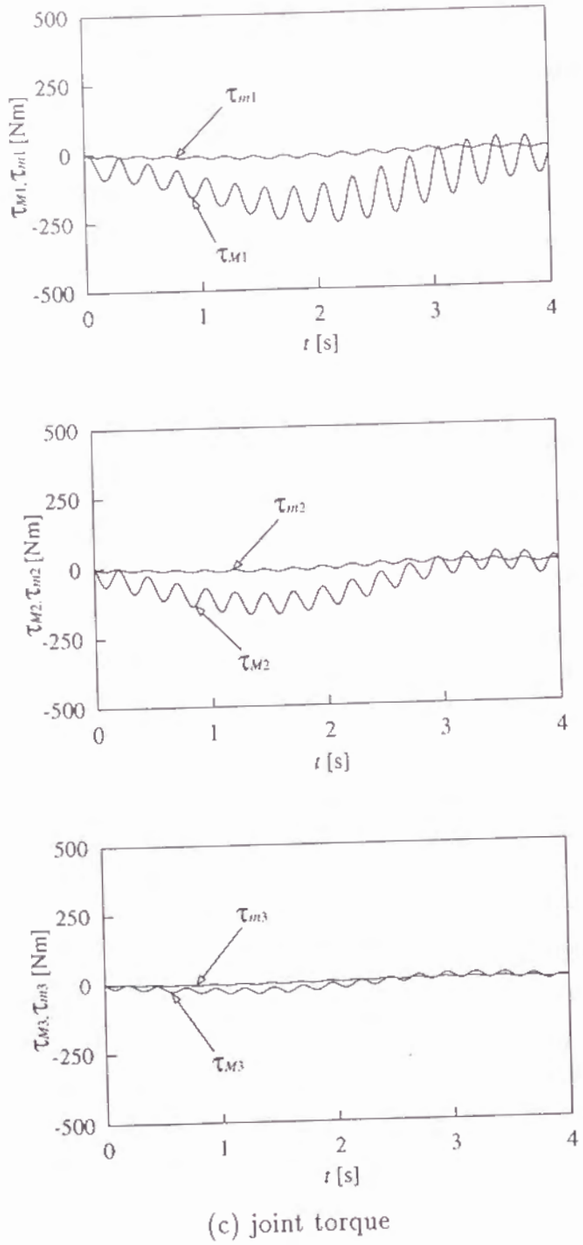

(c) joint torque

Fig. 5.6. Simulation results when external force is composite sine wave.

5.6 Conclusion

The main results obtained in this chapter are summarized as follows.

1) An impedance control scheme of redundant macro-micro manipulators is proposed. In the controller, not only the desired mechanical impedance of the endpoint, but also that of the macro manipulator are specified by considering the internal force applied at the tip of the macro manipulator. This control scheme can utilize both merits of the macro and micro manipulators, that is, the wide motion range of the macro manipulator and the high capability of compliant motion of the micro manipulator.

2) The validity of the proposed controller is shown by several simulation results. It is shown that the macro manipulator moves according to the lower frequency element of the external force, and the micro manipulator moves according to its higher frequency element.

Applying the proposed control scheme to macro-micro manipulators without the need for enough redundancy and to arms with multifingered hands is among the future topics.

Chapter 6

Grasping and Manipulation by Robotic Arm/Multifingered-Hand Mechanisms

6.1 Introduction

Multifingered hands have the capability of high band width regarding positioning and force control, because of their small inertia. This is one of advantages of multifingered hands, however, small motion range is one of their disadvantages. Consequently, it is necessary for multifingered hands to be attached to an arm. In such a case, manipulation can be realized by either part. This kind of combination is also a topic of the redundant macro-micro manipulators, where the multifingered hands correspond to the micro manipulators and the arms correspond to the macro manipulators. Therefore, the proposed control scheme for these redundant macro-micro manipulators in the previous chapter can be the base of the discussion in this chapter. However, it is necessary to realize simultaneously a non-slip grasping during manipulation.

In this chapter, a new control scheme, which brings the ability of multifingered hands and arms into full play, is proposed. This control scheme has advantages not only to make the band width of manipulation high but also to use the big motion range of the arms. Moreover, the control scheme can realize secure grasping during manipulation like the control scheme proposed in Chapter 3. In Section 6.2, basic equations are provided. In Section 6.3, a new control scheme is proposed. In Section 6.4, the simulation results illustrate the validity of the proposed control scheme. In Section 6.5, the experimental results also illustrate the validity of it.

6.2 Basic Equation

6.2.1 Arm-Hand Mechanism

Arm-hand mechanisms, discussed in this chapter, consist of arms and multifingered hands. The arms are assumed to have six DOF. The multifingered hands have three fingers, and each finger has three joints to make frictional point contact. The assumptions on the hands are same as in Chapter 2.

In this section, basic equations of arm-hand mechanisms, shown in Fig. 6.1, are shown. The nomenclatures in this chapter are as follows:

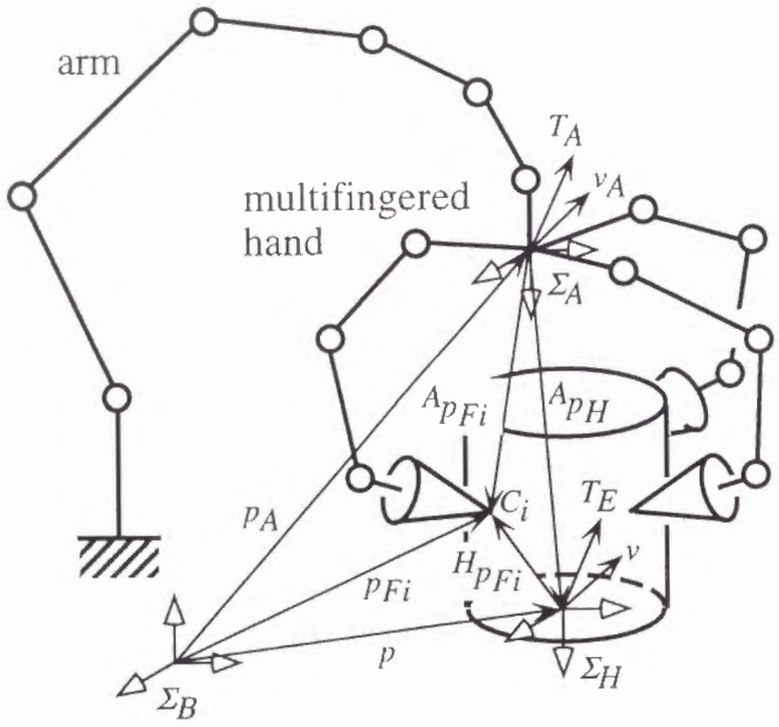

Fig. 6.1. Arm-hand mechanism.

Σ_B : Base coordinate frame, the origin O_B
Σ_A : Arm coordinate frame, the origin O_A
Σ_H : Hand coordinate frame, the origin O_H
C_i : Contact point of i-th fingertip, $i = 1, 2, 3$
$\boldsymbol{p}_{Fi} \in \mathrm{R}^3$: Position vector of C_i from O_B
${}^A\boldsymbol{p}_{Fi} \in \mathrm{R}^3$: Position vector of C_i from O_A
${}^H\boldsymbol{p}_{Fi} \in \mathrm{R}^3$: Position vector of C_i from O_H

$\boldsymbol{p} \in \mathrm{R}^3$: Position vector of O_H from O_B
$\boldsymbol{p}_A \in \mathrm{R}^3$: Position vector of O_A from O_B
${}^A\boldsymbol{p}_H \in \mathrm{R}^3$: Position vector of O_H from O_A
$\boldsymbol{\phi} \in \mathrm{R}^3$: Orientation(roll-pitch-yaw) of Σ_H represented by Σ_B
$\boldsymbol{\phi}_A \in \mathrm{R}^3$: Orientation(roll-pitch-yaw) of Σ_A represented by Σ_B
${}^A\boldsymbol{\phi}_H \in \mathrm{R}^3$: Orientation(roll-pitch-yaw) of Σ_H represented by Σ_A
$\boldsymbol{r} = [\boldsymbol{p}^{\mathrm{T}} \ \boldsymbol{\phi}^{\mathrm{T}}]^{\mathrm{T}} \in \mathrm{R}^6$: Position and orientation of Σ_H represented by Σ_B
$\boldsymbol{r}_A = [\boldsymbol{p}_A^{\mathrm{T}} \ \boldsymbol{\phi}_A^{\mathrm{T}}]^{\mathrm{T}} \in \mathrm{R}^6$: Position and orientation of Σ_A represented by Σ_B
${}^A\boldsymbol{r}_H = [{}^A\boldsymbol{p}_H^{\mathrm{T}} \ {}^A\boldsymbol{\phi}_H^{\mathrm{T}}]^{\mathrm{T}} \in \mathrm{R}^6$: Position and orientation of Σ_H represented by Σ_A
$\boldsymbol{\omega} \in \mathrm{R}^3$: Angular velocity vector of Σ_H represented by Σ_B
$\boldsymbol{\omega}_A \in \mathrm{R}^3$: Angular velocity vector of Σ_A represented by Σ_B
${}^A\boldsymbol{\omega}_H \in \mathrm{R}^3$: Angular velocity vector of Σ_H represented by Σ_A
$\boldsymbol{v} = [\dot{\boldsymbol{p}}^{\mathrm{T}} \ \boldsymbol{\omega}^{\mathrm{T}}]^{\mathrm{T}} \in \mathrm{R}^6$: Velocity of object
$\boldsymbol{v}_A = [\dot{\boldsymbol{p}}_A^{\mathrm{T}} \ \boldsymbol{\omega}_A^{\mathrm{T}}]^{\mathrm{T}} \in \mathrm{R}^6$: Velocity of endpoint of arm
${}^A\boldsymbol{v}_H = [{}^A\dot{\boldsymbol{p}}_H^{\mathrm{T}} \ {}^A\boldsymbol{\omega}_H^{\mathrm{T}}]^{\mathrm{T}} \in \mathrm{R}^6$: Velocity of object represented by Σ_A
${}^B\boldsymbol{A}_H \in \mathrm{R}^{3\times3}$: Rotational matrix from Σ_B to Σ_H
${}^B\boldsymbol{A}_A \in \mathrm{R}^{3\times3}$: Rotational matrix from Σ_B to Σ_A
${}^A\boldsymbol{A}_H \in \mathrm{R}^{3\times3}$: Rotational matrix from Σ_A to Σ_H
$\boldsymbol{q}_A \in \mathrm{R}^6$: Joint valuable vector of arm
$\boldsymbol{q}_{Fi} \in \mathrm{R}^3$: Joint valuable vector of i-th finger. $i = 1, 2, 3$
$\boldsymbol{q}_F = [\boldsymbol{q}_{F1}^{\mathrm{T}} \ \boldsymbol{q}_{F2}^{\mathrm{T}} \ \boldsymbol{q}_{F3}^{\mathrm{T}}]^{\mathrm{T}} \in \mathrm{R}^9$: Joint valuable vector of hand
$\boldsymbol{q} = [\boldsymbol{q}_A^{\mathrm{T}} \ \boldsymbol{q}_F^{\mathrm{T}}]^{\mathrm{T}} \in \mathrm{R}^{15}$: Joint valuable vector of arm-hand mechanism
$\boldsymbol{\tau}_A \in \mathrm{R}^6$: Joint driving force vector of arm
$\boldsymbol{\tau}_{Fi} \in \mathrm{R}^3$: Joint driving force vector of i-th finger
$\boldsymbol{\tau}_F \in \mathrm{R}^9$: Joint driving force vector of hand
$\boldsymbol{\tau} = [\boldsymbol{\tau}_A^{\mathrm{T}} \ \boldsymbol{\tau}_F^{\mathrm{T}}]^{\mathrm{T}} \in \mathrm{R}^{15}$: Joint driving force vector of arm-hand mechanism
$\boldsymbol{f}_i \in \mathrm{R}^3$: Fingertip force of i-th finger
$\boldsymbol{F} = [\boldsymbol{f}_1^{\mathrm{T}} \ \boldsymbol{f}_2^{\mathrm{T}} \ \boldsymbol{f}_3^{\mathrm{T}}]^{\mathrm{T}} \in \mathrm{R}^9$: Fingertip force
$\boldsymbol{T} \in \mathrm{R}^6$: Total force applied at object
$\boldsymbol{T}_A \in \mathrm{R}^6$: Force applied at endpoint of arm
$\boldsymbol{T}_E \in \mathrm{R}^6$: External force applied at object

where left-superscript expresses the coordinate frame. It is omitted when it expresses base coordinate frame, except for the rotational matrix.

6.2.2 Kinematics before Grasping

In this subsection, basic kinematical equations are shown before the hand grasps an object. Here, the position and velocity of the fingertips should be made absolutely clear.

The position and orientation of the end point of arm, and the position of i-th fingertip

represented by Σ_A are given as follows:

$$\boldsymbol{p}_A = \boldsymbol{p}_A(\boldsymbol{q}_A) \tag{6.1}$$

$${}^B\boldsymbol{A}_A = {}^B\boldsymbol{A}_A(\boldsymbol{q}_A) \tag{6.2}$$

$${}^A\boldsymbol{p}_{Fi} = {}^A\boldsymbol{p}_{Fi}(\boldsymbol{q}_{Fi}) \tag{6.3}$$

Then, contact position $\boldsymbol{p}_{Fi}$ is,

$$\boldsymbol{p}_{Fi} = \boldsymbol{p}_A + {}^B\boldsymbol{A}_A\,{}^A\boldsymbol{p}_{Fi} \tag{6.4}$$

By using Eqs. (6.1) $\sim$ (6.3), the velocity of the endpoint of arm, $\boldsymbol{v}_A$, and the velocity of fingertip, ${}^A\dot{\boldsymbol{p}}_{F_i}$, are:

$$\boldsymbol{v}_A = \boldsymbol{J}_A\dot{\boldsymbol{q}}_A \tag{6.5}$$

$${}^A\dot{\boldsymbol{p}}_{Fi} = {}^A\boldsymbol{J}_{Fi}\dot{\boldsymbol{q}}_{Fi} \tag{6.6}$$

where, $\boldsymbol{J}_A$ and ${}^A\boldsymbol{J}_{Fi}$ are the Jacobian matrices of the arm and of i-th finger on Σ_A, respectively. Based on Eq. (6.4), the velocity of the contact point, ${}^A\dot{\boldsymbol{p}}_{Fi}$, is shown to be,

$$\dot{\boldsymbol{p}}_{Fi} = \boldsymbol{J}_{AFi}\boldsymbol{v}_A + {}^B\boldsymbol{A}_A\,{}^A\dot{\boldsymbol{p}}_{Fi} \tag{6.7}$$

The velocity of fingertip, $\dot{\boldsymbol{p}}_F = \left[\dot{\boldsymbol{p}}_{F1}^{\mathrm{T}}\ \dot{\boldsymbol{p}}_{F2}^{\mathrm{T}}\ \dot{\boldsymbol{p}}_{F3}^{\mathrm{T}}\right]^{\mathrm{T}} \in \mathrm{R}^9$, is then obtained by using Eqs. (6.5) $\sim$ (6.7) for $i = 1, 2, 3$:

$$\dot{\boldsymbol{p}}_F = \boldsymbol{J}\dot{\boldsymbol{q}} \tag{6.8}$$

where,

$$\boldsymbol{J} = \begin{bmatrix} \boldsymbol{J}_{AF1}\boldsymbol{J}_A & {}^BA_A\,{}^A\boldsymbol{J}_{F1} & 0 & 0 \\ \boldsymbol{J}_{AF2}\boldsymbol{J}_A & 0 & {}^BA_A\,{}^A\boldsymbol{J}_{F2} & 0 \\ \boldsymbol{J}_{AF3}\boldsymbol{J}_A & 0 & 0 & {}^BA_A\,{}^A\boldsymbol{J}_{F3} \end{bmatrix} \in \mathrm{R}^{9\times 15} \tag{6.9}$$

6.2.3 Kinematics after Grasping

In this subsection, basic kinematical equations are described after the hand grasps the object. Here, the relation between the two velocities should be made absolutely clear, where one is a set of velocities of the arm endpoint and the object, and the other one is the joint velocity.

The position and orientation of the object are represented as follows:

$$\boldsymbol{p} = \boldsymbol{p}_A + {}^B\boldsymbol{A}_A\,{}^A\boldsymbol{p}_H \tag{6.10}$$

$${}^B\boldsymbol{A}_H = {}^B\boldsymbol{A}_A\,{}^A\boldsymbol{A}_H \tag{6.11}$$

When only the part of the hand is considered, the position of the i-th fingertip is represented by,

$${}^A\boldsymbol{p}_{Fi} = {}^A\boldsymbol{p}_H + {}^A\boldsymbol{A}_H\,{}^H\boldsymbol{p}_{Fi} \tag{6.12}$$

The velocity of fingertip, ${}^A\dot{\boldsymbol{p}}_F = \left[{}^A\dot{\boldsymbol{p}}_{F1}^{\mathrm{T}}\ {}^A\dot{\boldsymbol{p}}_{F2}^{\mathrm{T}}\ {}^A\dot{\boldsymbol{p}}_{F3}^{\mathrm{T}}\right]^{\mathrm{T}} \in \mathrm{R}^9$, is then obtained by differentiating Eq. (6.12) for $i = 1, 2, 3$ and integrating them:

$${}^A\dot{\boldsymbol{p}}_F = {}^A\boldsymbol{J}_{HF}\,{}^A\boldsymbol{v}_H \tag{6.13}$$

On the other hand, the velocity of fingertip is shown by integrating Eq. (6.6) for $i = 1, 2, 3$:

$${}^A\dot{\boldsymbol{p}}_F = {}^A\boldsymbol{J}_F\dot{\boldsymbol{q}}_F \tag{6.14}$$

In case of non-slip grasping, a kinematical constraint exists among the fingers, and obtained by using Eqs. (6.13) and (6.14):

$${}^A\boldsymbol{J}_F\dot{\boldsymbol{q}}_F = {}^A\boldsymbol{J}_{HF}\,{}^A\boldsymbol{v}_H \tag{6.15}$$

This constraint can be expressed by using the joint velocity of the whole mechanism. In this case, first, the position of the i-th fingertip on Σ_B, $\boldsymbol{p}_{F_i}$ is given by,

$$\boldsymbol{p}_{Fi} = \boldsymbol{p}_H + {}^B\boldsymbol{A}_H\,{}^H\boldsymbol{p}_{Fi} \tag{6.16}$$

The velocity of fingertip is then obtained by differentiating Eq. (6.16) for $i = 1, 2, 3$ and integrating them:

$$\dot{\boldsymbol{p}}_F = \boldsymbol{J}_{HF}\boldsymbol{v} \tag{6.17}$$

By using Eqs. (6.17) and (6.8), the following equation can be obtained:

$$\boldsymbol{J}\dot{\boldsymbol{q}} = \boldsymbol{J}_{HF}\boldsymbol{v} \tag{6.18}$$

Equation (6.18) shows the kinematical constraint from the viewpoint of the whole mechanism.

The following describes the relation between the velocity of joint velocity $\dot{\boldsymbol{q}}$ and a set of the velocities of the endpoint of arm $\boldsymbol{v}_A$ and object $\boldsymbol{v}$.

First, by using Eq. (6.5) and (6.15), the relation between the joint valuables and the set of the velocity of the arm and hand can be obtained:

$$\begin{bmatrix} \dot{\boldsymbol{q}}_A \\ \dot{\boldsymbol{q}}_F \end{bmatrix} = \begin{bmatrix} \boldsymbol{J}_A^{-1} & 0 \\ 0 & {}^A\boldsymbol{J}_F^{-1}\,{}^A\boldsymbol{J}_{HF} \end{bmatrix} \begin{bmatrix} \boldsymbol{v}_A \\ {}^A\boldsymbol{v}_H \end{bmatrix} \tag{6.19}$$

On the other hand, the velocity of object $\boldsymbol{v} \in \mathrm{R}^6$ is shown as follows:

$$\boldsymbol{v} = \boldsymbol{J}_{AH}\boldsymbol{v}_A + {}^B\boldsymbol{R}_A\,{}^A\boldsymbol{v}_H \tag{6.20}$$

where,

$$\boldsymbol{J}_{AH} = \begin{bmatrix} E_3 & -P \\ 0 & E_3 \end{bmatrix} \tag{6.21}$$

$$P = \begin{bmatrix} 0 & -p_z & p_y \\ p_z & 0 & -p_x \\ -p_y & p_x & 0 \end{bmatrix}, \quad \boldsymbol{p} = [p_x\ p_y\ p_z]^{\mathrm{T}} = {}^{B}\boldsymbol{A}_{A}{}^{A}\boldsymbol{p}_{H}$$

$${}^{B}\boldsymbol{R}_{A} = \begin{bmatrix} {}^{B}\boldsymbol{A}_{A} & \boldsymbol{0} \\ \boldsymbol{0} & {}^{B}\boldsymbol{A}_{A} \end{bmatrix} \in \mathrm{R}^{6\times 6} \tag{6.22}$$

By modifying Eq. (6.20), the following equation can be obtained.

$$\begin{bmatrix} \boldsymbol{v}_{A} \\ \boldsymbol{v} \end{bmatrix} = \begin{bmatrix} \boldsymbol{E}_{6} & \boldsymbol{0} \\ \boldsymbol{J}_{AH} & {}^{B}\boldsymbol{R}_{A} \end{bmatrix} \begin{bmatrix} \boldsymbol{v}_{A} \\ {}^{A}\boldsymbol{v}_{H} \end{bmatrix} \tag{6.23}$$

As a result, the following equation can be obtained by using Eqs. (6.19) and (6.23),

$$\dot{\boldsymbol{q}} = \tilde{\boldsymbol{J}}\tilde{\boldsymbol{v}} \tag{6.24}$$

where,

$$\tilde{\boldsymbol{v}} = \begin{bmatrix} \boldsymbol{v}_{A} \\ \boldsymbol{v} \end{bmatrix} \in \mathrm{R}^{12} \tag{6.25}$$

is the set of the velocities of the endpoint of the arm and object, and $\tilde{\boldsymbol{J}}$ is:

$$\tilde{\boldsymbol{J}} = \begin{bmatrix} \boldsymbol{J}_{A}^{-1} & \boldsymbol{0} \\ -{}^{A}\boldsymbol{J}_{F}^{-1}{}^{A}\boldsymbol{J}_{HF}{}^{B}\boldsymbol{R}_{A}^{-1}\boldsymbol{J}_{AH} & {}^{A}\boldsymbol{J}_{F}^{-1}{}^{A}\boldsymbol{J}_{HF}{}^{B}\boldsymbol{R}_{A}^{-1} \end{bmatrix} \in \mathrm{R}^{15\times 12} \tag{6.26}$$

Equation (6.24) means that the velocity of the hand-arm is determined uniquely, when the velocities of the end point of the arm and object are specified simultaneously.

The relations between two velocities, $\boldsymbol{v}_{A}$ and $\dot{\boldsymbol{r}}_{A}$, $\boldsymbol{v}$ and $\dot{\boldsymbol{r}}$ are as follows:

$$\boldsymbol{v}_{A} = \boldsymbol{W}_{A}\dot{\boldsymbol{r}}_{A} \tag{6.27}$$

$$\boldsymbol{v} = \boldsymbol{W}\dot{\boldsymbol{r}} \tag{6.28}$$

$\dot{\boldsymbol{r}}_{A}$ and $\dot{\boldsymbol{r}}$ are used in specifying the desired manipulation. Equations (6.27) and (6.28) can be integrated in the following way:

$$\tilde{\boldsymbol{v}} = \tilde{\boldsymbol{W}}\tilde{\dot{\boldsymbol{r}}} \tag{6.29}$$

$$\tilde{\dot{\boldsymbol{r}}} = \begin{bmatrix} \dot{\boldsymbol{r}}_{A} \\ \dot{\boldsymbol{r}} \end{bmatrix} \tag{6.30}$$

$$\tilde{\boldsymbol{W}} = \begin{bmatrix} \boldsymbol{W}_{A} & \boldsymbol{0} \\ \boldsymbol{0} & \boldsymbol{W} \end{bmatrix} \tag{6.31}$$

6.2.4 Equation of Motion of Mechanism and Object

The equations of motion of the arm-hand mechanism and object are:

$$\boldsymbol{M}_{q}\ddot{\boldsymbol{q}} + \boldsymbol{h}_{q} + \boldsymbol{J}^{\mathrm{T}}\boldsymbol{F} = \boldsymbol{\tau} \tag{6.32}$$

$$\boldsymbol{M}_{O}\dot{\boldsymbol{v}} + \boldsymbol{h}_{O} = \boldsymbol{T} + \boldsymbol{T}_{A} \tag{6.33}$$

where,

$$\boldsymbol{T} = \boldsymbol{J}_{HF}^{\mathrm{T}}\boldsymbol{F} \tag{6.34}$$

and $\boldsymbol{M}_{q} \in \mathrm{R}^{15\times 15}$ and $\boldsymbol{h}_{q} \in \mathrm{R}^{15}$ shows the inertia matrix and non-linear term of the mechanism $\boldsymbol{M}_{O} \in \mathrm{R}^{6\times 6}$ and $\boldsymbol{h}_{O} \in \mathrm{R}^{6}$ the inertia matrix and the non-linear term of the object, respectively.

6.2.5 Representation of Grasping and Manipulating Forces

In this subsection, the representations of the grasping and manipulating forces of three-fingered hands are described briefly.

The grasping force $\boldsymbol{F}_{g} = \left[\boldsymbol{f}_{g1}^{\mathrm{T}}\ \boldsymbol{f}_{g2}^{\mathrm{T}}\ \boldsymbol{f}_{g3}^{\mathrm{T}}\right]^{\mathrm{T}} \in \mathrm{R}^{9}$ and the manipulating force $\boldsymbol{F}_{m} = \left[\boldsymbol{f}_{m1}^{\mathrm{T}}\ \boldsymbol{f}_{m2}^{\mathrm{T}}\ \boldsymbol{f}_{m3}^{\mathrm{T}}\right]^{\mathrm{T}} \in \mathrm{R}^{9}$ are defined, in Chapter 2, as a component of the fingertip force $\boldsymbol{F} = \left[\boldsymbol{f}_{1}^{\mathrm{T}}\ \boldsymbol{f}_{2}^{\mathrm{T}}\ \boldsymbol{f}_{3}^{\mathrm{T}}\right]^{\mathrm{T}} \in \mathrm{R}^{9}$.

Representation of the grasping force is,

$$\boldsymbol{F}_{g} = \boldsymbol{B}_{g}\boldsymbol{h}_{g} \tag{6.35}$$

where, $\boldsymbol{h}_{g} \in \mathrm{R}^{3}$ is the grasp parameter to determine the grasping force.

Representation of the manipulating force is,

$$\boldsymbol{F}_{m} = \boldsymbol{B}_{m}\boldsymbol{h}_{m} \tag{6.36}$$

where, $\boldsymbol{h}_{m} \in \mathrm{R}^{6}$ is the manipulation parameter.

Fingertip force $\boldsymbol{F}$ is then shown as a sum of these forces in the following way.

$$\boldsymbol{F} = \boldsymbol{F}_{g} + \boldsymbol{F}_{m} \tag{6.37}$$

6.3 Control Law

In this section, a new control scheme of arm-hand mechanisms is proposed.

First, mechanical impedances are specified not only at the object but also at the endpoint of the arm:

$$\boldsymbol{M}_{Ad}\ddot{\boldsymbol{r}}_{A} + \boldsymbol{D}_{Ad}\dot{\boldsymbol{r}}_{Ae} + \boldsymbol{K}_{Ad}\boldsymbol{r}_{Ae} = \boldsymbol{T}_{A} \tag{6.38}$$

$$M_{rd}\ddot{\boldsymbol{r}} + D_{rd}\dot{\boldsymbol{r}}_e + K_{rd}\boldsymbol{r}_e = \boldsymbol{T}_E \tag{6.39}$$

where M_{Ad}, D_{Ad}, and K_{Ad} are the desired matrices of inertia, coefficient of viscous friction and stiffness of the endpoint respectively; M_{rd}, D_{rd}, and K_{rd} are those of the endpoint of the arm, respectively. $\boldsymbol{r}_e(=\boldsymbol{r}-\boldsymbol{r}_d)$ and $\boldsymbol{r}_{Ae}(=\boldsymbol{r}_A-\boldsymbol{r}_{Ad})$ are the position errors of the object and the endpoint of the arm. $\boldsymbol{r}_d$, $\boldsymbol{r}_{Ad}$ and ${}^A\boldsymbol{r}_{Hd}$ are the desired positions of the object, the endpoint of the arm and the hand part, respectively.

$$\boldsymbol{p}_{Ad} = \boldsymbol{p}_d - {}^B\boldsymbol{A}_{Ad}{}^A\boldsymbol{p}_{Hd} \tag{6.40}$$

$${}^B\boldsymbol{A}_{Ad} = {}^B\boldsymbol{A}_{Hd}{}^A\boldsymbol{A}_{Hd}^{-1} \tag{6.41}$$

$\boldsymbol{T}_A$ in Eq. (6.38) is the internal force applied at the end point of the arm from the hand. By utilizing this $\boldsymbol{T}_A$, the arm can move to compensate for any disadvantage of the small motion range of the hand.

Equations (6.38) and (6.39) can be represented as follows:

$$M_d\begin{bmatrix}\ddot{\boldsymbol{r}}_A\\ \ddot{\boldsymbol{r}}\end{bmatrix} + D_d\begin{bmatrix}\dot{\boldsymbol{r}}_{Ae}\\ \dot{\boldsymbol{r}}_e\end{bmatrix} + K_d\begin{bmatrix}\boldsymbol{r}_{Ae}\\ \boldsymbol{r}_e\end{bmatrix} = \begin{bmatrix}\boldsymbol{T}_A\\ \boldsymbol{T}_E\end{bmatrix} \tag{6.42}$$

$$\begin{aligned} M_d &= \begin{bmatrix} M_{Ad} & 0\\ 0 & M_{rd}\end{bmatrix},\quad D_d = \begin{bmatrix} D_{Ad} & 0\\ 0 & D_{rd}\end{bmatrix}\\ K_d &= \begin{bmatrix} K_{Ad} & 0\\ 0 & K_{rd}\end{bmatrix}\end{aligned}$$

Equation (6.42) is the desired manipulation.

On the other hand, the desired grasping is given as follows.

$$\boldsymbol{h}_g = \boldsymbol{h}_{gd} \tag{6.43}$$

where, $\boldsymbol{h}_{gd}$ is the desired value of grasp parameter $\boldsymbol{h}_g$. In the proposed controller, a secure grasp is realized by suitable $\boldsymbol{h}_{gd}$.

The control law of arm-hand mechanisms is then represented in the following way:

$$\boldsymbol{\tau}_C = \boldsymbol{\tau}_O + \boldsymbol{\tau}_{AH} \tag{6.44}$$

$$\boldsymbol{\tau}_O = \boldsymbol{J}^{\mathrm{T}}\boldsymbol{F}_d \tag{6.45}$$

$$\boldsymbol{F}_d = \boldsymbol{F}_{gd} + \boldsymbol{F}_{md} \tag{6.46}$$

$$\boldsymbol{F}_{gd} = \boldsymbol{B}_g\boldsymbol{u}_2 \tag{6.47}$$

$$\boldsymbol{F}_{md} = \boldsymbol{B}_m\left(\boldsymbol{J}_{HF}^{\mathrm{T}}\boldsymbol{B}_m\right)^{-1}\boldsymbol{T}_d \tag{6.48}$$

$$\boldsymbol{T}_d = \boldsymbol{M}_O\dot{\boldsymbol{v}}_d + \boldsymbol{h}_O - \boldsymbol{T}_E \tag{6.49}$$

$$\boldsymbol{\tau}_{AH} = \boldsymbol{M}_q\ddot{\boldsymbol{q}}_d + \boldsymbol{h}_q \tag{6.50}$$

$$\ddot{\boldsymbol{q}}_d = \tilde{\boldsymbol{J}}\dot{\tilde{\boldsymbol{v}}}_d + \dot{\tilde{\boldsymbol{J}}}\tilde{\boldsymbol{v}}_d \tag{6.51}$$

$$\dot{\tilde{\boldsymbol{v}}}_d = \begin{bmatrix}\dot{\boldsymbol{v}}_{Ad}\\ \dot{\boldsymbol{v}}_d\end{bmatrix} = \tilde{\boldsymbol{W}}\boldsymbol{u}_1 + \dot{\tilde{\boldsymbol{W}}}\tilde{\boldsymbol{r}} \tag{6.52}$$

$$\boldsymbol{u}_1 = \begin{bmatrix}\boldsymbol{u}_{1A}\\ \boldsymbol{u}_{1r}\end{bmatrix} = \boldsymbol{M}_d^{-1}\left\{\begin{bmatrix}\boldsymbol{T}_A\\ \boldsymbol{T}_E\end{bmatrix} - \boldsymbol{D}_d\begin{bmatrix}\dot{\boldsymbol{r}}_{Ae}\\ \dot{\boldsymbol{r}}_e\end{bmatrix} - \boldsymbol{K}_d\begin{bmatrix}\boldsymbol{r}_{Ae}\\ \boldsymbol{r}_e\end{bmatrix}\right\} \tag{6.53}$$

$$\boldsymbol{u}_2 = \boldsymbol{h}_{gd2} + \boldsymbol{K}_F\int(\boldsymbol{h}_{gd2} - \boldsymbol{h}_g)dt \tag{6.54}$$

$$\boldsymbol{h}_{gd2} = \boldsymbol{h}_{gd} - T_c\dot{\boldsymbol{h}}_{gd2} \tag{6.55}$$

where, T_c is the time constant in the first order lag for the desired response of the grasp parameter, and $\boldsymbol{K}_F$ is the integral gain.

The above control law can be divided into two parts. One is a compensator for linearizing the whole system, expressed by Eqs. (6.44) $\sim$ (6.52). By applying this compensator, the following relations can be yielded.

$$\ddot{\boldsymbol{r}}_A = \boldsymbol{u}_{1A} \tag{6.56}$$

$$\ddot{\boldsymbol{r}} = \boldsymbol{u}_{1r} \tag{6.57}$$

$$\boldsymbol{h}_g = \boldsymbol{u}_2 \tag{6.58}$$

The another part is the controllers expressed by Eqs. (6.53)$\sim$(6.55). Equation (6.53) should be called the impedance realizer.

6.4 Simulation

6.4.1 1 DOF Arm-Hand System

In this section, several simulation results show the validity of this controller.

Figure 6.2 shows a 1 DOF arm-hand system which consists of a 1 DOF arm and a two-fingered 1 DOF hand with linear motion. In the figure, m_A, m_H, m_{F1}, m_{F2} and m_O are the mass of the arm, base of the hand, 1st finger, 2nd finger, and object, respectively. The equations of motion of this mechanism are represented as follows:

$$\text{Arm} \;:\; m_A\ddot{q}_A = \tau_A + T_A \tag{6.59}$$

$$\text{Base of hand} \;:\; m_H\ddot{q}_A = -\tau_{F1} - \tau_{F2} - T_A \tag{6.60}$$

$$\text{1st finger} \;:\; m_{F1}(\ddot{q}_A + \ddot{q}_{F1}) = \tau_{F1} - f_1 \tag{6.61}$$

$$\text{2nd finger} \;:\; m_{F2}(\ddot{q}_A + \ddot{q}_{F2}) = \tau_{F2} - f_2 \tag{6.62}$$

Equations (6.59) and (6.60) are shown separately to specify the force applied at the endpoint of arm T_A, even if two parts move together. To integrate Eqs. (6.59) and (6.60), first, T_A is eliminated using Eqs. (6.59) and (6.60), and the following equation is derived:

$$(m_A + m_H)\,\ddot{q}_A = \tau_A - \tau_{F1} - \tau_{F2} \tag{6.63}$$

Then Eqs. (6.61) $\sim$ (6.63) are integrated into the following equation:

$$\boldsymbol{M}_q \ddot{\boldsymbol{q}} + \boldsymbol{J}^{\mathrm{T}} \boldsymbol{F} = \boldsymbol{\tau} \tag{6.64}$$

where, $\ddot{\boldsymbol{q}} \in \mathrm{R}^3$, $\boldsymbol{F} \in \mathrm{R}^2$, $\boldsymbol{\tau} \in \mathrm{R}^3$, and

$$\boldsymbol{M}_q = \begin{bmatrix} m_A + m_H + m_{F1} + m_{F2} & m_{F1} & m_{F2} \\ m_{F1} & m_{F1} & 0 \\ m_{F2} & 0 & m_{F2} \end{bmatrix} \in \mathrm{R}^{3\times 3}$$

$$\boldsymbol{J} = \begin{bmatrix} 1 & 1 & 0 \\ 1 & 0 & 1 \end{bmatrix} \in \mathrm{R}^{2\times 3}$$

Note that the dimensions of the vectors and the matrices are different from those in a general case.

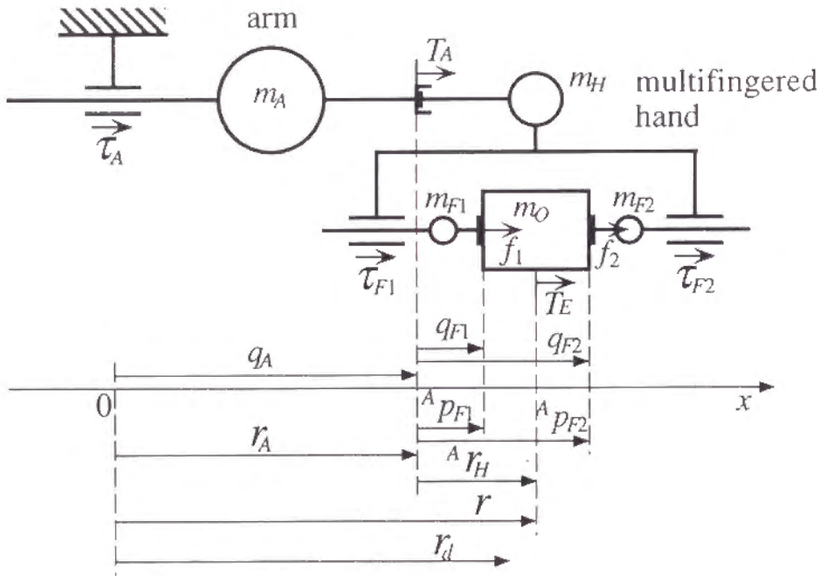

Fig. 6.2. 1 DOF arm-hand mechanism.

On the other hand, the equation of motion of the object is represented as follows:

$$M_O \dot{v} = T + T_E \tag{6.65}$$

$$T = \boldsymbol{J}_{HF}^{\mathrm{T}} \boldsymbol{F} \tag{6.66}$$

where, $\dot{v} \in \mathrm{R}^1$, $T \in \mathrm{R}^1$, $T_E \in \mathrm{R}^1$, and

$$M_O = m_O \in \mathrm{R}^{1\times 1}, \quad \boldsymbol{J}_{HF} = \begin{bmatrix} 1 \\ 1 \end{bmatrix} \in \mathrm{R}^{2\times 1}$$

Regarding basic equations concerning kinematics, the following equations hold:

$$\dot{\boldsymbol{q}} = \tilde{\boldsymbol{J}}\tilde{\boldsymbol{v}}, \quad \tilde{\boldsymbol{J}} = \begin{bmatrix} 1 & 0 \\ -1 & 1 \\ -1 & 1 \end{bmatrix} \in \mathrm{R}^{3\times 2} \tag{6.67}$$

$$v_A = W_A \dot{r}_A, \quad v = W\dot{r}, \quad W_A = W = 1 \tag{6.68}$$

The fingertip force, the grasping force and the manipulating force in this case are:

$$\boldsymbol{F} = \boldsymbol{F}_g + \boldsymbol{F}_m \tag{6.69}$$

$$\boldsymbol{F}_g = \boldsymbol{B}_g h_g, \; h_g \geq 0, \; \boldsymbol{B}_g = \begin{bmatrix} 1 \\ -1 \end{bmatrix} \in \mathrm{R}^{2\times 1} \tag{6.70}$$

$$\boldsymbol{F}_m = \boldsymbol{B}_m h_m, \; h_m \geq 0, \; \boldsymbol{B}_m = \begin{bmatrix} k \\ -(1-k) \end{bmatrix} \in \mathrm{R}^{2\times 1} \tag{6.71}$$

where, the value of $k(= 1 \text{ or } 0)$ is selected as h_m determined by Eqs. (6.66), (6.69) and (6.70):

$$h_m = \left(\boldsymbol{J}_{HF}^{\mathrm{T}} \boldsymbol{B}_m\right)^{-1} T \tag{6.72}$$

is plus or equal to zero, described in Chapter 2. Then, $\boldsymbol{F}_{md}$ in this case is calculated by using Eq. (6.48):

$$\boldsymbol{F}_{md} = \begin{cases} \begin{bmatrix} T_d \\ 0 \end{bmatrix}, & \text{when} \quad T_d \geq 0 \\ \\ \begin{bmatrix} 0 \\ T_d \end{bmatrix}, & \text{when} \quad T_d < 0 \end{cases} \tag{6.73}$$

The values of mass are determined in the following way:

$$m_A = 10[\mathrm{kg}], \quad m_H = 2.5[\mathrm{kg}], \quad m_{F1} = m_{F2} = 0.2[\mathrm{kg}]$$
$$m_O = 0.1[\mathrm{kg}]$$

6.4.2 Desired Grasping and Manipulation

In this section, the desired set of grasping and manipulation given to the proposed controller is described.

The desired grasping is given by desired grasp parameter h_{gd} and some constants in the servo controller for grasping. These values are:

$$h_{gd} = 20[\mathrm{N}], \quad K_F = 100[1/\mathrm{s}], \quad T_c = 0.05[\mathrm{s}]$$

On the other hand, the desired manipulations are given by a set of the parameters in the equations for the desired mechanical impedances:

$$\begin{array}{ll} M_{Ad} = 12.5[\mathrm{kg}] & M_{rd} = 0.5[\mathrm{kg}] \\ D_{Ad} = 140\,[\mathrm{N/(m/s)}] & D_{rd} = 28\,[\mathrm{N/(m/s)}] \\ K_{Ad} = 800\,[\mathrm{N/m}] & K_{rd} = 800\,[\mathrm{N/m}] \end{array}$$

The values of the parameters are determined the following guidelines:

1) The original mass characteristics of the mechanism grasping the object is considered.

2) The grasping posture of the hand goes to the initial one when an external force is constant.

3) The motion of the arm and the hand is stable.

The details of these guidelines are described as follows.

As for 1), the equation of motion of the mechanism grasping the object should be clear.

As for preparation, the following relation about the accelerations can be derived by Eq. (6.67)

$$\ddot{\boldsymbol{q}} = \tilde{\boldsymbol{J}}\ddot{\tilde{\boldsymbol{v}}} \tag{6.74}$$

where $\tilde{\boldsymbol{v}} = [\dot{v}_A \;\; \dot{v}]^{\mathrm{T}} \in \mathrm{R}^2$. The following relation about the forces can also be derived using Eq. (6.67)

$$\tilde{\boldsymbol{J}}^{\mathrm{T}}\boldsymbol{\tau} = \tilde{\boldsymbol{T}} \tag{6.75}$$

where $\tilde{\boldsymbol{T}} = [T_A \;\; T]^{\mathrm{T}} \in \mathrm{R}^2$. By using Eqs. (6.64), (6.74) and (6.75), and eliminating $\boldsymbol{\tau}$ and $\ddot{\boldsymbol{q}}$, the following equation can be derived:

$$\tilde{\boldsymbol{J}}^{\mathrm{T}}\boldsymbol{M}_q\tilde{\boldsymbol{J}}\ddot{\tilde{\boldsymbol{v}}} + \tilde{\boldsymbol{J}}^{\mathrm{T}}\boldsymbol{J}^{\mathrm{T}}\boldsymbol{F} = \tilde{\boldsymbol{T}} \tag{6.76}$$

By using the values of $\tilde{\boldsymbol{J}}$ and $\boldsymbol{J}$, the second term on the left side of Eq. (6.76) can be given as:

$$\tilde{\boldsymbol{J}}^{\mathrm{T}}\boldsymbol{J}^{\mathrm{T}}\boldsymbol{F} = \begin{bmatrix} 0 \\ f_1 + f_2 \end{bmatrix} \tag{6.77}$$

On the other hand, when external force T_E is not applied to the object, the equation of the object motion can be represented by using Eqs. (6.65) and (6.66):

$$m_O\dot{v} = f_1 + f_2 \tag{6.78}$$

Moreover, the next relation derived by Eq. (6.68) holds:

$$\ddot{\tilde{v}} = \ddot{\tilde{r}} \tag{6.79}$$

Therefore, by using Eqs. (6.76) $\sim$ (6.79), the equation of motion of the whole system can be derived as follows:

$$\boldsymbol{M}\ddot{\tilde{\boldsymbol{r}}} = \tilde{\boldsymbol{T}} \tag{6.80}$$

where,

$$\begin{aligned} \boldsymbol{M} &= \tilde{\boldsymbol{J}}^{\mathrm{T}}\boldsymbol{M}_q\tilde{\boldsymbol{J}} + \begin{bmatrix} 0 & 0 \\ 0 & m_O \end{bmatrix} \\ &= \begin{bmatrix} m_A + m_H & 0 \\ 0 & m_{F1} + m_{F2} + m_O \end{bmatrix} \end{aligned}$$

$\boldsymbol{M}$ means the original mass characteristics of the whole system. When the desired value of inertia $\boldsymbol{M}_d$ is different from the original value, the driving force corresponding to the difference is required. In the simulation, $\boldsymbol{M}_d$ is determined to be equal to $\boldsymbol{M}$:

$$M_{Ad} = m_A + m_H \tag{6.81}$$

$$M_{rd} = m_{F1} + m_{F2} + m_O \tag{6.82}$$

As for 2), due to the stiffness of the endpoint of the arm, K_{Ad} is determined as $K_{Ad} = K_{rd}$. These values are determined in which the natural frequency of the endpoint of the arm and object, ω_A and ω, are:

$$\omega_A = \sqrt{\frac{K_{Ad}}{M_{Ad}}} = 8[\mathrm{rad/s}], \quad \omega = \sqrt{\frac{K_{rd}}{M_{rd}}} = 40[\mathrm{rad/s}]$$

Generally, stiffness K_{Ad} should be determined as in Chapter 5:

$$K_{Ad} = \boldsymbol{J}_{AHd}^{\mathrm{T}}K_{rd}\boldsymbol{J}_{AHd} \tag{6.83}$$

$\boldsymbol{J}_{AHd}$ in Eq. (6.83) can be calculated using ${}^A\boldsymbol{p}_{Hd}$ for Eq. (6.21), where ${}^A\boldsymbol{p}_{Hd}$ is the position vector of $\mathrm{O_H}$ from $\mathrm{O_A}$ when the hand is in the desired position.

As for 3), D_{Ad} and D_{rd} are determined as the coefficients of damping ζ_A and ζ as 0.7:

$$\zeta_A = \frac{D_{Ad}}{2\sqrt{M_{Ad}K_{Ad}}} = 0.7, \quad \zeta = \frac{D_{rd}}{2\sqrt{M_{rd}K_{rd}}} = 0.7$$

The initial values of the position and velocities are:

$$r(0) = 0.5[\mathrm{m}], \quad {}^Ar_H(0) = 0.1[\mathrm{m}]$$

$$\dot{q}_A(0) = \dot{q}_{F1}(0) = \dot{q}_{F2}(0) = 0[\mathrm{m/s}]$$

and the desired values of r_d and ${}^Ar_{Hd}$ are determined so as to be equal to their initial values.

6.4.3 Simulation Results

In this section, the simulation results are described. However first, method for simulation is described prior to them.

The simulations in this chapter are for the arm-hand system moving under constraint among the fingertips. So it is necessary to get the motion of the mechanism which can satisfy the constraint and fingertip force simultaneously, for a given joint force. Therefore, the equation of motion of the mechanism is made clear considering as a regards the above intention.

As for acceleration, the next equation is obtained by Eq. (6.18).

$$J\ddot{q} + \dot{J}\dot{q} = J_{HF}\dot{v} + \dot{J}_{HF}v \tag{6.84}$$

The next equation is then obtained by eliminating $\dot{v}$ and T from Eqs. (6.84), (6.33) and (6.34).

$$J\ddot{q} - J_{HF}M_O^{-1}J_{HF}^{\mathrm{T}}F = J_{HF}M_O^{-1}(T_E - h_O) + \dot{J}_{HF}v - \dot{J}\dot{q} \tag{6.85}$$

Consequently, the equation of motion of the whole system can be derived using Eqs. (6.85) and (6.32):

$$\tilde{M}_q \begin{bmatrix} \ddot{q} \\ F \end{bmatrix} = \tilde{\tau} \tag{6.86}$$

where,

$$\tilde{M}_q = \begin{bmatrix} M_q & J^{\mathrm{T}} \\ J & -J_{HF}M_O^{-1}J_{HF}^{\mathrm{T}} \end{bmatrix} \in \mathrm{R}^{5\times 5}$$

$$\tilde{\tau} = \begin{bmatrix} \tau - h_q \\ J_{HF}M_O^{-1}(T_E - h_O) + \dot{J}_{HF}v - \dot{J}\dot{q} \end{bmatrix} \in \mathrm{R}^5$$

Since $\tilde{M}_q$ is a full rank matrix (see Appendix A), $\ddot{q}$ and F can be obtained simultaneously by solving Eq. (6.86) for given joint force τ. The sampling time for obtaining $\ddot{q}$ and F is 1 ms. $\dot{q}$ and q are obtained from $\ddot{q}$ using the Euler method such that the step-size of the numerical integration is 0.1 ms. T_A required in the control law is obtained using Eq. (6.60).

During the first 1[s] during each simulation, the object is assumed to be supported by a table at the initial position, because of realizing non-slip grasping. Therefore, the external force is applied after a second.

First, the position and the force responses are investigated when the external force is changed as the step function, shown in Fig. 6.3(a). T_A in this case is also shown in Fig. 6.3(a).

For manipulation, Fig. 6.3(b) shows that the motion of the object appears faster than that of the endpoint of the arm, so that of the hand appears faster as a result. The reasons for these motions are that the natural frequency given to object ω is larger than that given to the endpoint of arm ω_A. In addition, the position of hand ${}^A\boldsymbol{r}_H$ goes to the initial position, even when the deviation of the object is $T_E/K_{rd} = 0.05$[m]. That is, this control scheme utilizes the small motion range of the hand effectively against any additional external force.

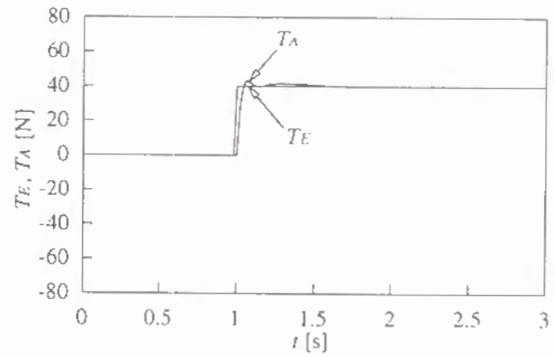

(a) External force

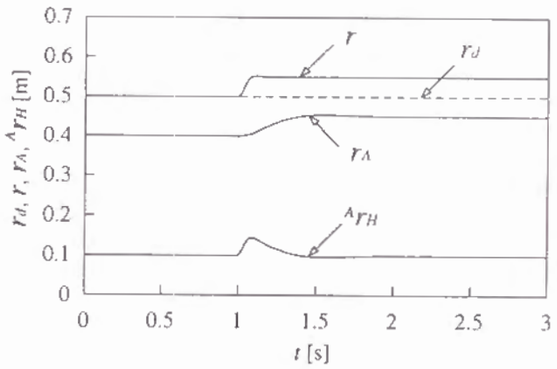

(b) Position

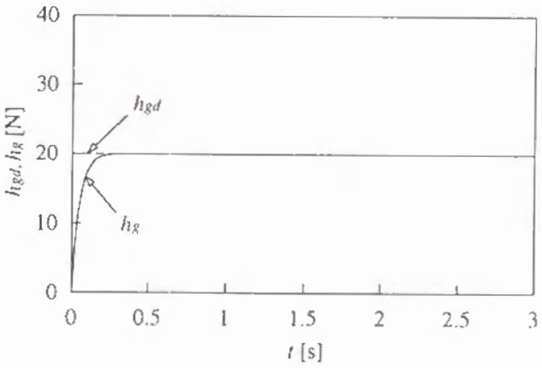

(c) Grasp parameter

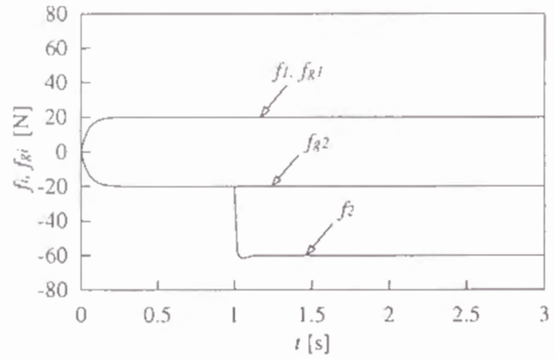

(d) Fingertip and grasping forces

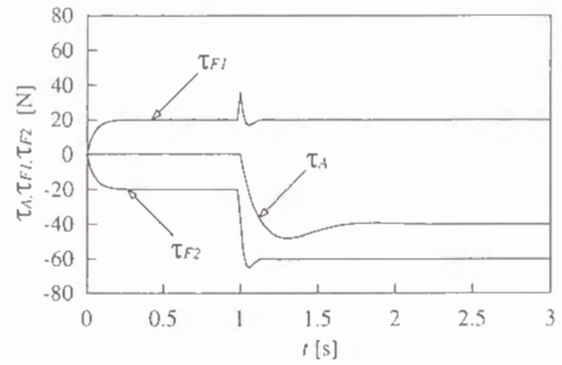

(e) Joint force

Fig. 6.3. Simulation results when the external force is changed as the step function.

For grasping, Fig. 6.3(c) shows that grasp parameter h_g converges to its desired value h_{gd} soon, and that it follows the desired value during manipulation. Fig. 6.3(d) shows that the magnitudes of grasping forces f_{g1} and f_{g2} are same as h_g, and that the magnitudes of fingertip forces f_{g1} and f_{g2} are equal to or larger than h_g during manipulation. Note that the difference between f_{gi} and f_i means manipulating force f_{mi} and f_{mi} appear such that it makes the magnitude of the fingertip force large. This f_{mi} does not disturb the non-slip grasping realized by f_{gi}.

The required driving force shown in Fig. 6.3(e) is not excessive, because the original mass characteristics of the system are considered in determination of the desired mass characteristics.

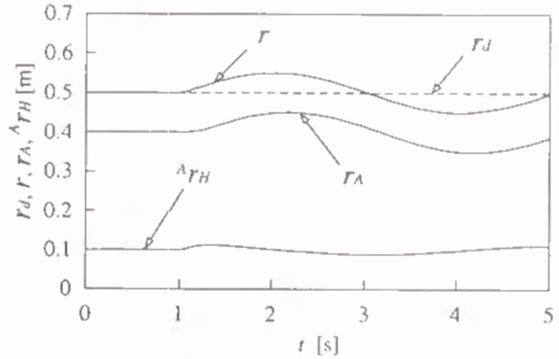

(a) Position when $f_r = 0.25$ [Hz]

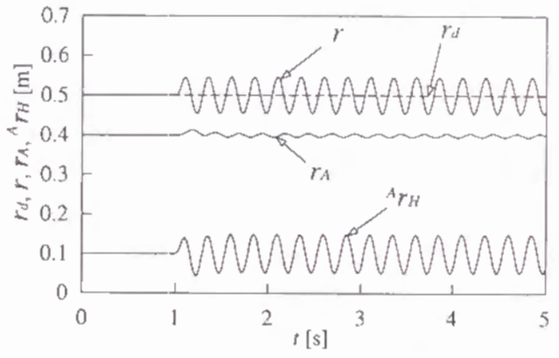

(b) Position when $f_r = 4$ [Hz]

Fig. 6.4. Simulation results when the external force is changed as the sine wave.

Second, the external force changed as sine wave is applied, and the position response is investigated. Figures 6.4(a) and 6.4(b) show the position responses when the frequencies are $f_r = 0.25$[Hz] and $f_r = 4$[Hz], respectively. We found that the arm part mainly moves when $f_r = 0.25$[Hz] and that the hand part mainly moves when $f_r = 4$[Hz]. This means that the motion distribution according to the frequency of the external force is possible.

Third, when thinking of a general case, the external force changed as the composite sine wave is applied, which is shown by the following equation.

$$T_E = a_1 \sin(2\pi f_{r1} t') + a_2 \sin(2\pi f_{r2} t') \tag{6.87}$$

where, $t' = t - 1$ (≥ 0). In this case, $a_1 = 40$[N], $a_2 = 10$[N], $f_{r1} = 0.25$[Hz], $f_{r2} = 4$[Hz]. This external force is shown in Fig. 6.5(a).

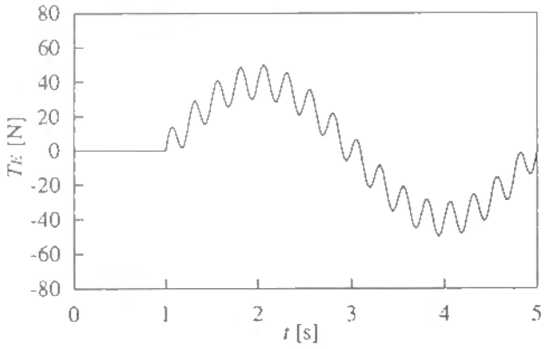

(a) External force

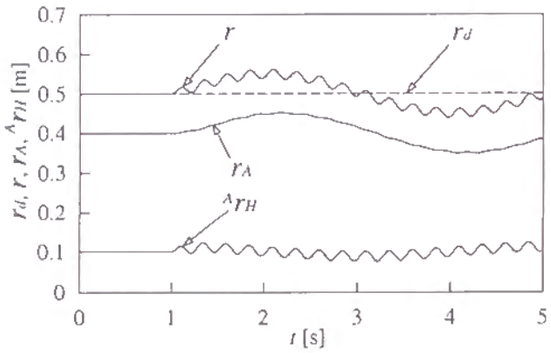

(b) Position

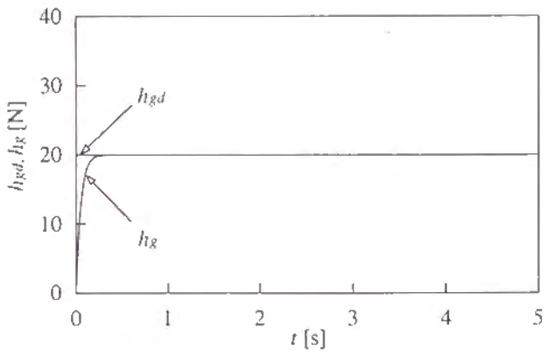

(c) Grasp parameter

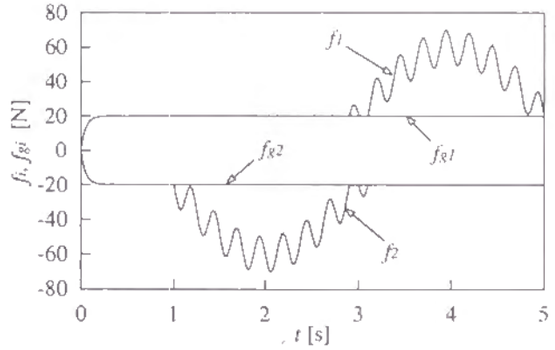

(d) Fingertip and grasping forces

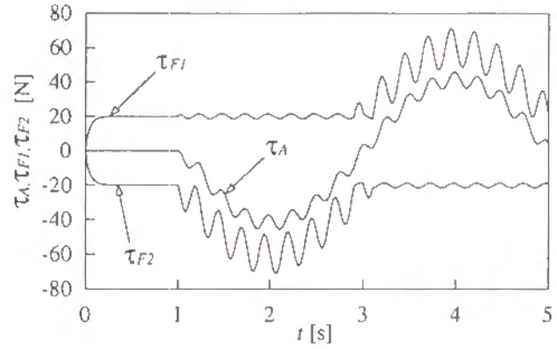

(e) Joint force

Fig. 6.5. Simulation results when external force is changed as the composite sine wave.

Figure 6.5(b) shows that the endpoint of the arm part moves according to the lower frequency element of the external force, but the hand part moves according to its higher frequency element. This results suggest to us that the mechanical impedances could be determined as the above motion distribution occurs. Putting it more concretely, M_{Ad} and M_{rd} should be determined as the natural frequency of the endpoint of the arm, ω_A is smaller than that of object ω. The control of the mechanism based on this idea makes it possible to utilize both merits of the arm and hand, that is the big motion range of the arm and the high capability of compliant motion of the hand.

Figures 6.5(c) and 6.5(d) show the responses of the grasp parameter, the grasping force and the fingertip force. Grasp parameter h_g converges on h_{gd} and follows it, the magnitudes of the fingertip forces are equal to or larger than h_g during manipulation. These behaviors are the same as those in Fig. 6.3.

Figure 6.5(e) shows that the required joint force is not excessive.

In the above simulations, using the grasping and manipulating forces seems to work well so as to realize secure grasping. To verify the above supposition, lets construct the controller without the grasping and manipulating forces and compare both results.

As one example of the controller without the grasping and manipulating forces, there is a method to calculate desired fingertip force $\boldsymbol{F}_d$ using the following equations instead of Eqs. (6.46) $\sim$ (6.48), (6.54) and (6.55):

$$\begin{aligned}
\boldsymbol{F}_d &= \tilde{\boldsymbol{F}}_{gd} + \tilde{\boldsymbol{F}}_{md} && (6.88)\\
\tilde{\boldsymbol{F}}_{gd} &= \tilde{\boldsymbol{F}}_{gd2} + \boldsymbol{K}_F \int (\tilde{\boldsymbol{F}}_{gd2} - \tilde{\boldsymbol{F}}_g) dt && (6.89)\\
\boldsymbol{K}_F &= \mathrm{diag.}(k_{F1}, k_{F2}) \\
\tilde{\boldsymbol{F}}_{gd2} &= \begin{bmatrix} 1 \\ -1 \end{bmatrix} h_{gd} - T_c \dot{\boldsymbol{F}}_{gd2} && (6.90)\\
\tilde{\boldsymbol{F}}_{md} &= \left(\boldsymbol{J}_{HF}^{\mathrm{T}}\right)^{\dagger} T_d = \begin{bmatrix} T_d/2 \\ T_d/2 \end{bmatrix} && (6.91)
\end{aligned}$$

In the above method, $\tilde{\boldsymbol{F}}_{gd}$ for grasping is calculated by $\tilde{\boldsymbol{F}}_g = [\tilde{f}_{g1} \quad \tilde{f}_{g2}]^{\mathrm{T}} \in \mathrm{R}^2$ as the control input $\tilde{\boldsymbol{F}}_{md}$ for manipulation is calculated by solving Eq. (6.34) for $\boldsymbol{F}$ using the pseudoinverse of $\boldsymbol{J}_{HF}^{\mathrm{T}}$. In Eq. (6.90), the desired value of element of the fingertip force for grasping is determined by h_{gd} so as to make it agree with that in Figure 6.5. A method to detect $\tilde{\boldsymbol{F}}_g$ from $\boldsymbol{F}$ is described in Appendix B.

Figure 6.6 shows the responses of position f_i and f_{gi} when the external force is the same as that in Figure 6.5, where the parameters are determined similar to these in Fig. 6.5 in the following way:

$$h_{gd} = 20[\mathrm{N}], \quad k_{Fi} = 100[1/\mathrm{s}], \quad T_c = 0.05[\mathrm{s}]$$

Figure 6.6(b) shows that the response of the fingertip force f_i is different even when the position response in Fig. 6.6(a) is the same as in Fig. 6.5(b). The magnitudes of f_i are not only equal to or larger than h_{gd}, and are also sometimes in the inverse direction of the object inward. The reason for this behavior is caused from the calculation of $\tilde{\boldsymbol{F}}_{md}$ by Eq. (6.91), and we find that the constant internal force can not be enough as the desired value for secure grasping in this case. This means that the proposed controller which uses the grasping and manipulating forces is suitable for secure grasping.

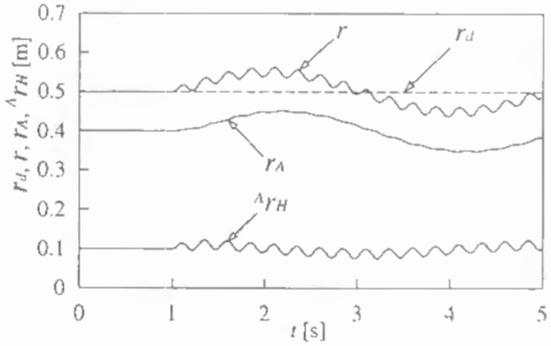

(a) Position

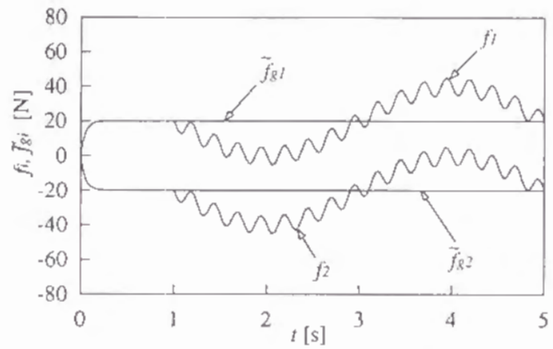

(b) Fingertip force and its component for grasping

Fig. 6.6. Simulation results without the grasping and manipulating forces when the external force is changed as the composite sine wave.

6.5 Experiment

In this section, several experimental results are presented to demonstrate the validity of the proposed control scheme, which correspond to the results of the simulation in the previous section.

A 1 DOF arm-hand mechanism used in the experiments is shown in Fig. 6.7. The both parts of the arm and two-fingered hand can manipulate an object along the common line. Indeed, the two fingers which have links with a length of 0.08[m] are driven by revolute joints. However, the hand is treated as a hand with 1 DOF linear motion by converting the parameters of dynamics into those in linear motion. The values of mass of the mechanism are as follows:

$$m_A = 8.7[\mathrm{kg}], \quad m_H = 4.3[\mathrm{kg}], \quad m_{F1} = m_{F2} = 0.15[\mathrm{kg}]$$
$$m_O = 0.15[\mathrm{kg}]$$

The friction of the arm are not negligible, therefore they are identified based on the method of identification[41]. The static friction forces are estimated as 30[N] in plus direction and -31[N] in minus direction. The motion friction forces and the viscous frictional coefficients are also estimated as 16.0[N] and 57.7[N/(m/s)] in plus direction, -17.0[N] and 65.7[N/(m/s)] in minus direction.

First, an external force like step function with a magnitude of 20[N] is applied by using a weighting mass and a pulley. Figure 6.8(a) shows detected external force, T_E, calculated by,

$$T_E = -J_{HF}^{\mathrm{T}} F \tag{6.92}$$

and the force applied at the endpoint of the arm, T_A. Indeed, the exact external force is calculated by using Eqs. (6.65) and (6.66) with an acceleration of the object. However, the inertia term $M_O \dot{v}$ is neglected in this experiment, because the mass of the object M_O is not big. Figure 6.8(b) shows that the motion of the object appears faster than that of the endpoint of the arm, and the hand goes to a position close to the initial position, those are similar to the results of simulation shown in Figure 6.3. In addition, Figs. 6.8(c) and 6.8(d) show that the responses of the grasp parameter, the fingertip force and the grasping force are also similar to the results of simulation. The joint force shown in Fig. 6.8(e) are also similar to the results of simulation, even τ_A includes the joint force elements which compensate the friction forces.

Second, the applied external force is changed like a sine wave. Figure 6.9 shows that the distribution of motion is possible according to the frequency of the external force, which is similar to the case in the simulation shown in Fig. 6.4.

Finally, the applied force is changed like a composite sine wave in Fig. 6.10(a). By the figure, the two frequencies of the external force elements are found as about 0.25[Hz] and 4[Hz]. Figure 6.10(b) shows that the endpoint of the arm part moves according to the lower frequency element of the external force, on the other hand, the hand part moves according to its higher frequency element. This results is qualitatively same as that in the simulation shown in Fig. 6.5. Figure 6.10(d) shows that the fingertip force keeps to be a push force, even the response of the grasp parameter shown in Fig. 6.10(c) is not so good. Figure 6.10(e) shows that the required joint force is not excessive.

Above results correspond to those in the simulation, and illustrate the validity of the proposed control scheme.

(a) Whole mechanism and object

(b) Two-fingered hand

Fig. 6.7. 1 DOF arm-hand mechanism for experiment.

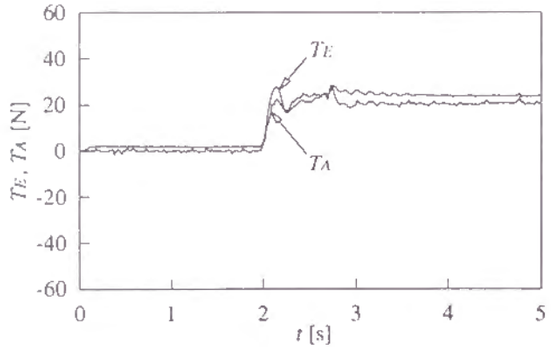

(a) External force

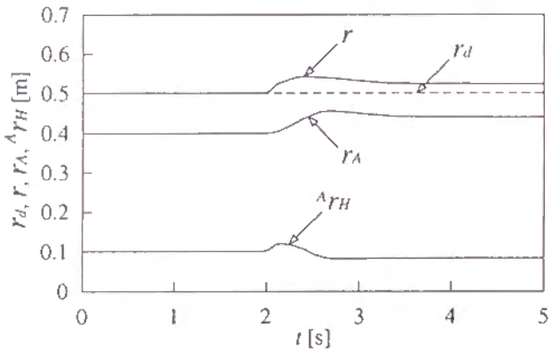

(b) Position

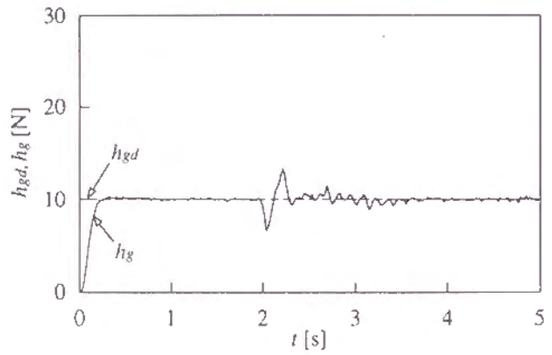

(c) Grasp parameter

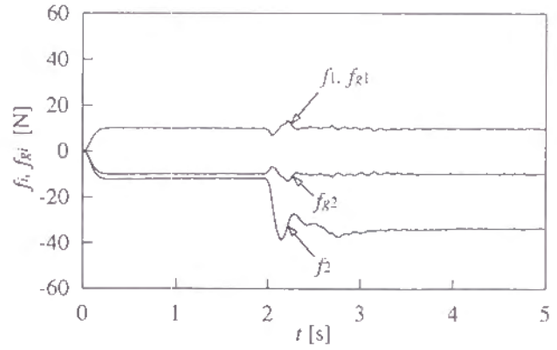

(d) Fingertip and grasping forces

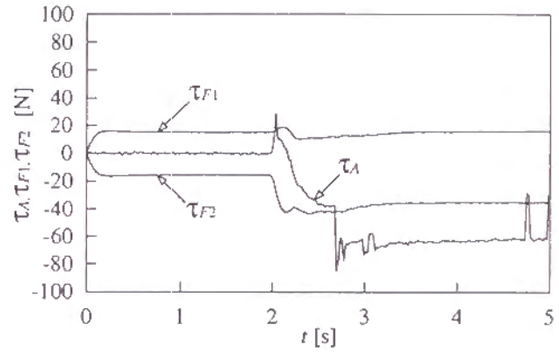

(e) Joint force

Fig. 6.8. Experimental results when the external force is changed like the step function.

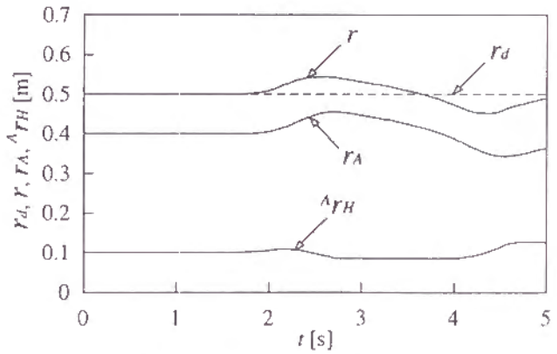

(a) Position when frequency of the external force is low

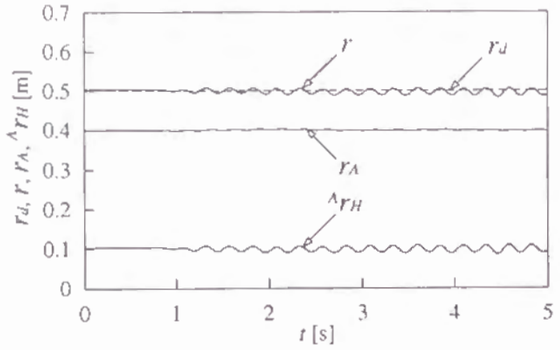

(b) Position when frequency of the external force is high

Fig. 6.9. Experimental results when the external force is changed like the sine wave.

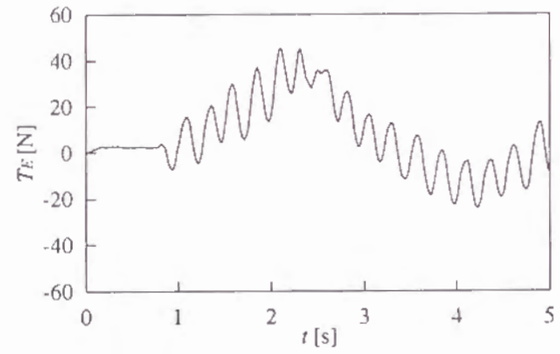

(a) External force

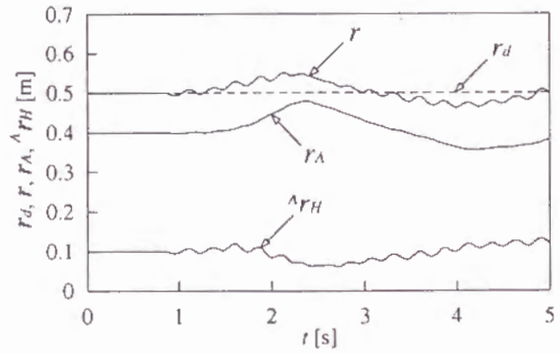

(b) Position

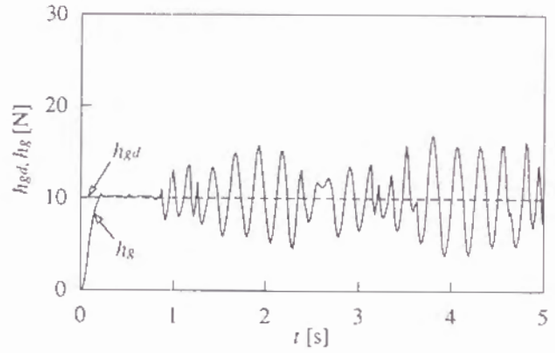

(c) Grasp parameter

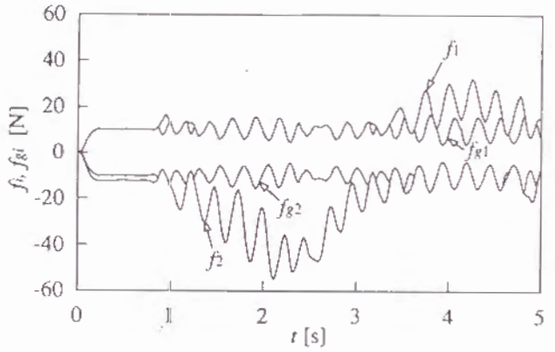

(d) Fingertip and grasping forces

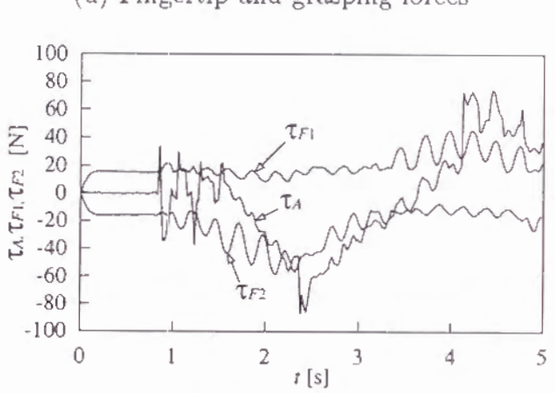

(e) Joint force

Fig. 6.10. Experimental results when the external force is changed like the composite sine wave

6.6 Conclusion

The major results obtained in this chapter are as summarized as follows.

1) A motion control scheme is proposed. For manipulation, this control scheme is based on the impedance control scheme of redundant macro-micro manipulators introduced in Chapter 5. In the control scheme, the arm is considered as the macro manipulator and the hand is considered as the micro manipulator. This control scheme can utilize both merits of the arm and hand, that is, the big motion range of the arm and the high capability of compliant motion of the hand. This control scheme can also obtain secure grasping during manipulation.

2) Simulation and experimental results illustrate the validity of the controller.

The capability of the hand controlled by the proposed control scheme includes the capability of RCC proposed by Whitney[54]. Moreover, this control scheme can compensate for the small motion range of the hand which is a defect of RCC. Therefore, this control scheme is thought to be a major advancement regarding manipulation technology.

Appendix A Proof that $\tilde{M}_q$ is Full Rank Matrix

It is utilized in a way that the rank of the matrix does not change when a regular matrix is multiplied.

$$\begin{aligned}
&\mathrm{rank}\left(\tilde{M}_q\right) \\
&= \mathrm{rank}\left(\begin{bmatrix} E_3 & 0 \\ -JM_q^{-1} & E_2 \end{bmatrix}\tilde{M}_q\right) \\
&= \mathrm{rank}\left(\begin{bmatrix} M_q & J^{\mathrm{T}} \\ 0 & -JM_q^{-1}J^{\mathrm{T}} - J_{HF}M_O^{-1}J_{HF}^{\mathrm{T}} \end{bmatrix}\right) \\
&= \mathrm{rank}\,(M_q) \\
&\quad + \mathrm{rank}\left([J \quad J_{HF}]\begin{bmatrix} -M_q^{-1} & 0 \\ 0 & -M_O^{-1} \end{bmatrix}[J \quad J_{HF}]^{\mathrm{T}}\right) \\
&= 3+2 \\
&= 5
\end{aligned} \tag{6.a}$$

Appendix B detection of $\tilde{F}_g$ without the Grasping and Manipulating Forces

The following equations holds:

$$\tilde{F}_g = F - \tilde{F}_m \tag{6.b}$$

$$\tilde{F}_m = (J_{HF}^{\mathrm{T}})^{\dagger}T \tag{6.c}$$

$$T = J_{HF}^{\mathrm{T}}F \tag{6.d}$$

$\tilde{F}_g$ can be detected by the next equation using the above equations:

$$\begin{aligned}
\tilde{F}_g &= \left\{E_2 - \left(J_{HF}^{\mathrm{T}}\right)^{\dagger}J_{HF}^{\mathrm{T}}\right\}F \\
&= \begin{bmatrix} 1/2 & -1/2 \\ -1/2 & 1/2 \end{bmatrix}F \\
&= \begin{bmatrix} (f_1 - f_2)/2 \\ (-f_1 + f_2)/2 \end{bmatrix}
\end{aligned} \tag{6.e}$$

Chapter 7

Concluding Remarks

7.1 Results of This Thesis

Grasping and manipulation are two of the most important topics in the robotics field, which are very closely related to each other. Multifingered hands have the capability of grasping and manipulation. It is important for them to have a suitable fingertip force for secure grasping and desired manipulation. Moreover, the hand has to be attached to an arm in order to obtain a big motion range. In such a case, cooperative manipulation of the arm and the hand with secure grasping is important.

In the first half of this thesis, Chapters 2 through 4, grasping and manipulation by multifingered hands have been discussed. In the second half of the thesis, Chapters 5 and 6, cooperative manipulation by redundant macro-micro manipulators and cooperative manipulation with secure grasping by arm-hand systems has been discussed.

In Chapter 2, a new definition of grasping and manipulating forces has been proposed for multifingered robot hands. The concept of grasp mode has also been introduced. An algorithm for decomposing a given fingertip force into the grasping and manipulating forces has been presented. This decomposition is required for the controller proposed in Chapter 3.

In Chapter 3, a dynamic manipulation/grasping controller of multifingered robot hands has been proposed, based on the dynamic control and hybrid position/force control. This controller, using the concept of the manipulating and grasping forces, consists of a compensator which linearizes the whole grasping system and a servo-controller for the linearized system. The distinctive features of the proposed controller are: 1) It uses a grasp parameter, which has the same number of elements as that of the essential dimension of the internal force, as the controlled variables for the grasping control. 2) It decomposes the total force applied to the grasped object into the manipulating force which is a part of the fingertip force.

In Chapter 4, a new method of the adaptive grasping for multifingered hands with the

constraints of static friction and joint torque, under the repeated manipulation tasks has been discussed. Then, a new algorithm of the adaptive grasping has been proposed. This algorithm realizes the desired manipulation without any slipping of the fingertips, adjusting the grasp parameter to the specified manipulation task.

In Chapter 5, an impedance control scheme of redundant macro-micro manipulators has been proposed. In this control scheme, we can specify not only the desired mechanical impedance of the end effector but also that of the macro manipulator by considering the internal force applied at the tip of the macro manipulator. This control scheme can utilize both merits of the macro and micro manipulators. That is, by specifying a suitable set for the desired mechanical impedance, a compliant motion can be obtained without any excessive joint torque of the macro manipulator, and a big motion range of the macro manipulator can be used effectively to compensate for the small motion range of the micro manipulator.

In Chapter 6, a control scheme for grasping and manipulation by arm-hand mechanisms has been proposed. The arm-hand mechanisms, consist of an arm and multifingered hand, have the same features as that of redundant macro-micro manipulator regarding manipulation. That is: 1) manipulation is possible not only the arm but also using the hand, 2) the hand is suitable for compliant motion compared to the arm because of the small inertia, and the motion range of the arm is larger than that of the hand. The control scheme can utilize both merits of the arm and hand. Simultaneously, it can realize secure grasping during manipulation.

The author believes that the results obtained in this thesis will contribute to advanced manipulation technology, and also help to realize dexterous manipulation, which can be had by the cooperative motions by the human arm and hand.

7.2 Further Research Topics

There are several further research topics about grasping and manipulation by multifingered hands and arm-hand systems.

For multifingered hands, one of the topics is the problem of the contact between the fingertips and an object. In this thesis, the point contact is assumed because it makes the problem on grasping and manipulation much clearer. However, we need to consider the rolling contact and elasticity of the fingertips as practical matters.

Uncertainty is another topic of multifingered hands. A clearance in assembly tasks like insertion is often smaller than $10[\mu\mathrm{m}]$, and it is beyond the position accuracy of the robot hand. Toward such a problem, an intelligent motion control may be required based on task understanding.

For arm-hand systems, the proposed control scheme must be a reasonable way to realize

cooperative motion of the arm and hand. However, there may be a more advanced control algorithm that is more flexible to the variety of real tasks. In such a case, a learning algorithm may be necessary to obtain a suitable mechanical impedance.

To develop artificial hands for physically disabled persons is one of the most important topics for the author. Since, the author believes that our society can be a truly affluent one, if these disabled people do not feel to be the weak by utilizing the technology in the robotics field.

Bibliography

[1] J. M. Abel, W. Holzmann, and J. M. McGarthy: "On grasping planar objects with two articulated fingers," Proc. IEEE Int. Conf. on Robotics and Automation, pp.576-581, 1985.

[2] T. E. Alberts and D. I. Soloway: "Force Control of a Multi-Arm Robot System," Proc. IEEE Int. Conf. on Robotics and Automation, pp.1490-1496, 1988.

[3] A. Bicchi: "Analysis and Control of Power Grasping," Proc. of 1991 IEEE/RSJ Int. Workshop on Intelligent Robots and Systems (IROS'91), pp.691-697, 1991.

[4] T. L. Boullion and P. L. Odell: "Generalized Inverse Matrices," New York: Wiley, pp.1-11, 1971.

[5] C. Cai: "LP Problem Formulation of Extremal Path Accelerations for a Rigid Body Handled by Multiple Linkages," IEEE Trans. Robotics and Automation, Vol.6, No.3, pp.342-347, 1990.

[6] A. B. A. Cole, J. E. Hauser, and S. S. Sastry: "Kinematics and Control of Multifingered Hands with Rolling Contact," IEEE Trans. Automatic Control, Vol.34, No.4, pp.398-404, 1989.

[7] M. R. Cutkosky and P. K. Wright: "Friction, Stability and the Design of Robotic Fingers," Int. Journal of Robotic Research, vol.5, No.4, pp.20-37, 1986.

[8] M. R. Cutkosky: "On Grasp Choice, Grasp Models, and the Design of Hands for Manufacturing Tasks," IEEE Trans. Robotics and Automation, Vol.5, No.3, pp.269-279, 1989.

[9] M. R. Cutkosky and I. Kao: "Computing and Controlling the Compliance of a Robot Hand," IEEE Trans. Robotics and Automation, Vol.5, No.2, pp.151-165, 1989.

[10] J. Demmel and G. Lafferriere: "Optimal Three Finger Grasps," in Proc. IEEE Int. Conf. Robotics and Automation, pp.936-942, 1989.

[11] R. S. Fearing: "Simplified Grasping and Manipulation with Dexterous Robot Hands," IEEE Journal Robotics and Automation, Vol.2, No.4, pp.188-195, 1986.

[12] H. Hanafusa and H. Asada: "Stable Prehension by a Robot Hand with Elastic Fingers," Proc. 7th Int. Symp. Industrial Robots pp.361-368, 1977.

[13] H. Hanafusa, T. Yoshikawa, and Y. Nakamura: "Analysis and Control of Articulated Robot Arms with Redundancy," Prep. 8th IFAC World Congress, XIV, pp.78-83, 1981.

[14] H. Hanafusa, T. Yoshikawa, Y. Nakamura, and K. Nagai "Structural Analysis and Robust Prehension of Robotic Hand-Arm System," Proc. Int. Conf. Advanced Robotics, Tokyo, pp.311-318, 1985.

[15] H. Hanafusa and M. A. Adli: "Effect of Internal Forces on Stiffness of Closed Mechanisms," Journal of RSJ, vol.10, No.1, pp.128-134, 1992. (in Japanese)

[16] N. Hogan : Impedance Control; "An Approach to Manipulation, Parts I–III, ASME Journal of Dynamic Systems, Measurement, and Control," Vol.107, No.1, pp.1-24, 1985.

[17] S. C. Jacobsen et al.: "The version I UTA/MIT dexterous hand," in Robotics Research, 2nd Int. Symp. Cambridge, MA: MIT Press, pp.301-308, 1985.

[18] Z. Ji and B. Roth: "Direct computation of grasping force for three-finger tip-prehension grasps," ASME Journal Mechanisms, Transmissions, Automat. Design, vol.110, pp.405-413, 1988.

[19] M. Kaneko, N. Imamura, K. Yokoi, and K. Tanie: "Stiffness Model Based Grasp Stability Analysis of Multi-Fingered Hand with Friction," Journal of RSJ, Vol.7, No.3, pp.161-170, 1989. (in Japanese)

[20] K. Kawase, H. Ishikawa, C. Sawada, and M. Takata: "Cooperative Compliant Motion Control of Wrist and Arm," Journal of RSJ, Vol.9, No.4, pp.401-408, 1991. (in Japanese)

[21] J. Kerr and B. Roth: "Analysis of multifingered hands," Int. Journal Robotics Research, vol.4, no.4, pp.3-17, 1986.

[22] J. Kerr and B. Roth: "Special Grasping Configurations with Dexterous Hands," Proc. of IEEE Int. Conf. on Robotics and Automation, pp.1361-1367, 1986.

[23] O. Khatib : "Reduced effective inertia in macro-/mini-manipulator systems," Proc. of ACC, pp.2140-2147, 1988.

[24] M. Kitagawa, H. Asada, and H. Tokumaru: "Mechanics of Grasping using Potential Function," Trans. of JAACE, 1986.

[25] V. Kumar and K. J. Waldron: "Sub-optimal algorithms for force distribution in multifingered grippers," in Proc. IEEE Int. Conf. Robotics Automat., pp.252-257, 1987.

[26] V. Kumar and K. J. Waldron: "Suboptimal Algorithms for Force Distribution in Multifingered Grippers," IEEE Trans. Robotics and Automation, Vol.5, No.4, pp.491-498, 1989.

[27] H. Kobayashi: "Control and geometrical consideration for an articulated robot hand," Int. Journal Robotics Research, vol.4, no.1, pp.3-12, 1985.

[28] H. Kobayashi: "On the articulated hands," in Robotics Research 2nd Int. Symp. Cambridge, MA: MIT Press, pp.293-300, 1985.

[29] Z. Li and S. Sastry: "Task oriented optimal grasping by multifingered robot hands," in Proc. IEEE Int. Conf. Robotics and Automation, pp.389-394. 1987.

[30] Z. Li, P. Hsu and S. Sastry: "Grasping and Coordinated Manipulation by a Multifingered Robot Hand," Int. Journal of Robotics Research, Vol.8, No.4, pp.33-50, 1989.

[31] Z. Li and J. Canny: "Motion of Two Rigid Bodies with Rolling Constraint," IEEE Trans. Robotics and Automation, Vol.6, No.1, pp.62-72, 1990.

[32] M. T. Mason and J. K. Salisbury: "Robot Hands and the Mechanics of Manipulation," Cambridge, MA: MIT Press, 1985.

[33] D. J. Montana: "The Kinematics of Contact and Grasp," Int. Journal of Robotic Research, Vol.7, No.1, pp.3-8, 1988.

[34] Y. Nakamura, K. Nagai, and T. Yoshikawa: "Mechanics of Coordinative Manipulation by Multiple Robotic Mechanisms," Journal of RSJ, Vol.4, No.5, pp.489-498, 1986.(in Japanese)

[35] Y. Nakamura, K. Nagai, and T. Yoshikawa: "Mechanics of Coordinative Manipulation by Multiple Robotic Mechanisms," Proc. IEEE Int. Conf. on Robotics and Automation, pp.991-998, 1987

[36] Y. Nakamura, K. Nagai, and T. Yoshikawa: "Dynamics and Stability in Coordination of Multiple Robotic Mechanisms," The Int. Journal of Robotics Research, Vol.8, No.2, pp.44-61, 1989.

[37] W. S. Newman and M. E. Dohring: "Augmented Impedance Control: An Approach to Compliant Control of Kinematically Redundant Manipulators," Proc. IEEE Int. Conf. on Robotics and Automation, pp.30-35, 1991.

[38] V. D. Nguyen: "Constructing force-closure grasps," Int. Journal Robotics Research, vol. 7, no. 3, pp.3-16, 1988.

[39] V. Nguyen: "Constructing Stable Grasps," Int. Journal Robotics Research, Vol.8, No.1, pp.26-37, 1989.

[40] T. Okada: "Object-handling system for manual industry," IEEE Trans. Syst . Man Cybern., Vol.SMC-9, No.2, pp.79-89, 1979.

[41] K. Osuka and H. Mayeda: "A New Identification Method for Manipulators," Trans. of SICE, Vol.22, No.6, pp.41-47, 1986. (in Japanese)

[42] M. Raibert and J. Craig: "Hybrid Position/Force Control of Manipulators," Journal of Dynamic Systems, Measurement and Control, Vol.103, No.2, pp.126-133, 1981.

[43] J. K. Salisbury and J. J. Craig: "Articulated hands: Force control and kinematic issues," Int. Journal Robotics Research, vol.1, no.1, pp.4-17, 1982.

[44] J. K. Salisbury and B. Roth: "Kinematic and force analysis of articulated mechanical hands," ASME Journal Mechanisms, Transmissions, Automat. Design, vol.105, pp.35-41, 1983.

[45] J. T. Schwartz and M. Sharir: "Finding effective force-targets for two-dimensional multifinger frictional grips," in Proc. 25th Allerton Conf. Commun., Control, Computing, pp.843-848, 1987.

[46] A. Sharon, N. Hogan, and D. E. Hardt: "Controller Design in the Physical Domain," Proc. of the IEEE Conference on Robotics and Automation, pp.552-559, 1989.

[47] G. P. Starr: "Experiments in Assembly Using a Dexterous Hand," IEEE Trans. Robotics and Automation, Vol.6, No.3, pp.342-347, 1990.

[48] T. Sugie and T. Yoshikawa: "General Solution of Robust Tracking Problem in Two-Degrees-of-Freedom Control Systems," IEEE Trans. on Automatic Control AC-31-6, pp.552-554, 1986.

[49] T. Sugie, K. Kumashita, and T. Ono: "Coordinative Manipulation by Multiple Manipulators," Trans. of SYSTEM AND CONTROL, Vol.1, No.4, pp.144-151, 1988 (in Japanese)

[50] J. C.Trinkle, J. M. Abel, and R. P. Paul: "Enveloping, frictionless, planar grasping," in Proc. IEEE Int. Conf. Robotics Automat., pp.246-251, 1987.

[51] T. Tsuji, T. Takahashi, and K. Ito: "Joint Compliance Regulation for Manipulators Utilizing Redundant Degrees of Freedom" Trans. of SICE, Vol.26, No.5, pp.557-563, 1990. (in Japanese)

[52] T. Tsuji, T. Takahashi, and K. Ito: "Multi-Point Compliance Control for Redundant Manipulators," Trans. of SICE, Vol.26, No.12, pp.1406-1413, 1990. (in Japanese)

[53] T. Tsuji, T. Takahashi, and K. Ito: "Multi-Point Compliance Control for Manipulators Constrained by Task Objects," Trans. of SICE, Vol.27, No.1, pp.85-92, 1991. (in Japanese)

[54] D. E. Whitney: "Quasi-Static Assembly of Compliantly Supported Rigid Parts," ASME Journal of Dynamic Systems, Measurement, and Control, Vol.104, No.1, pp.65-77, 1982.

[55] K. Yokoi, H. Maekawa, and K. Tanie: "A Method of Compliance Control for a Robotic Arm with Redundant Degrees of Freedom," Journal of RSJ, Vol.11, No.1, pp.121-130, 1993. (in Japanese)

[56] T. Yoshikawa: "Manipulability of Robotic Mechanisms," Int. Journal of Robotics Research, Vol.4, No.1, pp.3-9, 1985

[57] T. Yoshikawa: "Dynamic Hybrid Position/Force Control of Robot Manipulators - Description of Hand Constraints and Calculation of Joint Driving Force," IEEE Trans. on Robotics and Automation, Vol.3, No.5, pp.386-392, 1987

[58] T. Yoshikawa and K. Nagai: "Evaluation and Determination of Grasping Forces for Multi-Fingered Hands," Proc. IEEE Int. Conf. on Robotics and Automation, pp.245-248, 1988.

[59] T. Yoshikawa and X. Zheng: "Coordinated Dynamic Hybrid Position/Force Control for Multiple Robot Manipulators Handling One Constrained Object," Proc. 1990 JAPAN-U.S.A. Symp. on Flexible Automation, pp.401-407, 1990.

[60] T. Yoshikawa, K. Hosoda, and T. Doi: "Quasi-Static Trajectory Tracking Control of Flexible Manipulator by Macro-Micro Manipulator System," Journal of RSJ, Vol.11, No.1, pp.140-147, 1993. (in Japanese)

[61] T. Yamashita: "Mechanical Fingers Controlled by Machine and Their Applications to Materials Handling," Trans. of SICE, Vol.3, No.6, pp.429-439, 1964. (in Japanese)

Published Papers by the Author

Chapter 2:

- T. Yoshikawa and K. Nagai: "Manipulating and Grasping Forces in Manipulation by Multi-Fingered Hands," Proc. IEEE Int. Conf. on Robotics and Automation, pp.1998-2004, 1987.
- T. Yoshikawa and K. Nagai: "Manipulating and Grasping Forces of Multi-Fingered Hands," Trans. of SICE, Vol.23, No.11, pp.1206-1213, 1987. (in Japanese)
- T. Yoshikawa and K. Nagai: "Manipulating and Grasping Forces in Manipulation by Multifingered Robot Hands," IEEE Trans. on Robotics and Automation, Vol.7, No.1, pp.67-77, 1991.

Chapter 3:

- K. Nagai and T. Yoshikawa: "Dynamic Manipulation/Grasping Control of Multifingered Robot Hands" Proc. IEEE Int. Conf. on Robotics and Automation, pp. 1027-1033, 1993.
- K. Nagai and T. Yoshikawa: "Dynamic Manipulation/Grasping Control of Multifingered Robot Hands," Trans. of SICE, Vol.30, No.1, pp.39-47, 1994. (in Japanese)

Chapter 4:

- K. Nagai and T. Yoshikawa: "Adaptive Grasping by Multifingered Hands," J. of RSJ, Vol.11, No.1, pp.111-120, 1993. (in Japanese)

Chapter 5:

- K. Nagai and T. Yoshikawa: "Impedance Control of Redundant Macro Micro Manipulators," Journal. of RSJ, Vol.12, No.5, pp.766-772, 1994. (in Japanese)

- K. Nagai and T. Yoshikawa: "Impedance Control of Redundant Macro Micro Manipulators," Proc. of the 1994 IEEE/RSJ Int. Conf. on Intelligent Robots and Systems (IROS'94), pp.1438-1445, 1994.

Chapter 6:

- K. Nagai and T. Yoshikawa: "Grasping and Manipulation by Robotic Arm/Multifingered-Hand Mechanisms," (submitted to Journal. of RSJ, in Japanese)